Chemopreventive potential of Se-enriched broccoli and kale sprouts *in vitro* and in a human prostate cancer xenograft model

German Cancer Research Center, Heidelberg

(Division of Epigenomics and Cancer Risk Factor)

University of Heidelberg

(Biology)

DISSERTATION

Inaugural-Dissertation zur

Erlangung der Doktorwürde der Ruprecht-Karls-Universität

Heidelberg

2010

vorgelegt von

Jung-Hyun KIM

Presented by

Jung-Hyun KIM

References: Prof. Dr. Thomas Rausch

Prof. Dr. Bernard Watzl

Jesus Christ

"A man's heart deviseth his way: but the LORD directeth his steps"
KING JAMES (PROVERBS 16:9)

I. TABLE OF CONTENTS

II. LIST OF ABBREVIATIONS

5-aza-dC	5-aza-2'-deoxycytidine	**FACS**	Fluorescence assisted cell sorting
Ab	Antibody	**Flu**	Flutamide
ABC	Avidin biotin complex	**g**	Gram
Akt/PkB	Protein Kinase B	**GAPDH**	Glyceraldehyde 3-phosphate dehydrogenase
AP-1	Activator protein 1		
APC	Adenomatous polyposis coli	**GPx**	Glutathione peroxidase
APS	Ammonium persulfate	**GR**	Glutathione reductase
AR	Androgen receptor	**GSH**	Glutathione (Reduced)
Aza C	Cytidine analogues	**GSSG**	Glutathione (Oxidized)
		GST	Glutathione-S-transferase
BCA	Bicinchoninic acid	**GSTP1**	Glutathione-S-transferase π
Bcl-2	B-cell lymphoma 2		
BfEL	Institute of Nutritional Physiology, Federal Research Centre for Nutrition	**h**	Hour
		HAT	Histone acetyl transferase
		HDAC	Histone deacetylase
BITC	Benzylisothiocyanate	**HE**	Hematoxylin-Eosin
BPH-1	Benign prostatic hyperplasia-1	**HIF1-a**	Hypoxia inducible factor 1 alpha
BSA	Bovine serum albumin	**HIP**	Heidelberg Institute of Plant sciences
b.w.	Body weight		
		HO-1	Heme oxygenase 1
CBP/p300	CREB binding protein	**HPLC**	High performance liquid chromatography
CD	Concentration required to double the specific activity of		
QR	NAD(P)H:quinine oxidoreductase	**HRP**	Horseradish peroxidase
		HSP	Heat shock protein
cDNA	Complementary deoxyribonucleic acid		
		IC$_{50}$	Half maximal inhibitory concentration
CO$_2$	Carbondioxide	**IGF-1**	Insulin like growth factor 1
Cox	Cyclooxygenase	**INDO**	Indomethacin
CpG	Cytidine-guanine-dinucleotide	**iNOS**	Inducible nitric oxide synthase
Cyp1A1	Cytochrome P450 1A1		
		kDa	kiloDalton
		kg	Kilogram
DAB	3,3'-Diaminobenzidine	**KS**	Kale sprouts
DAF	Deutsche Forschungsanstalt fur Lebensmittelchemie		
		l	Liter
DHT	Dihydrotestosterone	**LNCaP**	Lymph node cancer of the prostate (a hormone dependent prostate cancer cell line)
DKFZ	German Cancer Research Center		
DMSO	Dimethylsulfoxide		
DNA	Desoxyribonucleic acid	**LPS**	Lipopolysaccharide
DNase	Desoxyribonuclease		
DNMT	Dimethylsulfoxide	**MAPK**	Mitogen activated protein kinase
dNTP	2-Desoxynucleotide-5'-triphosphate	**MCip**	Methyl-CpG immunoprecipitation
DPPH	1,1-Diphenyl-2-picrylhydrazyl	**mg**	Milligram
DTT	Dithiothreitol	**min**	Minute
		ml	Milliliter
EDTA	Ethylenediamine tetraacetic acid	**MOPS**	3-(N-Morpholino)-propanesulphonic acid
EGCG	(+)-Epigallocatechingallate		
ELISA	Enzyme linked immuno sorbent assay	**MMP**	Matrix metalloproteinase
		mRNA	Messenger ribonucleic acid
ERK	Extracellular signal-regulated kinase		
		NAC	N-acetylcysteine
Ex/Em	Excitation/Emission	**NAD(P)H**	β-Nicotinamide adenine dinucleotide (phosphate)

11

LIST OF ABBREVIATIONS

NF-kB	Nuclear factor-κB	**TBS-T**	TBS containing Tween 20
NKX3.1	NK3 homeobox 1	**TCA**	Trichloroacetic acid
NO	Nitric oxide	**TEMED**	N,N,N',N'-
NOS	Nitric oxide synthase		tretramethylethylenediamine
Nrf-2	Nuclear Factor-EE-related factor 2	**TGF**	Transforming growth factor
		TNFa	Tumor necrosis factor alpha
		U	Unit
OD	Optical density	**UV**	Ultraviolet
ORAC	Oxygen radical absorbance capacity	**V**	Volt
		VEGF	Vascular endothelial growth factor
PARP	Poly(ADP ribose) polymerase	**vs.**	versus
PBS	Phosphate-buffered saline	**Wt**	Wild type
PCNA	Proliferating cell nuclear antigen		
PCR	Polymerase chain reaction		
PEITC	Phenethylisothiocyanate		
PI3K	Phosphatidyl-inositol 3-kinase		
PIA	Proliferative inflammatory atrophy		
PIN	Prostatic intraepithelial neoplasia		
PSA	Prostate specific antigen		
PTEN	Phophatase and tensin homologue		
PKC	Protein kinase C		
PMSF	Phenylmethyl sulfonyl fluoride		
PlGF	Placenta growth factor		
PVDF	Polyvinyliden fluoride		
QR	NAD(P)H:quinone oxidoreductase		
RT-PCR	reverse transcriptase PCR		
r	Correlation coefficient		
RNA	Ribonucleic acid		
ROS	Reactive oxygen species		
rpm	Rotations per minute		
RT	Reverse transcriptase		
RPMI	Roswell Park Memorial Institute (cell culture media)		
RR	Relative risk		
s	Second		
s.c.	Subcutaeous		
SD	Standard deviation		
SDS	Sodium dodecyl sulfate		
SDS-PAGE	Sodium dodecylsulfate-polyacrylamide gel electrophoresis		
Se	Selenium		
SEM	Standard error of mean		
SFN	Sulforaphane		
SOD	Superoxide dismutase		
TBE	Tris/borate/EDTA		
TBS	Tris-buffered saline		

1. INTRODUCTION

1.1 Prostate cancer

1.1.1 Prostate cancer incidence

Prostate cancer is the most common cancer and the second leading cause of cancer death in men in Western countries. The American Cancer Society estimated lately that about 217,000 new cases of prostate cancer will be diagnosed and 32,000 men will die of prostate cancer in 2010 in United States (1). Despite a recent increase in prostate cancer cases and related death, the prevalence of prostate cancer in Asian countries is 20 times lower than in Western countries (2). This geographic variation most likely reflects differences in lifestyle. Many factors like diet, environmental carcinogens, and inflammatory diseases have been linked to an increased risk of prostate cancer (3).

1.1.2 Multistep process of prostate carcinogenesis

The development of prostate cancer is believed to be a multi-step process with distinct cellular and molecular alterations in each phase. A number of mutations are required to initiate, promote and progress the disease through a series of morphological defined stages (4). Genetic and epigenetic alterations promote transformation of normal glandular epithelium to preneoplastic lesions to invasive carcinoma (5, 6). Proliferative inflammatory atrophy (PIA) is a precursor of prostatic intraepithelial neoplasia (PIN) and characterized by down-regulated p21/WAF gene expression which functions as a regulator of cell cycle progression. PIN lesions are highly proliferative and often show silencing of tumor suppressor genes such as GSTPi and NKX3.1. Hypermethylation of the promoter CpG islands of GSTPi is the most common epigenetic alterations that is also observed in prostatic adenocarcinoma (6, 7). During further progression of prostate adenocarcinoma, the tumor suppressor gene PTEN is frequently silenced, which is a negative regulator of the serine/threonine protein kinase Akt that plays a key role in cell proliferation and migration (8, 9). The final stage of prostate cancer is characterized by hormone-independent proliferation with AR mutations and down-regulation of p53 (6, 10) (schematic description in Fig. 1).

Normal prostate epithelium

↓ p21^{cip1}

Prostate inflammatory Atrophy (PIA)

↓ GSTP1
↓ NKX3.1
Telomerase
activation

Prostatic Intraepithelial Neoplasia (PIN)

↓ PTEN

AR mutations
or amplications
↑ Bcl2
↓ P53
↓ ET-1

Prostatic Adenocarcinoma

Hormone Refractory Prostate Cancer
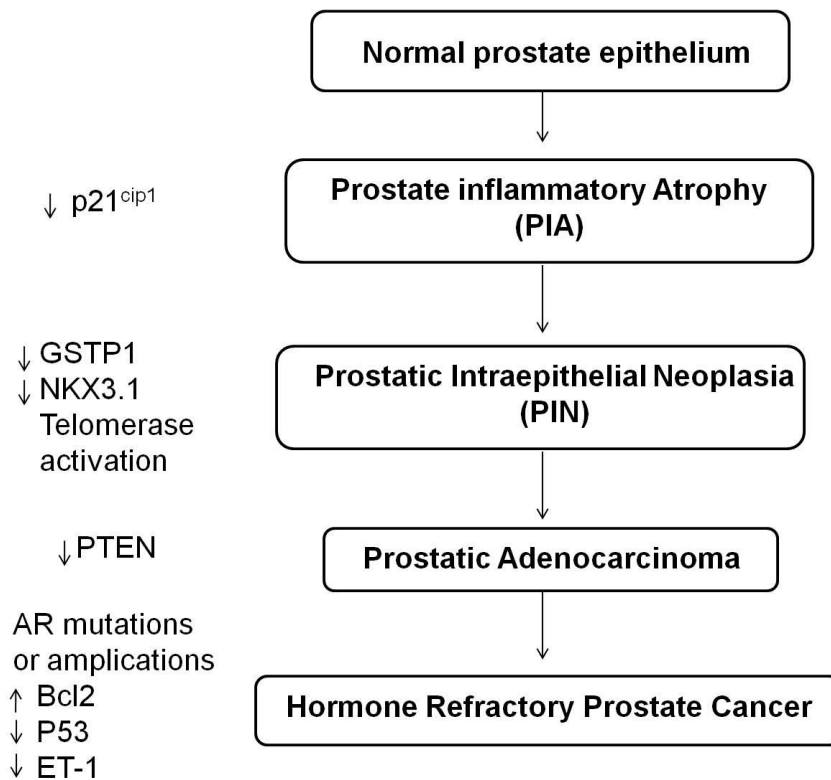
Fig. 1: Model for the progression of prostate carcinogenesis. The normal prostate epithelium progresses through a series of morphological changes forming PIA and PIN lesions followed by adenocarcinoma to hormone refractory prostate cancer. Genetic alterations of each stage of prostate cancers are shown. Modified from (11).

1.1.3 AR signaling in prostate cancer progression

Early-stage prostate cancers depend on androgens for growth and survival, and androgen ablation therapy causes them to regress. However, during prostate cancer progression, hormone-responsive prostate cancer may turn into a hormone-refractory stage. More aggressive, invasive and metastatic prostate cancer cells move to other organs where they do not need hormones to proliferate. Therefore they do not respond to hormone withdrawal therapy. Testosterone is the main circulating androgen, secreted primarily by the testes. When free circulating testosterone enters prostate cells, 90% is converted to dihydrotestosterone (DHT) by the enzyme 5α reductase. DHT is the more active hormone, having fivefold higher affinity to the androgen receptor (AR) than does testosterone. Like other nuclear receptors, in the basal state, the AR is bound to heat shock proteins (HSPs) and other proteins in a conformation that prevents DNA binding. Binding to androgens induces a conformational change in the AR that leads to dissociation from the heat-shock proteins and receptor phosphorylation, in part mediated by protein kinase A. The ligand-induced conformational

change facilitates the formation of AR homodimer complexes that can then bind to androgen response elements (AREs) in the promoter regions of target genes. The activated DNA-bound AR homodimer complex recruits co-regulatory proteins, co-activators or co-repressors, to the AR complex. The co-activators allow interaction of the AR complex with the general transcription apparatus to stimulate target gene transcription. Many AR target genes have been identified, including prostate specific antigen (PSA), insulin-like growth factor-1 (IGF-1), prostate binding protein C3 (PBPC3), resulting in proliferation and survival of prostate cancer (reviewed in (12) and schematic description in Fig. 2).
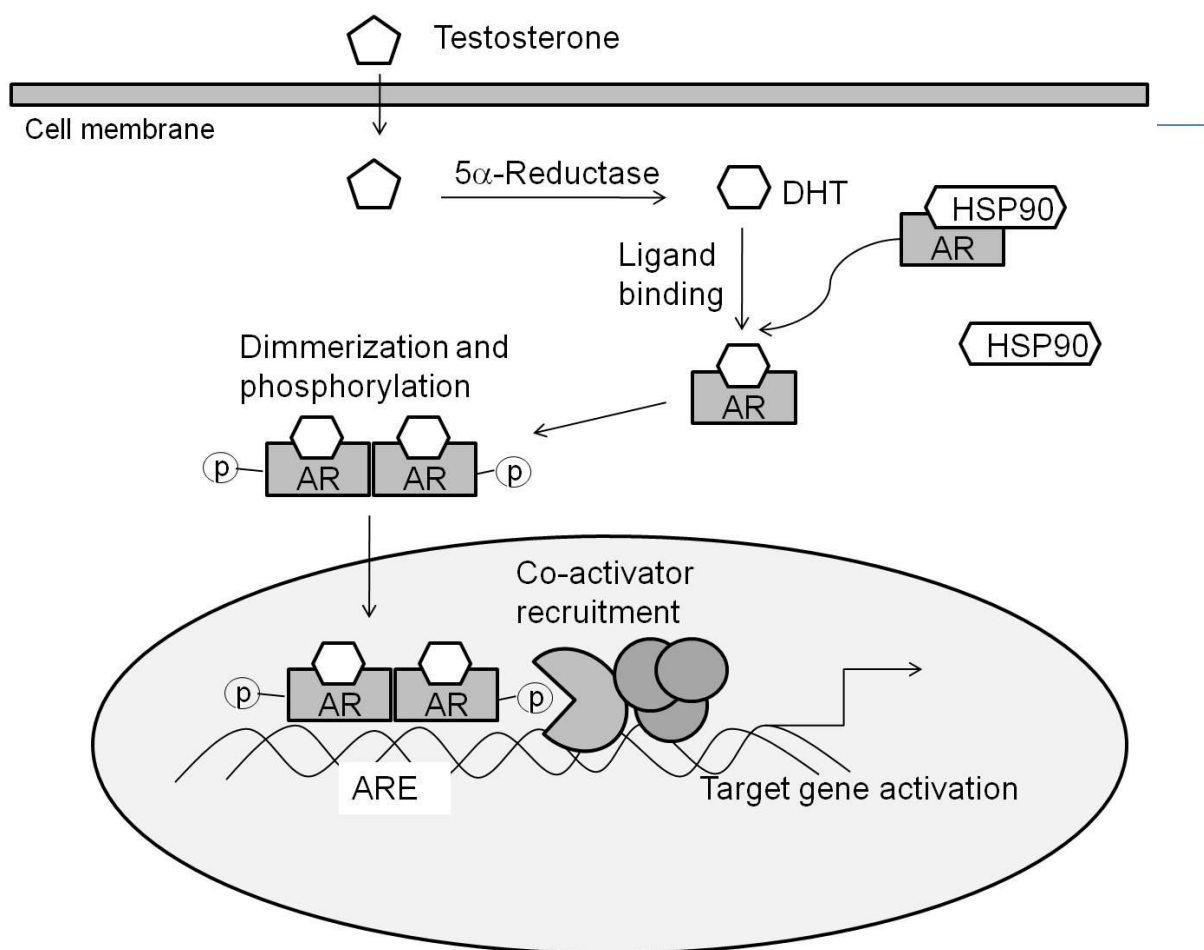
Fig. 2: AR signaling Free testosterone enters prostate cells and is converted to DHT by active 5α-reductase. Binding of DHT to the AR induces dimerization and phosphorylation of AR which leads to conformational changes of the AR. Translocated AR dimer can bind to the androgen response element (ARE). One of the major target genes is PSA, which leads to biological responses including cell growth. Adapted from (12).

INTRODUCTION

1.1.4 Prostate cancer cell lines

Various cell lines have been established from prostatic tissue and different stages of prostate cancer. Benign prostatic hyperplasia cell line (**BPH-1**) has been derived from highly proliferative human prostate tissue (13). Primary epithelial cell cultures were immortalized with SV40 large T antigen. Tumor suppressor genes PTEN and p53 are expressed in this cell line, which is induced to proliferate by growth factors; however testosterone has no direct effect on BPH-1 cell proliferation. Although 5α-reductase is detected in BPH-1 cells, expression of AR and the secretory markers, PSA and prostatic acid phosphatase, are not detectable (13). The **LNCaP** cell line was established from a metastatic lesion of human prostatic adenocarcinoma. The LNCaP cell line is characterized by GSTPi mutation, loss of PTEN and low levels of p53 expression. High-affinity specific AR is present in the cytosol and nuclear fractions of LNCaP cells (14). Estrogen receptors (ER) are detectable in the cytosol. This cell culture model is hormone-responsive, and produces PSA in response to testosterone. The **PC-3** cell line is from a human prostatic adenocarcinoma metastatic to bone. PC-3 cells have a greatly reduced dependence upon serum for growth when compared to normal prostatic epithelial cells and do not respond to androgens, glucocorticoids, or epidermal or fibroblast growth factors. The tumor suppressor genes GSTPi and p53 are mutated (15). The **DU145** cell line is a highly aggressive and metastatic prostate cancer cell line. This long-term tissue culture cell line has been derived from a human prostate adenocarcinoma metastatic to the brain (16). Among the prostate cancer cell lines, LNCaP cells are hormone dependent and express AR and PSA secretion. However, more aggressive PC-3 and DU145 cell lines show hormone independent growth and do not produce PSA.

1.2 Chemoprevention

The association between life style and prostate cancer risk has been widely studied and indicate that diet, alcohol consumption, obesity and lack of exercise are considered as cancer risk factors (17). It has been estimated that more than 60% of human cancers could be prevented through appropriate lifestyle modification (18). There has been a lot of effort to precisely assess the mechanisms by which components of fruit and vegetables prevent different types of cancer in laboratory studies (17) .

Chemoprevention is defined as the use of specific agents to delay or block the development,

progression or recurrence of carcinogenesis. The aim of chemoprevention is to reduce the cancer incidence by delaying or suppressing the process of cancer development (19). The NCI has determined that more than 1,000 different phytochemicals, plant-derived compounds, possess cancer-preventive activity.

Many of the prominent chemopreventive agents have multiple intracellular targets. Carcinogenesis is generally recognized as a multistep process in which distinct molecular and cellular alterations occur. Tumor development is considered to consist of tumor initiation, promotion and progression. Fig. 3 shows several key mechanisms during the multistep process of carcinogenesis that serve as targets for cancer prevention.
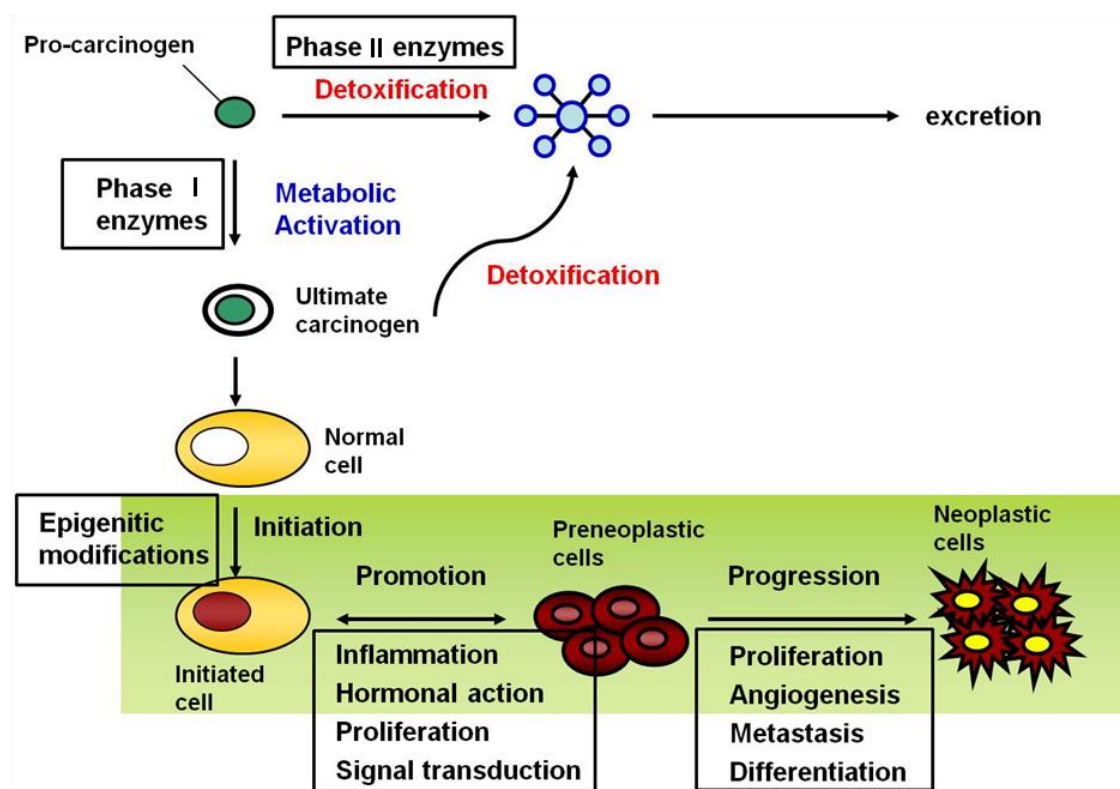
Fig. 3: Multistep process of carcinogenesis and target mechanisms of chemoprevention. Carcinogenesis is initiated by transformation of a normal cell into a cancer cell (initiated cell). These cells undergo tumor promotion into preneoplastic cells and progression into neoplastic cells. Distinct mechanisms are involved in each step of carcinogenesis. Modified from (17).

During the rapid and irreversible initiation stage, a reactive carcinogen, either directly or after metabolic activation through Phase I enzymes, reacts with DNA and leads to DNA damage, which may lead to DNA mutations if not repaired. Inhibition of Phase I metabolic enzymes may block the activation of pro-carcinogen, and induction of Phase II enzymes contributes to increased detoxification of pro-carcinogens. The Phase II enzyme system of

xenobiotic metabolism is an important component of the cellular stress response by which a diverse array of electrophilic and oxidative toxicants can be removed from the cell before they are able to damage the DNA. The induction of Phase II enzymes is mediated *via* the activation of the transcription factor Nrf-2, which induces the transcription of several detoxifying enzymes, such as glutathione-*S*-transferase (GST), NAD(P)H:quinone oxidoreductase, uridine diphosphate glucuronosyl-transferases (UGTs), Thioredoxin reductase (TRx-R) and many others. Modulation of xenobiotic metabolizing enzymes is a target of several chemopreventive agents including isothiocyanates derived from cruciferous vegetables (19) (further detailed description in Chapter 1.2.2.2).

Another target of the initiation step of carcinogenesis is epigenetic gene regulation. Interest in targeted epigenetic modifications by chemopreventive agents has been recently raised. Inhibition of histone deacetylase (HDAC) activity results in histone hyperacetylation and consequently an open chromatin which facilitates gene transcription. HDAC inhibitors up-regulate the cyclin-dependent kinase inhibitor p21 and increased cell cycle arrest and cell differentiation (20, 21). Another epigenetic modification often observed in cancer is DNA methylation that causes inhibition of gene transcription of tumor suppressor genes and other key regulators. Inhibition of DNA methyltransferases by chemopreventive agents such as genistein from soy and EGCG from green tea is considered as a novel interesting chemopreventive mechanism to block carcinogenesis (22).

In contrast to the initiation stage, tumor promotion stage is considered to be a relatively long-lasting event, in which actively proliferating cells accumulate to preneoplastic lesions. In this phase, inhibition of inflammation, induction of cell cycle arrest and modulation of signal transduction may postpone the development of carcinogenesis. Inflammation is a driving force of the progression of carcinogenesis and possibly reduced by inhibition of pro-inflammatory mediators, such as nuclear factor κB (NF-κB), subsequently leading to reduce transcriptional activation of inflammation mediators, inducible nitric oxide synthase (iNOS), cyclooxygenase2 (Cox2), tumor necrosis factor α (TNFα), and hypoxia inducible factor α (HIF-1α). Anti-inflammatory properties by modulating pro-inflammatory signaling mediated by these factors is also considered as effective target of chemoprevention by dietary compounds such as quercetin, curcumin and sulforaphane (reviewed in (17)).

The final progression stage involves malignant transformation of pre-neoplastic cells to neoplastic lesions, resulting in tumor growth with metastasizing potential. Therefore the target can be the inhibition of cell proliferation, angiogenesis, metastasis and differentiation.

Chemopreventive drugs, such as resveratrol and PEITC have been reported to potentially inhibit tumor angiogenesis and metastasis by inhibition of HIF-1α–mediated induction of vascular endothelial growth factor (VEGF) (19, 23).

1.2.1 Chemoprevention of prostate cancer

A large body of evidence describes the role of dietary factors and physical activity in the development and progression of prostate cancer. Dietary factors are major elements accounting for the international and inter-ethnic differences in the rate of prostate cancer. Identifying molecular mechanisms involved in carcinogenesis provides the rationale for developing strategies for prostate cancer prevention. When we consider the multistep progress of prostate cancer (Fig. 1) as well as many risk factors to develop prostate cancer, dietary intervention targeting multiple pathways might be particularly effective to prevent prostate cancer.

1.2.2 Chemopreventive agents of prostate cancer

Many agents have been evaluated for their primary and secondary chemopreventive capacities to targets different stages and molecular signaling of prostate cancer, including selenium, vitamin E, isothiocyanates, lycopene, polyphenols and green tea. These agents potentially interact with a range of carcinogenic pathways in the prostate. An overview is given in Table 1. Prominent examples of prostate cancer chemopreventive agents are described in the following sections.

Table 2. Summary of chemopreventive agents and target mechanisms against prostate cancer adapted from (24).

Dietary agent	Model system	Targets/mechanism of action
Selenium		
Selenomethionine	In vitro cell culture	Cell cycle arrest (G_2/M)
		Apoptosis
		Androgen receptor-mediated response
Sodium selenite	In vitro cell culture	Redox mechanism
Methylseleninic acid	In vitro cell culture	Caspase-mediated, cytochrome c release and DNA fragmentation
		Phosphorylation of c-Jun and p38
		p53 phosphorylation
		TRAIL-mediated apoptosis
		Regulation of phosphor-Akt
		Modulate androgen-regulated genes

	In vivo (Lady transgenic)	No reduction in prostate cancer incidence
Cruciferous vegetables		
Sulforaphane	In vitro cell culture	Cell death, caspase-mediated apoptosis Generation of ROS Activation of MAPK Modulation of NF-κB and AP-1 Inhibition of HDAC Destabilization of AR associated with HSP90 Lowered AR protein/ gene expression
Sulforaphane	In vivo	Protective against tumorigenesis Induction of phase II enzymes
Broccoli sprouts	In vivo xenografts TRAMP mice	Retards tumor growth Inhibition tumor growth Apoptosis with suppression of Akt pathway
Vitamin E		
α-Tocopherol	In vitro cell culture	Cell cycle arrest(G1 or G2/M) Induced apoptosis Inhibition AR and PSA expression
	In vivo-Lady transgenic	No reduction in prostate cancer incidence
	Xenograft	Reduced incidence of prostate cancer
Lycopene		
	In vitro cell culture	Inhibition of DNA strand breaks Mitotic arrest Apoptosis and altered mitochondrial function Reversal of the effect of DHT Reduces AR and β catenin level Inhibits IGF
	In vivo	Increased necrosis
Green tea polyphenols		
Epigallocatechin gallate	In vitro cell culture	Cell cycle arrest TRAIL-induced apoptosis Inhibition of NF-κB and AP-1 Inhibits biomarkers of angiogenesis/metastasis
	In vivo	Inhibits prostate cancer development and progression IGF-1 inhibition
	TRAMP mice	Inhibition of MMP-2 activation and invasion PSA-triggered basement membrane degradation

1.2.2.1 Selenium

The micro-nutrient selenium exists naturally in food such as button mushrooms, cod, calf's

liver, tuna and salmon predominantly in the organic form as selenomethionine and selenocysteine. Several large prospective studies reported 50-65% reductions in risk of developing prostate cancer associated with high versus low selenium levels as measured in plasma (25, 26). The Nutrition Prevention of Cancer Trial (NPC) observed a 50% reduction in prostate cancer incidence among men randomized to selenium supplements (27).

The benefit of selenium was also tested in SELECT (Selenium and Vitamin E Cancer Prevention Trial), a phase III randomized, placebo-controlled study, designed to determine whether selenium and vitamin E, alone or in combination, decrease the risk of prostate cancer in healthy men. A total of 35,534 men randomized from 400 clinical sites across United States, Puerto Rico and Canada received selenium (200 μg/day of selenomethionine) and/or vitamin E (400 IU/day of all rac-α-tocopheryl acetate) supplementation or placebo for a minimum of 7 years (maximum 12 years) (28). The result was that selenium or vitamin E, alone or in combination at the doses and formulations used, did not prevent prostate cancer in this population of relatively healthy men (28). The difference between the earlier NPC study was that NPC study used selenized yeast, whereas SELECT used selenomethionine. These forms of selenium may have significantly differences in their biologic effects.

Selenium has several activities and targets different mechanisms, depending on its form (29). Selenomethionine inhibits proliferation and induces cell cycle arrest of human prostate cancer cells (30). Selenium in the form of selenomethionine induces apoptosis and inhibits angiogenesis, mediated in part by the androgen receptor, reviewed in (24, 31). Another form of selenium, methylseleninic acid, induces apoptosis through a caspase-mediated pathway, mediated through the release of cytochrome c, cleavage of poly[ADP-ribose]polymerase (PARP) and DNA fragmentation (32). Methylseleninic acid also modulates expression of many androgen-regulated genes in human prostate cancer cells *in vitro* (33). The anticancer effects of sodium selenite are thought to be mediated *via* a redox-related mechanism involving induction of oxidative stress (34).

Generally, most of the selenium (inorganic/organic) serves as a precursor to the synthesis of selenoproteins, such as glutathione peroxidase (GPx), TRx-R, and selenoprotein P. Polymorphisms of selenoprotein P and Sep15, by altering their ability to incorporate selenium, may be important in protecting against the development of prostate cancer (35). GPx is a major Se-containing protein which converts toxic H_2O_2 to harmless H_2O (36). Five different members of the GPx family have been reported. GPx-1 is the major cytoplasmic glutathione peroxidase, GPx-4 acts on lipid hydroperoxides and cholesterol ester

hydoperoxides within cell membranes, and GPx-3, called plasma glutathione peroxidase, is mainly expressed in lung and kidney (35, 37). TRx-R is another key selenoprotein that is the primary catalyst for the NADPH-dependent reduction of thioredoxin (36).

Modulation of the redox status by selenium seems to have dual effects on prostate cancer proliferation − on one hand inhibition of therapeutic effectiveness (34), on the other hand induced apoptotic potential and increased sensitivity of cells to radiation-induced killing (38). Regarding these opposing effects, we may have to consider the concentration of selenium. Regarding the relation between selenium dose and prostate carcinogenesis, it was showed that over-accumulation of selenium intake may be potentially dangerous, indicated by a U-shaped dose-response curve of Se in association with increased DNA damage in aging dogs (39, 40). Thus, optimization of the use of selenium as potential prostate cancer chemopreventive agent is required.

1.2.2.2 Cruciferous vegetables

Cruciferous vegetables of the family *Brassicaceae* include vegetables such as broccoli, cauliflower, kale, Brussels sprouts and Chinese cabbage have been suggested as promising candidates to modulate prostate cancer risk (41). Evidence for the protective effect of cruciferous vegetable against prostate cancer comes from epidemiological studies of dietary intake (42). Table 2 listed several epidemiological studies that analyzed the association between intake of cruciferous vegetables and prostate cancer risk.

Table 2. List of epidemiology studies of cruciferous vegetables and prostate cancer risk

Country	Participants	No. of Cases	Effect	Reference
USA	>45.000	3000	10% ↓	Giovannucci *et al.,* 2003 (42)
USA	>80.000	3000	No	Stram *et al.,* 2006 (43)
Canada	>29.000	1.300	40% ↓ (advanced)	Kirsh *et al.,* 2007 (44)
Germany	>11.000	300	40% ↓ (low-grade)	Steinbrecher et *al.,* 2009 (45)
USA	>3.000 cases + controls		30% ↓ (advanced)	Kolonel *et al.,* 2000 (46)
USA	>1.200 cases + controls		40% ↓	Cohen *et al.,* 2000 (47)

A prospective study in the US with more than 45,000 participants demonstrated that there is

no compelling evidence for a protective influence of cruciferous vegetables on prostate cancer risk, and only a slight inverse association between cruciferous vegetable intake and prostate cancer risk was found (42). Another prospective study reported no significant protective association of any vegetable consumption and prostate cancer risk (43). However, two other recent prospective studies showed significantly negative associations between prostate cancer risk and consumption of cruciferous vegetables, although the number of cases of these studies were smaller that in earlier studies (45). Two case-control comparisons of people with histological confirmed prostate cancer and cancer-free controls demonstrated that intake of cruciferous vegetables was inversely related to prostate cancer (46). Although the results of these studies are not conclusive, most of the studies show a trend to an inverse relationship between the consumption of cruciferous vegetables and prostate cancer risk (Table 1).

Reduction of prostate cancer risk by dietary cruciferous vegetables is attributed to glucosinolates (GS) in the vegetables. GS are substituted β-thioglucoside N-hydroxysulfates, formed by the plant. Over 115 naturally occurring glucosinolates have been identified. Each cruciferous vegetable contains a mixture of glucosinolates that varies according to the strain of the plant. Inhibition of carcinogenesis by glucosinolates is not primarily attributable to this class of compound, but is rather due to their break-down products. Hydrolysis of these phytochemicals is catalyzed by myrosinase, an enzyme that is stored in 'myrosin' cells in the plant. Upon wounding of the vegetable, for example during harvesting, freeze–thawing, food preparation, or chewing while being eaten, myrosinase is released from the 'myrosin' cells and catalyses the hydrolysis of glucosinolates within the damaged plant. In addition, myrosinase activity may be present in human colonic microflora, suggesting that it is possible that glucosinolates are hydrolysed in the gastrointestinal tract during digestion of food (48). Fig. 4 illustrated examples of hydrolysis of GS by active myrosinase. Glucoraphanin, which is an abundant GS in broccoli, is catalyzed to sulforaphane by active myrosinase. A indolyl glucosinolates, glucobrassicin, generates indole-3-carbinol at neutral pH by active myrosinase. In the acidic environment of the stomach, I3C condenses to form various condensation products including 3,3'-diindolymethane (DIM) (48).

Various chemopreventive mechanisms stimulated by ITCs in many cancers, including prostate cancer, have been demonstrated over the years. Basically all the steps of carcinogenesis have been identified as targets of ITCs. Early studies focused on the modes of action of isothiocyanates as inhibitors of phase I enzyme CYP450 and inducers of phase II

detoxification, thereby blocking the metabolic activation of pro-carcinogens and facilitating carcinogen excretion. Recent studies suggest that ITCs also offer protection against tumor development during the "post-initiation" phase and mechanisms for suppression effects of ITCs including cell cycle arrest and apoptosis induction in prostate cancer. Mechanisms of ITCs include induction of antioxidant and detoxification genes mediated by activation of Nrf-2 and AhR (arylhydrocarbon receptor), inhibition of pro-inflammatory reactions by repression of NF-κB (49), AP-1 (activator protein 1) signaling, inhibition of cytochrome P450 enzyme activity, inhibition of histone deacetylase, and stimulation of cell cycle arrest and apoptosis, and inhibition of metastasis and angiogenesis, as reviewed in (24, 50). There is a dose-dependency in these responses. Generally induction of metabolic genes occurs at relatively low concentrations of ITCs, whereas activation of cell cycle arrest and apoptosis occurs at higher concentration (51, 52).

A major mechanism of anti-proliferative effects of ITCs on prostate cancer is related to cell cycle arrest and apoptosis. The first report on the involvement of caspases in SFN-mediated apoptosis was by Chiao and colleagues in prostate LNCaP cells [116]. Induction of apoptosis by ITCs are mediated by caspase activation, death ligand induction, ROS formation, mitogen-activated protein kinase (MAPK) activation, modulating Bcl/Bax protein expression in prostate cancer *in vitro* and *in vivo* (reviewed in (50)). Subsequently, SFN was shown to activate the mitochondrial/ intrinsic apoptotic pathway. This involves release of cytochrome c from the mitochondria into the cytosol, which in turn binds to the apoptosis protease activation factor-1 (Apaf-1) and leads to activation of caspase-9 (53). Recently, SFN was also shown to activate the death receptor/extrinsic pathway of apoptosis in prostate cancer cells. This pathway is initiated when the death ligands, such as Fas-L and TRAIL or tumor necrosis factor α (TNFα) through their cell surface receptors activate the downstream intracellular apoptotic machinery, which involves induction of caspase-8 and subsequent activation of effector caspases (54). More recently, SFN and PEITC mediated apoptosis was linked with the generation of ROS in prostate cells (55, 56). Increased levels of ROS in response to SFN and PEITC treatment were accompanied by disruption of mitochondrial membrane potential, cytosolic release of cytochrome c and apoptosis.

Anti-proliferative effects of ITC on prostate cancer are also related to cell cycle arrest (57). Inhibition of proliferation of SFN was link to irreversible G_2/M phase cell cycle arrest by activation of checkpoint kinase 2 (Chk2) and increased phosphorylation of cell division cycle protein 25C (Cdc25C) (50, 58). Allyl isothiocyanate (AITC) significantly inhibits

proliferation of cultured PC-3 (androgen-independent) and LNCaP (androgen-dependent) human prostate cancer cells in a dose-dependent manner associated with reduction in the expression of cyclin B1 protein cycle dependent kinase 1 (Cdk1), Cdc25B and Cdc25C (59). Re-expression of the p21 tumor suppressor gene mediated by histone acetylation also causes cell cycle arrest in LNCaP cells treated by PEITC and SFN (60, 61). Another mechanism to induce cell cycle by ITCs is mediated by proteasome-mediated degradation of Cdc25C and Cdk1 in PC-3 human prostate cancer cells (62).

Androgen signaling is a key mechanism to maintain proliferation of prostate cancer. Androgen signaling targeted by ITCs has been reported in many studies. PEITC represses AR transcription and expression in both androgen-dependent and -independent prostate cancer cell lines (63). Recent study newly defined that SFN treatment enhances HSP90 acetylation by inhibition of HDAC6, thereby inhibiting its association with AR. Moreover, AR is subsequently degraded in the proteasome, which leads to reduced AR target gene expression (64). DIM, the condensed form of I3C, suppresses DHT-stimulated cell proliferation by inhibiting AR translocation into the nucleus. This study suggested that DIM binds to AR competitively to DHT (65).

In addition to single ITC's effects on prostate cancer, effects of dietary cruciferous vegetables have been investigated. Studies in TRAMP mice have evaluated the pharmacodynamic action of broccoli against prostate tumorigenesis (66). Mice given 240 mg broccoli sprouts per day exhibited a significant inhibition of prostate tumor growth, accompanied by increased expression of cleaved caspase-3, cleaved PARP and apoptosis regulator Bax, and decreased levels of Bcl-xL protein.

1.2.2.3 Vitamin E

Vitamin E contains a group of naturally occurring compounds such as the tocopherols, tocotrienols, and their natural and synthetic derivatives which can classified into α, β, γ and δ isoforms (67). Vitamin E is rich in many dietary sources including vegetable oils, nuts and egg yolks. Several epidemiological studies suggest that men in the highest quintile of plasma concentration of γ-tocopherol had reduced risk of prostate cancer (68). In addition, the ATBC trial (Alpha-tocopherol, Beta-carotene cancer prevention study) indicated that daily supplementation of vitamin E potently reduce the incidence of prostate cancer among men who smoked (69). The mechanisms which were targeted by vitamin E in prostate cancer have

been investigated in several studies. The biologically active form of vitamin E is a potent intracellular antioxidant which inhibits lipid peroxidation and DNA damage (70). Besides its antioxidant function, vitamin E and its analogues can modulate transforming growth factor and AR/PSA signaling pathway and regulate cell cycle through DNA synthesis arrest in LNCaP, PC-3, and DU-145 prostate cancer cells (71). Induction of apoptosis by causing depletion of cytosolic death receptor Fas, inhibition of VEGF production, and inhibition of matrix metalloproteinases (MMPs) are other mechanisms through which vitamin E inhibits prostate carcinogenesis (72).

1.2.2.4 Lycopene

Lycopene is a lipophilic carotenoid presented in tomatoes at high concentration (73). In a recent clinical study, consumption of tomato paste resulted in a significant reduction in mean plasma PSA levels in patients with benign prostatic hyperplasia (74). The chemical structure of lycopene is a linear hydrocarbon containing a series of conjugated and un-conjugated double bonds. This structure contributes to the limiting of oxidative damage and confers high affinity for quenching singlet oxygen molecules (73, 75). For the target mechanisms of lycopene against prostate cancer, cell cycle arrest, apoptosis, and growth factor signaling have been demonstrated with lycopene administration. Lycopene induced mitotic arrest in the G_0/G_1 phase, with decreased levels of cyclins D and E as well as CDK in LNCaP, PC3 and DU145 human prostate cancer cells (76). Lycopene mediated apoptosis in a concentration-dependent manner in LNCaP cells shown by decreased mitochondrial trans-membrane potential (77). Lycopene, in dietary relevant concentration, reversed the androgen-regulated effects of dihydrotestosterone by reducing androgen receptor and β-catenin nuclear localization and inhibiting IGF-1 stimulation (78).

1.2.2.5 Green tea polyphenols

Tea consumption has been associated with a reduced prostate cancer risk, partly *via* the antioxidative properties of tea polyphenols (Table 1) (79). Two randomized clinical trials testing green tea in patients with high-grade prostatic intraepithelial neoplasia and advanced prostate cancer demonstrated negative result, which might reflect a lack of power to confirm a modest benefit of green tea (80-82). However, several molecular anticancer mechanisms

have been proposed, including cell cycle arrest in both androgen-sensitive and androgen-insensitive prostate cancer cells (24). Induction of apoptosis via inhibition of transcription factors, such as NF-κB and AP-1 has been reported (83). Epigallocatechin gallate (EGCG), a polyphenolic compound, is abundant in green tea. Administration of EGCG led to negative regulation of the NF-κB pathway, which caused a decrease in the expression of the pro-apoptotic protein Bcl-2. In addition, several studies have indicated that this compound inhibited the IGF-1 pathway (84).

Similar benefits of tea polyphenols have been observed in preclinical models. In the TRAMP mouse model, which mimics the pathogenesis of human prostate cancer, the consumption of green tea polyphenols significantly inhibited the development of prostate cancer and metastasis (85, 86). Consumption of polyphenol early in life might be important; intervention of green tea polyphenols by 6 weeks of age demonstrated the absence of tumors in TRAMP mouse model, whereas delaying intervention beyond this time resulted in high-grade prostatic intraepithelial neoplasia followed by well-differentiated cancer with metastasis (86).

1.3 Selenium-enriched broccoli

As described above, chemopreventive agents target distinct mechanisms to prevent or inhibit prostate carcinogenesis. The idea to combine potent dietary agents to prevent prostate cancer may increase effects of individual compounds.

One such idea is to increase selenium levels in cruciferous vegetables to combine potential preventive activities of Se and glucosinolates breakdown products. Se is accumulated in accumulator plants primarily in methylated forms such as SeMSC, γ-glutamyl SeMSC, selenocystathione, γ-glutamyl selenocystathione, and methyl selenol (87). Broccoli (*B. oleacea* var. italica) has high glucosinolate content, but it also has a high capacity for SeMSC biosynthesis. However, under field conditions SeMSC formation is limited by low selenate availability in most soils. By addition of sodium selenate in the soil broccoli accumulated almost 1,000 *m*g Se per gram of dry plant tissue (88). However, something to consider is whether modulation of Se levels has no side effects.

In the plant, sulfate and selenate share the initial route for uptake, absorption and incorporation into O-acetylserine, follow by the formation of cysteine and seleno-cysteine, respectively (89, 90). The predicted competition between sulfate and selenate for uptake and assimilation has been suggested by using same transporter and enzymes (91); accumulation

of SeMSC was dependent on selenate addition to the growth medium, addition of sulfate reduced the formation of SeMSC by selenate inoculation (91). Although there is predictable competition in the biosynthesis of these two chemopreventive agents in one plant, an optimal range of selenium accumulation may increase the chemopreventive efficacy of broccoli.

As described previously, consumption of broccoli was inversely correlated with prostate cancer incidence. This was mainly attributed to glucosinolates derivatives. Several studies reported that addition of Se to cruciferous vegetables could provide even greater protection from cancer, including prostate cancer (88, 92-94). There has been an investigation in a prostate cancer model that Se-enriched broccoli sprouts were superior to normal broccoli sprouts in inhibiting cell proliferation, decreasing prostate-specific antigen secretion, and inducing apoptosis of prostate cancer cells. (92). In addition to prostate cancer prevention, high-Se broccoli has been proven to be protective against colon cancer in the $Apc^{Min/+}$ mouse model. The $Apc^{Min/+}$ mouse mimics the rapid development of adenomatous polyps that affect humans with germ line inactivation of one Apc gene. Mice fed high-Se broccoli (2 mg Se per g of diet) showed significantly fewer total tumors and a lower total tumor burden (by almost 50%) than mice fed low-Se broccoli (88, 93). In the DMBA-induced rat mammary tumor model, high-Se broccoli significantly reduced tumor incidence, total tumor number, and tumor burden about 30% compared to animals fed adequate amounts of Se (0.1 mg/g) without broccoli (94). Similar effects have also been shown in another study with Sprague-Dawley rats that consumed diets containing 3 µg of Se/g of diet supplied as high-Se broccoli. High-Se broccoli fed rats had significantly fewer mammary tumors than rats fed 0.1 µg of Se as selenite with or without the addition of regular broccoli (94). Besides Se-enriched broccoli florets, Se-enriched broccoli sprouts have been investigated in a similar model. Fisher F-344 rats fed 2 µg of Se/g of diet supplied as high-Se broccoli sprouts had significantly fewer aberrant colon crypts than rats fed 0.1 or 2 µg of Se/g of diet supplied as selenite with or without the addition of low-Se broccoli (94). Although these report suggest the possibility of Se-enriched broccoli as a potential chemopreventive agent, there is only a few studies regarding prostate cancer prevention. Therefore optimization of Se accumulation in broccoli and detailed mechanisms for the protection against prostate cancer have to be further investigated.

1.4 Kale sprouts – a potential dietary agent for prostate cancer prevention

Another possibility to prevent prostate cancer development by dietary chemopreventive agents may be to increase the level of active compounds in the vegetables. For example, recently a super broccoli has been developed without any genetically modification of the plant. It contains three fold more of glucosinolate compared to standard broccoli and consumption resulted in increasing sulforaphane metabolites in human plasma (95). Also, it induced gene expression associated with xenobiotics and cell cycle arrest in human gastric mucosa (96).

Sprouts of cruciferous vegetables are also a good source of glucosinolates. Sprouts were shown to contain about 10-100 fold more of glucoraphanin than the corresponding mature cruciferous vegetables (97). For example, broccoli sprouts, grown from broccoli seeds, contain glucoraphanin in quantities similar to seed levels which range from 5-100 μmol/g (98). Hence, small quantities of sprouts may protect against risk of cancers as effectively as much larger quantities of mature vegetables of the same variety. Not only the quantities but also dramatic differences in the glucosinolate profiles are presented. Young broccoli sprouts contain glucoraphanin as a major glucosinolates and less than 10% of glucobrassicin is present. However in mature broccoli, although the composition varies considerably among the cultivars, on average, 67% of the total glucosinolates is glucobrassicin (98).

Following this concept, kale sprouts may have powerful potential to prevent prostate cancer carcinogenesis because they contain about five fold higher levels of glucosinolates compared to standard broccoli (Fig. 5). Kale sprouts have not been investigated so far with respect to prostate cancer preventive potential. Mature kale is a family member of *Brassica oleracea* which is also referred to as cruciferous vegetable. It is widely cultivated and popular in North Western Europe and served as food vegetable. Kale is considered to be highly nutritious with β-carotene, vitamin K, vitamin C and is rich in glucosinolates. Because of its high contents in glucosinolates, kale is considered a candidate to protect against prostate cancer (42, 44).

The major group of glucosinolates in the kale sprouts is aliphatic glucosinolates. The most abundant glucosinolate is sinigrin, which will be converted to allyl isothiocyanate (AITC) during digestion. The chemopreventive effects of AITC on prostate cancer have been shown in many studies (59, 99-101). AITC induces cell cycle arrest and apoptosis, and inhibits HDAC activities and angiogenesis (59, 99-101). The second leading ITC in the kale sprouts is glucoiberin which will be converted to iberin by hydrolysis during consumption. Recently

the potential of iberin to prevent prostate cancer development has been suggested by gene expression profiling after treatment of primary prostate epithelial and stromal cells with iberin (102) in comparison to sulforaphane. Iberin induced mainly genes related to detoxification and cell cycle arrest. The comparison on between iberin and SFN showed that iberin is more effective on stromal cells than epithelial cells whereas SFN caused opposite effect (102).
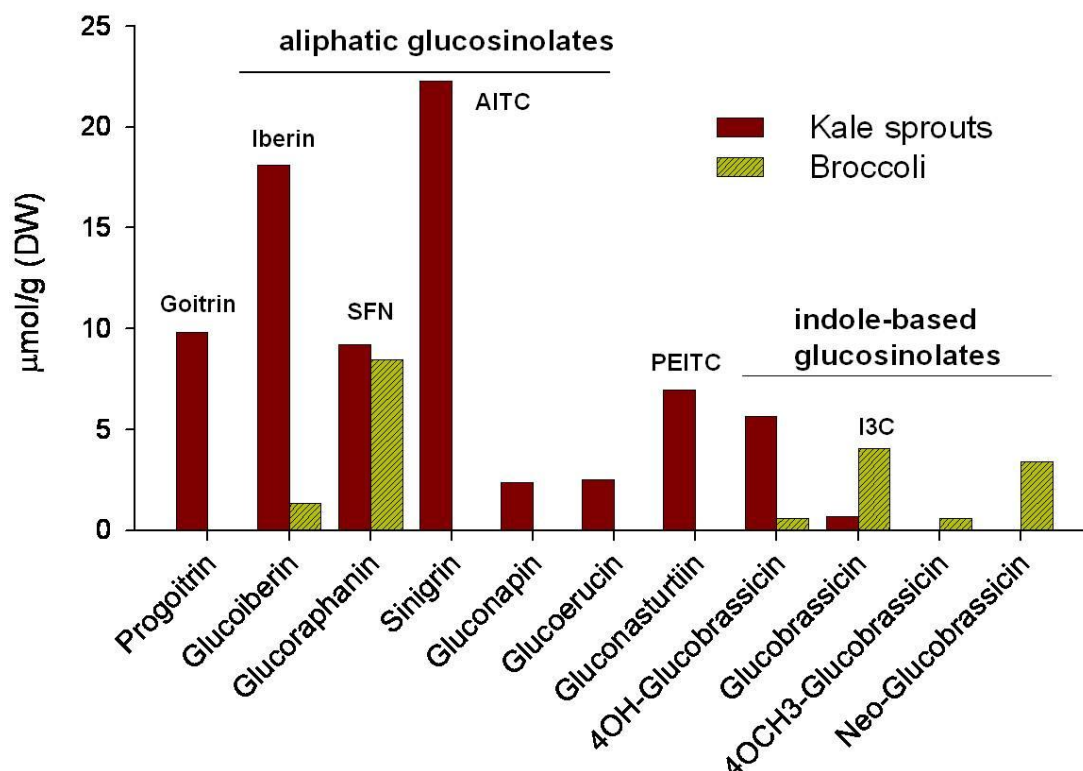
Fig. 5: Glucosinolate contents of kale sprouts compared to standard broccoli. The names of glucosinolate-derived products are indicated beside or above bars.

The glucoraphanin content in kale sprouts is relatively similar to broccoli. The role of SFN against prostate cancer development was described earlier (Chapter 1.2.2.2) Another ITC abundant in kale sprouts but almost not presented in broccoli is PEITC. Mechanisms to prevent prostate cancer development by PEITC include induction of caspase-mediated apoptosis, inhibition of EGFR signaling and induction of p21 by epigenetic modification (61, 103-106). When summing up the potential prostate cancer preventive effects of different types of ITCs abundantly present in combination in kale sprouts, kale sprouts can be regarded as an interesting novel potential chemopreventive cruciferous vegetables against prostate cancer progression.

1.5 Inhibition of angiogenesis as a promising target mechanism of cruciferous vegetables

As described above, ITCs have been shown to alter cancer development by multiple mechanisms. One mechanism, which was discovered relatively recently, is the inhibition and prevention of angiogenesis (107-109).

1.5.1 The process of angiogenesis

Angiogenesis, the formation of new vessels from pre-existing vasculature, usually occurs during development, is involved in tissue regeneration and in chronic inflammatory conditions (110). Cancer cells begin to promote angiogenesis early in tumorigenesis and consequently, angiogenesis is an important mechanism used by tumors to promote growth and metastasis (110). Tumor angiogenesis features are significantly different from physiological angiogenesis. Differences include aberrant vascular structure, altered endothelial-cell–pericyte interactions, abnormal blood flow, increased permeability and delayed maturation (111). Tumor angiogenesis is regulated by an intricate balance between pro-angiogenic factors and anti-angiogenic factors (111). Pro-angiogenic factors include oncogene-driven pro-angiogenic proteins, such as vascular endothelial growth factor (VEGF), basic fibroblast growth factor (bFGF), interleukin- 8 (IL-8), placenta-like growth factor (PlGF), transforming growth-factor-β (TGF-β), matrix metallo-proteinase (MMPs) and others (112-114). As a consequence of fast growing and large consumption of oxygen, environmental conditions of nearby tumor cells are usually hypoxic. Tumor-associated hypoxic condition activate hypoxia-inducible factor-1α (HIF-1α), which promotes up-regulation of several angiogeneic factors (112). These pro-angiogenic factors are secreted from the tumor cell itself, vascular endothelial cells, fibroblasts, invaded immune cells and inflammatory cells in or near the tumor site (Fig. 6). Triggering of angiogenesis also involves down-regulation of angiogenesis suppressor proteins, such as angiostatins, thrombospondin and prostate specific antigen in case of prostate cancer cell (112, 115). The orchestrated induction of pro-angiogenic factors and inhibition of anti-angiogenic factors initiates the degradation of vascular basement membrane and leads to proliferation and migration of vascular endothelial cells. New vascular structures are then covered with new basement membrane and connected with pre-existing vasculature. For further facilitated construction, endothelial cells are covered with pericytes (mural cells) (Fig. 6).
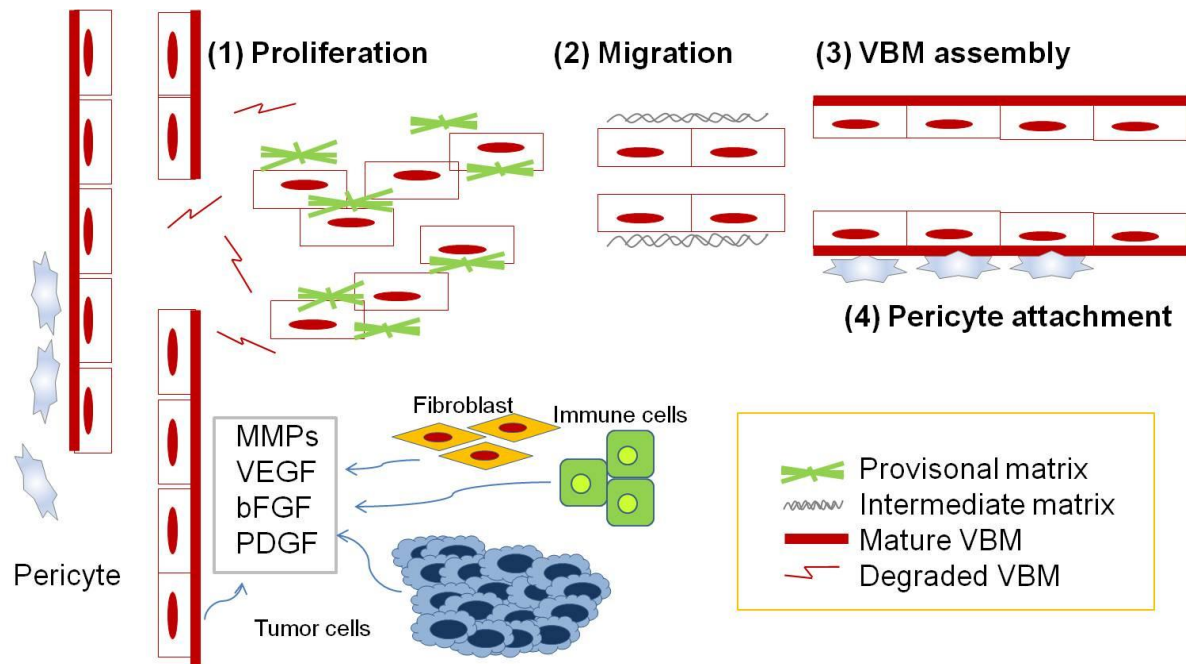
Fig. 6: New blood-vessel formation in cancer. Initiation of new blood vessels is started by release of proangiogenic factors such as VEGF, bFGF and PDGF secreted from the indicated cell types. These factors activate MMPs, which degrade the vascular basement membrane (VBN). Proliferation (1) and migration (2) of endothelial cells contribute to the construction of new blood vessel with reforming of VBM assembly (3) and pericyte coverage (4). Adapted from (116).

Evidence is accumulating to indicate that tumors cannot grow without being connected to the blood vessel system necessary for delivery of oxygen and nutrients to the tumor (112, 117). Therefore, targeting of angiogenesis for anti-tumor therapy has been investigated intensively in many clinical and laboratory studies (117). For example, targeting of VEGF has been validated in various types of human cancers (118-120). Different agents including antibodies, peptides and small molecules have been extensively investigated to block VEGF and some of these agents currently used in clinical trials (121-123).

1.5.2 Vascular normalization as an anti-angiogenic approach

During cancer progression un-organized vascular structure is rapidly formed. It permits the growth and invasiveness of cancer cells leading to metastasis to distant organs. Unlike normal angiogenesis which is tightly regulated by pro- and anti-angiogenic factors, cancer angiogenesis is structurally and functionally abnormal and caused a by persisting unbalance of these pro- and anti-angiogenic factors (Fig. 7)(124, 125).
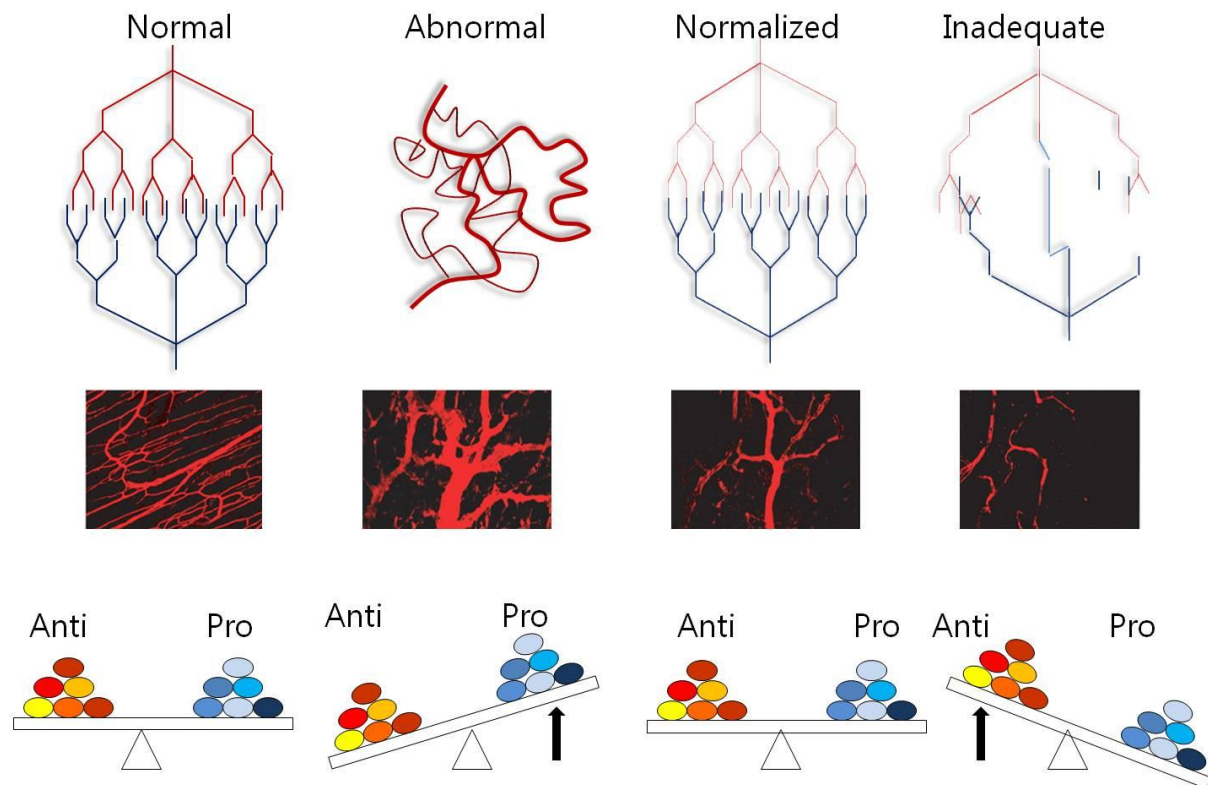
Fig. 7: Vascular normalization by anti-angiogenic therapy. Oppose to normal pathological angiogenesis tumor angiogenesis is structurally un-organized and functionally abnormal. The balance between anti- and pro- angiogenic factors is collapsed. Treatment with anti-angiogenic drugs promotes normalization of blood vasculature and function by re-balancing of anti- and pro-angiogenic factors. Adapted from (124)

The stabilizing pericytes that cover normal vessels are often absent or have an abnormal distribution among tumor vessels that show chaotic feature of mal-functional vessels (124). This leads to hemorrhage, characterized by leaky blood which leads to necrosis of tumor. Normalization of tumor vasculature has been proposed as a new rationale for anti-angiogenic therapy. Hellmann *et al.* found first evidence of drug-induced normalization of tumor blood vessels, and described that use of razoxane, a drug targeting VEGF signaling, normalized the characteristically chaotic tumor vasculature and prevented tumor hemorrhages, necrosis, blood-borne tumor-cell dissemination and metastasis (125, 126). The normalization of blood vessels could improve the availability of oxygen to cancer cells to prevent hypoxic conditions and angiogenesis as well as tumor growth (124). Suggested targets underlying the vascular normalization were restoring the balance between anti-angiogenic and pro-angiogenic factors to the levels of non-pathogenic angiogenesis.

1.5.3 ITCs as anti-angiogenic agents

Several reports have described effects of ITCs on endothelial cell functions essential for angiogenesis in HUVEC cells, human vascular endothelial cells, mainly targeting pro-angiogenic factors expression (100, 108, 127, 128). SFN was shown to inhibit microcapillary growth in an *ex vivo* model of angiogenesis with an IC_{50} value of 0.08 μM. Using human micro-vascular endothelial cells as a model, it inhibited cell migration and prevented hypoxia-induced up-regulation of VEGF, HIF1α, c-Myc, and MMP2 mRNA expression (109). SFN inhibited hypoxia-induced HIF-1α expression through activating JNK and ERK signaling pathways, but not Akt pathway which is involved in cell survival. Further, inhibition of HIF-1α resulted in decreased expression of VEGF in human tongue squamous cell carcinoma and prostate cancer DU145 cells (107).

The capillary-like tube structure formation (in vitro neovascularization) and migration (invasion potential) by HUVEC was inhibited significantly in the presence of PEITC at pharmacologically relevant concentrations (< 1μM). The PEITC-mediated inhibition of angiogenic features of HUVEC *in vitro* was associated with suppression of vascular endothelial growth factor (VEGF) secretion, down-regulation of VEGF receptor 2 protein levels, and inactivation of pro-survival serine-threonine kinase Akt (108). The PEITC treatment reduced migration by PC-3 human prostate cancer cells, which correlated with inactivation of Akt and suppression of VEGF, epidermal growth factor (EGF), and granulocyte colony-stimulating factor (G-CSF) secretion (108). Anti-angiogenic efficacy of AITC has also been shown. The pro-inflammatory cytokine TNFα is a mediator of nitric oxide synthesis. AITC inhibited tumor angiogenesis through down regulation of NO and TNFα production in B16F-10 melanoma cells (100). Another study with ATIC also supported previous findings that AITC significantly inhibited tumor proliferation and VEGF expression in tumor-bearing mice *in vivo*. It also reduced vessel sprouting and exhibited potent anti-angiogenic activity in the chorioallantoic membrane and cornea of the rat (129). These studies indicate that prevention or inhibition of angiogenesis represents an important mechanism contributing to the cancer preventive potential of ITCs.

1.6 Epigenetic regulation of gene expression through HDAC inhibition

Another mechanism which was recently identified as a contributor to the cancer preventive potential of ITCs and other sulfur-containing compounds is the inhibition of histone acetylation.

1.6.1 Regulation of histone acetylation

Chromatin is composed of histone octamers wrapped with DNA. Pairs of core histones (H2A, H2B, H3, H4) assemble to form an octamer which is positively charged and wrapped with DNA which is negatively charged. All four core histones have an amino-terminal tail. This is lysine rich and contains about half of the positively charged residues and most of the post-translational modification sites of the core histone. The modification of the structure of the N-terminal tails of histones — by acetylation/deacetylation — is crucial in modulating gene expression, as it affects the interaction of DNA with transcriptional regulation (130). Increased histone acetylation results in an 'opened' chromatin structure and genes are transcribed. Reduced histone acetylation causes 'closed' chromatin structure which shuts down the transcription (130).
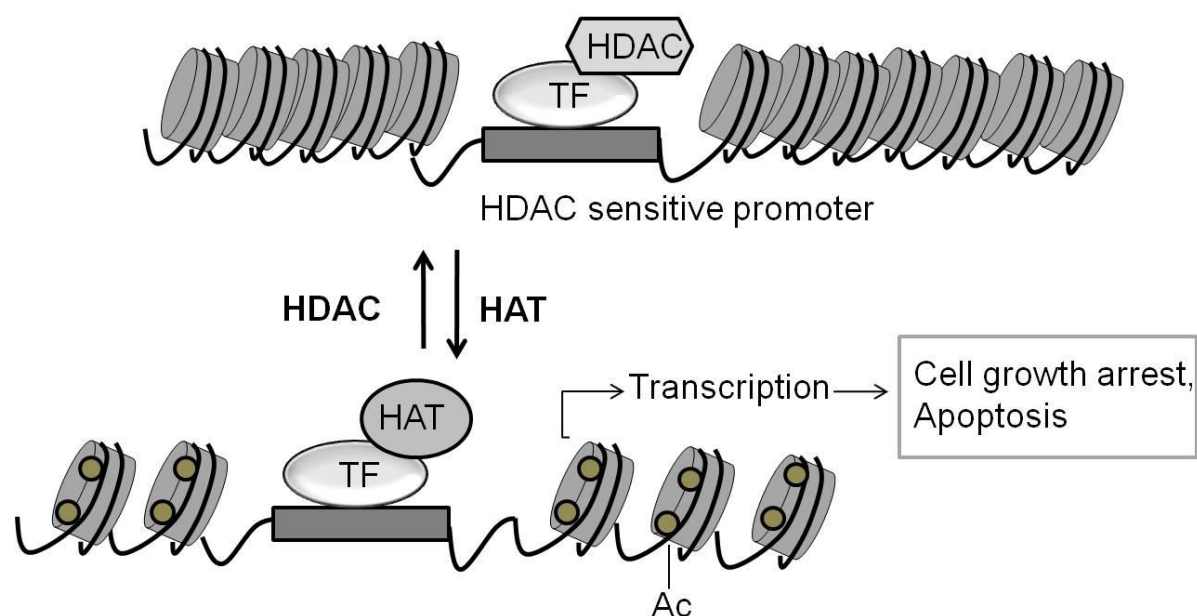
Fig. 8: Histone acetylation. Chromatin is composed of histone octamers wrapped with DNA. Histone acetylation leads to 'open' chromatin and increased transcription of genes which, in turn, leads to downstream effects that result in cell-growth arrest, differentiation and/or apoptotic cell death and, as a consequence, inhibition of tumors growth. Ac, acetyl group; HAT, histone acetyltransferase, HDAC; histone deacetylase. Modified from (130).

There are two key enzymes to modulate histone acetylation. Histone acetyl transferase (HAT) catalyze the addition of acetyl groups to lysine residues of the histone tails and histone deacetylase (HDAC) remove acetyl group from the histone tails (130) (Fig. 8).

HDACs can be divided into two subfamilies, that is the Zn^{2+}-dependent HDACs (classes I, II, and IV) and the NAD+-dependent sirtuins (SIRT) (class III). Class I, related to yeast RPD3 deacetylase, includes HDACs 1, 2, 3, and 8 that are primarily nuclear and ubiquitously expressed, whereas class II HDACs are primarily localized to the cytoplasm but are known to shuttle in and out of the nucleus. Class II HDACs are related to yeast Hda1 (histone deacetylase-1). This class is divided into class IIa, comprising HDACs 4, 5, 7, and 9; and class IIb, comprising HDACs 6 and 10, which contain two catalytic sites. Class III SIRTs are NAD+-dependent deacetylases that have been linked to regulation of caloric utilization in mammals and have non-histone proteins as substrates. Class IV is represented by HDAC 11, with limited identity to classes I and III, although it is most related to HDACs 3 and 8.

To date, many HATs have been identified and classified on the basis of a number of highly conserved structural motifs. GCN5, PCAF, HAT1 mainly acetylate lysines on the histone H3 and H4 tails. Mof and TIP60 are linked to acetylation of H4 and H2A. p300 and CBP acetylate substrate H2A and H2B. Likewise, different HATs have different preference to many substrates. However, target substrates of specific HATs are not yet clearly known. Also, direct cancer prevention by specific modulators of HAT has not been demonstrated so far (131).

1.6.2 Histone acetylation in prostate cancer

Alterations in aceylated histone levels may be important in the progression of prostate cancer. In contrast to the non-malignant prostatic cell lines, cancer cell lines like LNCaP, DU-145, and PC-3 possess histones which have reduced acetylation compared to non-malignant prostate epithelial cells (132). A previous study described that HDAC levels are up-regulated in prostate cancer compared to benign hyperplasia (133). Recently, several clinical trials and *in vivo* studies suggested therapeutic efficacy of HDAC inhibitors in many solid tumors (134-136). Inhibitors of HDAC, including suberoylanilide hydroxamic acid (SAHA), trichostatin (TSA), valproic acid, depsipeptide (137) and sodium butyrate, have been demonstrated to be effective against prostate cell lines and xenograft models (60, 138-142). For example, treatment of SAHA enhanced radiation-induced cytotoxicity in DU145 cell line and

synergistically induced cell death in the LNCaP and PC-3 cell lines in combination with zoledronic acid, a bisphosphonates anti-cancer drug (140). TSA can lead to TRAIL-induced cell death in prostate cancer xenograft model (139).

The beneficial effects of HDAC inhibitors (HDACi) in cancer treatment are mainly mediated through the activation of genes related to cell cycle arrest, apoptosis as well as angiogenesis (143). Inhibition of HDAC class I (HDAC1,2,3,8) and II (HDAC 4,5,6,7,9,10) showed changes of gene expression which have an impact on apoptosis and cell cycle arrest such as p21/Waf-1, cyclins, Bax and Bcl-2 (144, 145). Non-histone deacetylation-based gene repression involves deacetylation of transcription factors by HDACs. For example, increased p53 acetylation- induced transcriptional activity by inhibition of class III HDACs sirtuins has been reported (146-148).

1.6.3 Effects of ITCs on histone acetylation

Several isothiocyanates have been reported as HDAC inhibitors in various cancer models, including prostate cancer (101). SFN inhibits HDAC activity and increased histone acetylation status in BPH-1, LNCaP and PC-3 prostate cancer cell lines and in an *in vivo* xenograft model (143, 149). The HDAC inhibitory effect of SFN was also supported by a human intervention study with broccoli sprouts. Dietary broccoli sprouts led to an inhibition of HDAC activity and increased histone acetylation after ingestion in human peripheral blood cells (60). Phenylhexyl isothiocyanate, a synthetic isothiocyanate, also inhibited HDAC activity and increased p21 expression in prostate cancer (150) Phenylhexyl isothiocyanate induced HAT expression and remodeling of chromatins resulting in growth arrest in human leukemia cells (151). A study by Batra *et al*. showed that benzyl isothiocyanate-mediated inhibition of HDAC led to NF-κB turn off in a human pancreatic carcinoma cell line (152). Like these aliphatic isothiocyanate, indolic glucosinolate derivatives also presented potential to inhibit HDAC activity. DIM selectively induced proteasome-mediated degradation of class I histone deacetylases (HDAC1, HDAC2, HDAC3, and HDAC8) without affecting the class II HDAC proteins (153).

These reports indicated that the modification of histone acetylation by HDAC inhibition or modulation of HAT activity is a relevant mechanism for cancer chemoprevention by ITCs and other glucosinolate derivatives.

2. AIM OF THESIS

Cruciferous vegetables are rich in ITCs with a broad spectrum of chemopreventive activities in prostate cancer (154). The present thesis aimed to further investigate detailed mechanistic modes of action of two cruciferous vegetables, Se-enriched broccoli and kale sprouts.

The first aim of the thesis was to investigate the effects of Se-enriched broccoli on prostate cancer in *in vitro* and *in vivo* models. Targeted mechanisms included modulation of drug metabolism, anti-oxidant effects and anti-proliferative effects. Prior to evaluate these mechanisms we planned to optimize Se levels in broccoli by fertilization. Se and glucoraphanin contents were measured in broccoli and compared to the activities and expression of Se-containing antioxidant enzymes and phase II detoxifying enzymes in prostate cancer cell lines. Using optimized broccoli we further planned to compare the effects of Se-enriched broccoli in various preparations in an *in vivo* human prostate cancer xenograft model using LNCaP cells. In this study, endpoints to investigate were tumor growth and modulation of anti-oxidant and Phase II detoxifying enzymes in liver and tumor tissue. Furthermore, we intended to compare enzyme activities with levels of most abundant metabolites of broccoli constituents in mouse plasma, urine and feces samples.

The aim of the second part of this thesis was to elucidate the prostate cancer preventive potential of kale sprouts in the LNCaP xenograft model. Based on reported activities of ITCs as outlined above, we planned to focus our studies on putative anti-angiogenic and anti-necrotic modes of action. To detect effects on tumor vasculature, we intended to perform detailed histopathological analyses with H&E stained tissue sections. Further, we planned to use immunofluorescent staining of cryosections to detect endothelial and murals cells and to analyze pericyte coverage as a measure of vessel maturation. Mechanistic investigations were to include determinations of the expression of pro- and anti-angiogenic factors by quantitative RT-PCR and Western blotting. Another aspect of this study was to analyze the effect of kale sprout intervention on AR-mediated effects, including AR expression and PSA secretion. To clarify mechanistic details, concomitant incubations of LNCaP cells with kale sprouts in cell culture were planned.

Epigenetic alterations have been identified as a hallmark of prostate carcinogenesis. **The**

third part of the present thesis aimed to investigate the effects of kale sprouts on histone modifications. Alterations in acetylated histone levels may be important in the progression of prostate cancer. In this part of the project, we aimed to determine the effect of dietary kale sprouts on histone acetylation and tom investigate underlying mechanisms. Further we aimed to analyses functional consequences of increased histone acetylation, and planned to analyze p21 gene expression and phosphorylated H3 as a marker of mitotic cells by immunohistochemistry. To determine the relevance of these findings with kale sprouts for human ingestion, we planned a small pilot human intervention study with five female subjects.

Overall, we expected to gain insight into the potential use of Se-fertilized broccoli as a functional food for prostate cancer prevention. Another expected outcome was to clarify the potential role of kale sprouts to reduce prostate cancer growth, and to provide detailed information on mechanisms of cancer prevention, with a focus on anti-angiogenesis and histone modifications.

3 MATERIALS AND METHODS

3.1 Instruments

Name	Company
-20 ℃ freezer	Bosch, Stuttgart, Germany
20x gauge needle	BD, Heidelberg, Germany
-80 ℃ freezer	Thermo Fisher Scientific, Inc, Waltham, USA
Agfa Classic E.O.S developer	Siemens, Erlangen, Germany
Beckman Ultracentrifuge	Beckman, Fullerton, USA
Electrophoresis power supplier Power Pac	BioRad, Munich, Germany
Eppendorf Microfuge	Eppendorf, Hamburg, Germany
Eppendorf PCR Thermocycler	Eppendorf, Hamburg, Germany
Eppendorf spectrophotometer	Eppendorf, Hamburg, Germany
FACS Calibur	BD Biosciences, Heidelberg, Germany
Fluorimeter Cytoflour 4000	Perseptive Biosystems, Framingham, MA, USA
Fluorimeter SpectraMax Gemini XS	Molecular Devices, Munich, Germany
Gel Electrophoresis Chamber	BioRad, Munich, Germany
Forma Scientific Incubator	Thermo Fisher Scientific, Inc, Waltham, USA
Laminar Flow	Heraeus, Hanau, Germany
Microscope DM IL	Leica, Wetzlar, Germany
Nanodrop	Peqlab, Erlangen, Germany
Proteinmini-gel Wet Transfer System	BioRad, Munich, Germany
Real time PCR, iCycler Thermal Cycler IQ5	BioRad, Munich, Germany
Refrigerator	Liebherr, Biberach, Germany
Rocking Shaker	Eppendorf, Hamburg, Germany
SDS-PAGE electrophoresis equipment	BioRad, Munich, Germany
SpectraMax 340 PC	Molecular Devices, Munich, Germany
Tissue Lyser II	Qiagen, Hilden, Germany

3.2 Disposables

Name	Company
Cell culture flasks 75T and 25T	Falcon, BD, Heidelberg, Germany
Cell culture petri dishes	Falcon, BD, Heidelberg, Germany
Flat bottom 96well plates	Greiner, Frickenhausen, Germany
Photosensitive films	GE Healthcare, Fairfield, USA
Pipette tips	Gilson, Middleton, USA
Pipettes	Gilson, Middleton, USA
PVDF membrane	BioRad, Munich, Germany
RNase and DNase free filter tips	Starlba, Ahrensburg, Germany
Sterile pipettes	Falcon, BD, Heidelberg, Germany
Tuber	Falcon, BD, Heidelberg, Germany

3.3 Materials

3.3.1 Chemicals

Name	Company

5,5'-dithiobis(2-nitrobenzoic acid)	Sigma Aldrich, Taufkirchen, Germany
Adenosine diphosphate	Sigma Aldrich, Taufkirchen, Germany
Agarose	Sigma Aldrich, Taufkirchen, Germany
Ammonium persulfate	Sigma Aldrich, Taufkirchen, Germany
Avidin solution	DAKO, Hamburg, Germany
Blocking Solution	Invitrogen, Karlsruhe, Germany
Bradford reagent	BioRad, Hercules, USA
Broccoli extract powder	NIG, Magdeburg, Germany
Bromophenol blue	Sigma Aldrich, Taufkirchen, Germany
1-Chloro-2,4-dinitrobenzene	Sigma Aldrich, Taufkirchen, Germany
Chloroform	Sigma Aldrich, Taufkirchen, Germany
C 18 solid phase cartridges	Sigma Aldrich, Taufkirchen, Germany
Dextran	Sigma Aldrich, Taufkirchen, Germany
Dimethylsulfoxide	Sigma Aldrich, Taufkirchen, Germany
Dithiotheitol (DTT)	Sigma Aldrich, Taufkirchen, Germany
ECL Reagent (Western Lightning Plus)	PerkinElmer,Waltham, USA
EDTA	Sigma Aldrich, Taufkirchen, Germany
EGTA	Sigma Aldrich, Taufkirchen, Germany
Ethanol	Merck, Darmstadt, Germany
7-Ethoxyresorufin	Invitrogen GmbH, Karlsruhe
Ethidiumbromide	Sigma Aldrich, Taufkirchen, Germany
Fluorescein	Sigma Aldrich, Taufkirchen, Germany
G-Agarose/Salmon Sperm DNA beads	Millipore, Temecula, CA
Gelatin.	Sigma Aldrich, Taufkirchen, Germany
Glucose-6-phsophate-dehydrogenase	Sigma Aldrich, Taufkirchen, Germany
Glutathione reduced	Sigma Aldrich, Taufkirchen, Germany
Glutathione reductase	Sigma Aldrich, Taufkirchen, Germany
Glycerol	Sigma Aldrich, Taufkirchen, Germany
Hemoglobin	Sigma Aldrich, Taufkirchen, Germany
Hoechst dye	Sigma Aldrich, Taufkirchen, Germany
Hydrocortisone	Sigma Aldrich, Taufkirchen, Germany
Insulin	Sigma Aldrich, Taufkirchen, Germany
Isopropanol	Merck, Darmstadt, Germany
Kale sprouts powder	wHc service, Neuenbuerg, Germany
K_2HPO_4	Sigma Aldrich, Taufkirchen, Germany
KCl	Sigma Aldrich, Taufkirchen, Germany
LiCl	Sigma Aldrich, Taufkirchen, Germany
Matrigel™ Matrix Phenol Red-Free	BD biosciences, Heidelberg, Germany
Methanol	Sigma Aldrich, Taufkirchen, Germany
$MgCl_2$	Sigma Aldrich, Taufkirchen, Germany
Milk powder	Sigma Aldrich, Taufkirchen, Germany
MOPS	Serva, Heidelberg, Germany
3-(4,5-Dimethylthiazo-2-yl)-2,5-diphenyltetrazolium bromid	Sigma Aldrich, Taufkirchen, Germany
$NaHCO_3$	Sigma Aldrich, Taufkirchen, Germany
Na_2HPO4	Sigma Aldrich, Taufkirchen, Germany
Na_2SeO_3	Sigma Aldrich, Taufkirchen, Germany
Na_2SeO_4	Sigma Aldrich, Taufkirchen, Germany
$NADP^+$	Sigma Aldrich, Taufkirchen, Germany
PMSF	Sigma Aldrich, Taufkirchen, Germany
PVDF membrane	Bio-Rad, Munich, Germany
7- Pentoxyresorufin	Invitrogen Gmbh, Karlsruhe
SeMSC	Sigma Aldrich, Taufkirchen, Germany

Sodiumdodecylsulfate (SDS)	Serva, Heidelberg, Germany
Sucrose	Sigma Aldrich, Taufkirchen, Germany
Temed	Sigma Aldrich, Taufkirchen, Germany
Testosterone	Sigma Aldrich, Taufkirchen, Germany
Transferrin	Sigma Aldrich, Taufkirchen, Germany
Tris Base	Sigma Aldrich, Taufkirchen, Germany
Tris HCl	Sigma Aldrich, Taufkirchen, Germany
TRIzol	Invitrogen, Karlsruhe, Germany
Tween 20	Sigma Aldrich, Taufkirchen, Germany

3.3.2 Ready to use kit

Name	Company
BCA protein assay kit	Sigma Aldrich, Taufkichen, Germany
PSA Total Elisa Assay	DRG Diagnostics, Marburg, Germany
VECTASTAIN ABC Kit	Vector Laboratories, Inc., Burlingame, CA

3.3.3 Antibodies

Name	Company
GPX-1 (LF-MA0206)	AbFrontier, Seoul, Korea
GPX-3 (LF-MA0114	AbFrontier, Seoul, Korea
GPX-4 (LF-PA0055)	AbFrontier, Seoul, Korea
MnSOD (sc-30080)	SantaCruz, Heidelberg, Germany
β-actin (sc-4778)	SantaCruz, Heidelberg, Germany
TRx-R anti-serum	provided by Prof. John Arthur, Aberdeen, UK
AR (#3202)	Cell Signaling Technology, HD, Germany
TNFα (abb6671)	Abcam, Cambridge, UK
Angiostatin(ab2904)	Abcam, Cambridge, UK
Rat anti-mouse CD31 (#557355)	BD Bioscience, Heidelberg, Germany
Rabbit anti-mouse desmin (#ab15200-1)	Abcam, Cambridge, UK
Rabbit anti-rat-Alexa488 (#A21210)	Invitrogen, Karlsruhe, Germany
Biotinylated goat anti-rabbit (Dako, #X0590)	Vector Laboratories, Inc., Burlingame, CA, USA
anti-SMA-Cy3 (#C6198)	Sigma Aldrich, Taufkirchen, Germany
phospho-H3(ab5176)	Abcam, Cambridge, UK
p21 (sc-6246)	Santa Cruz Biotechnology, HD, Germany
HDACs ((#9928)	Cell Signaling Technology, HD, Germany
Sirt-1 (sc-15404)	Santa Cruz Biotechnology, HD, Germany
Ac-H3 (06-599)	Millipore, Temecula, CA, USA
Ac-H4 (06-598)	Millipore, Temecula, CA, USA
PCAF (#3378)	Cell Signaling Technology, HD, Germany

3.3.4 PCR reagents

Name	Company
dNTPs	Eppendorf, Hamburg, Germany
EvaGreen	Biotium, Inc., Hayward, USA

Fluorescein	Sigma Aldrich, Taufkirchen, Germany
Immolase Taq polymerase	Bioline, Inc., Taunton, USA
MgCl$_2$	Bioline, Inc., Taunton, USA
Moloney murine leukemia reverse transcriptase	Promega, Madison, USA
Nuclease free water	Qiagen, Hilden, Germany
Primers	Sigma Aldrich, Taufkirchen, Germany
Randeom Primers	Roche, Mannheim, Germany
RNase	Sigma Aldrich, Taufkirchen, Germany

3.4 Cell culture

3.4.1 Cell lines

Name	Company
BPH-1	Hayward et al., [12]
LNCaP	ATCC, Wesel, Germany
PC-3	DFKZ Tumorbank, Heidelberg, Germany

3.4.2 Cell culture reagents

Name	Company
RPMI1640 media	Invitrogen, Karlsruhe, Germany
Fetal bovine serum	PAA, Pasching, Austria
Transferin	Sigma Aldrich, Taufkirchen, Germany
Trypsin 0.25%	Invitrogen, Karlsruhe, Germany
Trypsin/EDTA	Invitrogen, Karlsruhe, Germany

3.4.3 Cell culture condition

BPH-1 cells, non-transformed human benign prostate hyperplasia were cultured in RPMI 1640 media, supplemented with 10% charcoal stripped fetal bovine serum (FBS) and 10 µg/ml hydrocortisone, 1 µg/ml insulin, 50 ng/ml testosterone and 5 µg/ml transferrin. The androgen-responsive prostate cancer LNCaP cell line, derived from a lymph node metastasis of human prostatic adenocarcinoma, was obtained from ATCC (Wesel, Germany). LNCaP cells were cultured in phenol red-free RPMI 1640 medium, supplemented with 10% FBS, 4.5 g/L glucose, 2.4 g/L HEPES, and 10 mM sodium pyruvate. PC-3 cells were cultured in RPMI 1640 medium with 10% FBS. All the media contained 10% antibiotics. The multiplex cell contamination test was conducted with all three cell lines.

For the experiments, 2 x 10^4 BPH-1 cells/ml , 5 x 10^4 LNCaP cells/ml , 4 x 10^4 PC3 cells/ ml were seeded for 24 hr (BPH-1, PC-3) to 48 hr (LNCaP) in 5% CO_2 incubator under humidified conditions at 37℃. Further detailed experimental conditions are described in

Chapter 3.6.3.

3.5 Animals

3.5.1 Animal strain

Name	Company
Balb-c nude mice	Charles River Laboratories, Sulzfeld, Germany

3.5.2 Animal diet

The diets for the animal study were prepared weekly in our laboratory. Broccoli sources were grounded by and electric mill and mixed with control diet powder (1:5) together with some water. Broccoli extract powder was mixed with control diet at a 1: 10 ratio. Diet sticks were dried for overnight at 30 ℃ under air blowing and stored at 4℃ until used. Detailed description about the broccoli sources are indicated below.

Broccoli Broccoli field cultivation (var. *Ironman*) was performed by a regional vegetable farmer (Gemüsebau Mohr, Frankental, Germany) between May and August 2008 according to the growers standard conditions (= standard broccoli). A subset cultivation received an additional foliar fertilization with selenium spray (300 L per ha of Na_2SeO_4 0.012%) (selenium-enriched broccoli). Directly after harvesting the broccoli was manually cut into florets and immediately transported to an industrial vegetable processor located nearby.

Frozen blanched broccoli: Florets from either standard or selenium-enriched broccoli were washed, blanched at 94℃ for 120 seconds, immediately frozen, packed and stored at -30℃ until use (Rheintal-Tiefkühlkost, Bobenheim-Roxheim, Germany).

Broccoli extract: Blanched frozen selenium broccoli florets were used to prepare extract (NIG, Magdeburg, Germany). Broccoli extract contains 443.99 μg/g sulforaphane and 201.97 μg/g sulforaphane-nitril.

Broccoli puree: Blanched frozen selenium broccoli florets were used for puree processing (Fruchtsaft Bayer, Ditzingen, Germany). Florets were thawed, puréed in a cutter with 125 ml lemon juice per kg florets, and filled in glasses. Sterilization was performed as follows:

continuous heating-up (40 min) to 121℃, temperature was held for 5 min. and cooled down to 98℃ in the course of 40 min. Then the glasses were allowed to cool down to room temperature. Broccoli puree was freeze-dried and stored at -20℃ until use.

3.5.3 LNCaP xenograft model

Pathogen-free, 5-6 week old male Balb-c nude mice were purchased and housed in sterile filter-capped microisolator cages, climate controlled room with a 12h light/12h dark cycle and provided with sterilized rodent diet and water. Animals were randomized and grouped with ten animals and started to feed with broccoli-contained diet or control diet one day before LNCaP cells injection until they sacrificed. In case of kale sprout diet, animals were started to feed one week before the cells injection. Mice were inoculated s.c. with 100 µl volume of 2×10^6 human prostate cancer LNCaP cells mixed with Matrigel™ Matrix Phenol Red-Free (BD biosciences, Heidelberg, Germany) 1:1 in both side of flanks. Tumor size, body weight and amount of food consumption were measured two times per week. After 7.5 - 9 weeks, animals were transferred to metabolic cages to collect urine and feces before they were euthanized through CO_2 asphyxiation in a numerical order across groups, equally representing the experimental groups throughout necropsy. After sacrifice, tumors, livers and lung tissues were excised, weighed, and stored in liquid nitrogen. Some parts of tissues were placed in phosphate-buffered formalin at room temperature for 48 h and then paraffin sections were prepared. Blood was collected by cardiac puncture and processed for separation of serum, plasma, and red blood cells.

3.6 Methods – Effects of Se-enriched broccoli

3.6.1 Fertilization of Se-enriched broccoli (Prepared by HIP)

3.6.1.1 Broccoli sprouts

Broccoli (*Brassica oleracea* var. *italica*) cv. Monaco was used to study the effects of Se-treatment at the seedling (liquid culture) and the adult plant stage (leaf application), respectively. 0.1g Monaco seeds were cultured in 100 ml half-strength MS (Murashige and Skoog) plant culture medium (pH 5.8) and treated with 50 µM sodium selenite or selenate for the last week before harvested. Seedlings were harvested at an age of 2 weeks and 3 weeks.

3.6.1.2 Broccoli florets

Three-month-old adult broccoli plants cultivated under field conditions and at a uniform stage of 2.0±0.5 cm head diameter were chosen. Sodium selenate solution was sprayed once onto the leaves (40 ml per plant, corresponding to 0, 2, or 20 mg Se per plant) after protection of soil and young broccoli heads from the direct contact with selenate by covering with aluminum foil. After 1 week, when the broccoli head diameter had reached 10 cm, they were harvested for further experiments.

3.6.2 Determination of enzyme activities in mouse liver tissue

3.6.2.1 Sample preparation

Approximately 150 mg of murine liver were homogenized in 3 ml of cold homogenizing buffer containing 60 mM Na_2HPO_4 and 60 mM $KHPO_4$, 0.5% KCl, 250 mM sucrose using a tissue grinder. Tissue homogenates were centrifuged at 9000 g for 10 minutes. Lipids were discarded using a cotton filter and supernatant were ultra-centrifuged for 45 minutes at 100.000 g. A clear supernatant was collected as cytosolic fraction. Microsome pellets were resuspended in 500 µl of microsome buffer (pH 7.4) containing 200 mM KH_2PO_4, 10 mM $MgCl_2$ as microsomal fraction. Eight livers in each group were used for the enzyme activity measurements. Glutathione *S*-transferase (GST), quinone reductase (QR), thioredoxin reductase (TrxR) activities and glutathione (GSH) were determined in cytosolic fractions and Cyp1A1/Cyp2B1 in microsomal fractions. Protein determination of both fractions was performed using the BCA method.

3.6.2.2 Cyp1A1/Cyp2B1

Cyp1A1 and Cyp2B1 activities were measured in liver microsomal fractions as described by Pohl and Fouts (155). Briefly, liver microsomal fraction (diluted 1:10 with phosphate buffer, contained 200 mM KH_2PO_4 and 10 mM $MgCl_2$, pH 7.4) was incubated with 2 µM 7-ethoxyresorufin (for Cyp1A1) or 25 µM 7-pentoxyresorufin (Cyp2B1), 1.3 mM $NADP^+$, 3.4 mM glucose-6-phosphate and 5 U glucose-6-phosphate dehydrogenase. Fluorescence intensity was measured at 37 ℃ every 30 s for 10 min using a microplate spectrofluorometer (Ex at 522 nm and Em at 580 nm). The results were quantified by using a resorufin standard (0.2 µM-20 µM) and normalized to the protein concentration. Reagents are indicated below.

Cyp1A1/Cyp2B1 activity determination	
Phosphate Buffer (KH_2PO_4, pH 7.4)	0.2 M
Glucose-6-phosphate	3.4 mM
Glucose-6-phosphate dehydrogenase	5 U
$NADP^+$	1.3 mM
7-Ethoxyresorufin	2 µM
7-Pentoxyresorufin	25 µM

3.6.2.3 NAD(P)H: quinone oxidoreductase (QR)

QR activity in mouse liver cytosolic fractions were determined by measuring the NADPH-dependent menadione-mediated reduction of MTT [3-(4,5-dimethylthiazo-2-yl)-2,5-diphenyltetrazolium bromid] to a blue formazan as described previously (156).

Liver cytosol was diluted 1:30 in homogenizing buffer and 50 µl each were used for determination. Plates were measured at 595 nm using a SpectraMax 340 PC plate reader every 30 s during a 15 min interval and the rate of MTT reduction was calculated using the molar extinction coefficient (ε) of 11,600 M^{-1} cm^{-1} and a path length of 0.75 cm. Values were normalized to protein content. Reagents are indicated below:

QR	
BSA	0.08 %
MTT	0.87 mM
Tris/HCl buffer pH 7.4	20 mM
Tween 20	0.01%
FAD^+	5 µM

NADP$^+$	23 µM
Glucose-6-phosphate	0.75 mM
Glucose-6-phosphate dehydrogenase	1.5 U
Menadione	38 µM

3.6.2.4 Glutathione *S*-transferase (GST)

GST activity was determined using cytosolic liver protein supernatants as source of GST and CDNB (1-chloro-2,4-dinitrobenzol) as described previously (157). The mix was incubated briefly at 37 ℃. Liver cytosols were diluted 1:300 in homogenizing buffer and 20 µl (approximately 30-80 µg protein) each were used for determination. The absorbance was recorded at 340 nm with a SpectraMax 340 PC plate reader at 37 ℃, using its kinetic mode at 15 s intervals during a 15 min reaction time. The rate of conjugated CDNB formation was calculated using the extinction coefficient (ε) 9.6 mM^{-1} cm^{-1} and normalized to protein concentration. Reagents are indicated below:

GST	
KH$_2$PO$_4$ / K$_2$HPO$_4$ buffer, pH 6.5	90 mM
CDNB	0.9 mM
GSH	2.25 mM

3.6.2.5 Thioredoxin reductase (TRx-R)

TRx-R activity was measured in cytosolic fractions *via* the NADPH-dependent reduction of DTNB [5,5-dithio*bis*-(2-nitrobenzoic acid] to 2-nitro-5-thiobenzoic acid at 412 nm. TR-independent reduction of DTNB was controlled by parallel incubations in the presence of the TR-inhibitor auranofin (158). Liver cytosolic fractions (40-90 µg) were incubated in the presence of auranofin (5 µM) or buffer. Plates were incubated at 37 ℃ for 20 minutes. The absolute TRx-R activity was calculated using the difference in absorbance of auranofin (total reductase enzymatic activity) and presence of auranofin (total reductase activity in absence of TRx-R activity). Kinetics was determined over 15 minutes taking one measure every 30 seconds at 412 nm. The rate of DTNB reduction was calculated using the molar extinction coefficient of 13,600 M^{-1} cm^{-1} and normalized to protein content. Reagents are indicated below:

TRx-R	
KH_2PO_4 buffer, pH 7.4	70 mM
EDTA	1.5 mM
BSA	0.004 %
DTNB	0.3 mM
NADPH	0.2 mM

3.6.2.6 Glutathione (GSH)

Determination of GSH was performed as described previously by Tietze *et al*. (159), using 5,5-dithiobis-(2-nitrobenzoic acid) (DTNB), Ellman's reagent. Cytosol was deproteinized using 1 % sulfosalicylic acid (SSA). One volume of cytosol was mixed with 2 volumes of 1 % SSA and centrifuged for 5 minutes at 10.000 rpm. After deproteinization, cytosol was diluted 1:10 in water and 40 µl was used for the assay. GSH standards (from 800 pmol to 20 pmol) were prepared from 100 µM GSH stock solution (diluted in water). Five minute kinetics were determined taking one measure every 30 seconds at 412 nm using a SpectraMax 340 PC plate reader. GSH content was calculated using the standard curve (10 µM to 0.25 µM GSH in stock buffer) and normalized to protein concentration measured prior to deproteinization. Reagents are indicated below:

GSH	
Tris-HCl, pH 7.4	16 mM
Glucose- 6- phosphate	0.61 mM
$NADP^+$	18.7 µM
DTNB	0.57 mM
Glucose-6-phosphate dehydrogenase	0.26 U
Gluthatione Reductase	0.24 U
Na_2HPO_4	125 m
Na-EDTA	6.3 mM

3.6. 3 Determination of protein expression by Western blotting

BPH-1 (2.5×10^4 cells/ml), PC-3 (4×10^4 cells/ml) and LNCaP (5×10^4 cells/ml) cells were seeded in 30 cm petri dish (30 ml per dish) and grown over night for BPH-1 and PC-3 or grown for two days for LNCaP. Cells were treated with extracts of freeze-dried sprouts or broccoli florets. Total cells were destroyed by using SDS lysis buffer containing 62.5 mM

Tris/HCl (pH 6.8), 2 % SDS, 10 % glycerin, 1 mM DTT, proteinase inhibitor and phosphatase inhibitor. Total lysates were boiled at 98 °C for 10 min and 30 µg of proteins were loaded to SDS-PAGE. After gel electrophoresis and transfer to PVDF membranes, membranes were incubated in 5% non-fat dried milk/TBS-T for 1 hr at room temperature before incubation with primary antibodies against GPX-1,3,4 (1:10000), TR (1:1000) and MnSOD (1:1000) over night at 4°C, followed by incubation with secondary antibodies for 2 hrs at room temperature. After washing three times with PBS-T, protein expression was detected by using ECL methodology on x-ray film.

3.6.4 Determination of sulforaphane metabolites in mouse plasma, urine and feces (performed and provided by Johanna Hauder, DFA)

Sample preparation: Plasma and urine samples for the analysis of glucoraphanin metabolites were prepared by first spiking the samples with the internal standards d_8-SFN and d_8-SFN-NAC and homogenizing for 1 min. Proteins were then precipitated from plasma using pre-cooled trifluoroacetic acid. After homogenization samples were centrifuged and the supernatant was subsequently loaded onto Discovery® C_{18} solid phase extraction cartridges (100 mg, 1 mL; Supelco, Taufkirchen, Germany) which had been conditioned with methanol and equilibrated with formic acid (0.1 % in water) previously. After a washing step with methanol/water (5/95; v/v), the metabolites were eluted with ACN/water (90/10; v/v), evaporated to dryness under a nitrogen stream and dissolved in formic acid (0.1 % in water). Ten microliters of each sample were injected into the HPLC-ESI(+)-MS/MS system. A mobile phase gradient starting from 100% aqueous formic acid (0.1 % formic acid in water), decreasing up to flux 100 % of the 0.1 % formic acid in acetonitrile phase within 15 min and keeping at the organic phase for 5 min was used.

HPLC-MS/MS analyses were carried out on a Finnigan Surveyor Plus HPLC system (Thermo Electron Corporation, Waltham, USA) equipped with a triple-quadrupole mass spectrometer (TSQ Quantum Discovery; Thermo Electron Corporation, Waltham, USA). For glucoraphanin metabolites, electrospray ionisation in positive mode and selected reaction monitoring (SRM) were selected. Analyses were performed on an Aqua C_{18} column (5 µm, 12.5 nm, 150 x 2 mm) as stationary phase equipped with a guard column (C_{18}, 4.0 x 2.0 mm; both from Phenomenex, Aschaffenburg, Germany). Mobile phase consisted of 0.1 % formic acid in water (A) and 0.1 % formic acid in ACN (B). It was operated with a flow rate of 0.2

mL/min and injection volume was 10 µL. UV detector wavelength was set at $\lambda = 210$ nm in this case. Quantifications of all metabolites in plasma and urine samples were performed by comparing the peak areas of characteristic mass fragments of analyses and standards.

3.6.5 Elemental analysis of total selenium (performed and provided by Fu-Chou Hsu, HIP)

Broccoli samples were dried at 65°C in an oven for 3 days. 20 mg of samples was incubated in 2 ml HNO_3 at room temperature for 3 days, 95°C for 3 hours and followed by addition of 1 ml H_2O_2 (30 %) and further incubation at 95°C for 1 hour. Thereafter, samples were diluted with double-distilled water to 10 ml. Total element contents were determined by inductively coupled plasma atomic emission spectrometry (ICP-AES, Thermo Elemental, Dreieich, Germany) using an IRIS Advantage Duo ER/S. Se was determined using the 196-nm line.

3.7 Methods-Anti-angiogenic potential of kale sprouts

3.7.1 RNA isolation, reverse transcription and quantitative real time PCR

RNA of prostate cancer LNCaP xenograft was isolated with TRIzol® following the manufacturer's instructions. 1 µg of total RNA was reverse transcribed with M-MLV (Moloney Murine Leukemia Virus) reverse transcriptase. mRNA expression of p21, HAT1, CBP, p300, PCAF was quantified by using iCycler iQ™ Real-Time PCR Detection System and normalized to the expression levels to the housekeeping gene HPRT-1 or β-actin. PCR reaction was performed in by standard procedures. The PCR program was consisted of denaturation step 95 °C for 10 min followed by 40 cycles of 30s at 95 °C, 15 s at individual annealing temperatures of primers and 45 s at 72 °C elongation step. After final elongation step for 10 min at 72 °C, product formation was confirmed by melting curve analysis (55 °C – 96 °C). Primer sequences are described below.

Primer Sequences for quantitative Real Time PCR

Gene	Species		Sequence 5'- 3'	T°[C]
PSA	Human	For	gtgcttgtggcctctcgt	60
		Rev	agcaagatcacgcttttgttc	
AR	Human	For	atggtgagcagagtgcccta	61

		Rev	gtggtgctggaagcctctcct	
uPA	Human	For	ggactacagcgctgacacg	61
		Rev	ggcaggcagatggtctgtat	
MMP-2	Human	For	ataacctggatgccgtcgt	62
		Rev	aggcacccttgaagaagtagc	
MMP-9	Human	For	gaaccaatctcaccgacagg	61
		Rev	gccacccgagtgtaaccata	
VEGF-c	Human	For	agtgtcaggcagcgaacaaga	63
		Rev	cctcctgagccaggcatctg	
TNFa	Human	For	cagcctcttctccttcctgat	60
		Rev	gccagagggctgattagaga	
HPRT-1	Human	For	tgaccttgatttattttgcatacc	60
		Rev	cgagcaagacgttcagtcct	
Actin	Human	For	ccatcatgaagtgtgacgtgg	62
		Rev	gtccgcctagaagcatttgcg	
FGFb	Mouse	For	cggctctactgcaagaacg	60
		Rev	tgcttggagttgtagtttgacg	
Prox-1	Mouse	For	cgacatctcaccttattcagga	60
		Rev	ttgcctttttcaagtgattgg	
TNFa	Mouse	For	tcttctcattcctgcttgtgg	61
		Rev	ggtctgggccatagaactga	
HPRT-1	Mouse	For	tcctcctcagaccgctttt	59
		Rev	cctggttcatcatcgctaatc	

3.7.2 Detection of AR, TNFα, angiostatin by Western blotting

Approximately 10 mg of LNCaP xenograft tumor tissue was homogenized by Tissue lyser II with 150 µl of pre-heated SDS lysis buffer containing 62.5 mM Tris/HCl, pH 6.8, 2 % SDS, 10% glycerol, 1 mM DTT, proteinase and phosphatase inhibitor tablets. Total lysates were boiled at 98 °C for 10 min, and 30 µg of proteins were loaded to SDS-PAGE gels. After electrophoresis and transfer to PVDF membranes they were incubated in 5% non-fat dried milk/TBS-T for 1 hr at room temperature before incubation with primary antibodies against AR, TNFα and angiostatin over night at 4 °C, and secondary antibodies at room temperature for 2 hrs. ECL was used for protein detection by standard methods.

3.7.3 Chromatin Immunoprecipitation-PSA promoter

Approximate 50 mg of frozen tissue was crushed with liquid nitrogen. Chromatin immunoprecipitation assays were conducted as described previously (160). Briefly, cells were cross-linked at room temperature for 10 min by using 1% formaldehyde containing 20 mM Na-butyrate, protease inhibitor and 1 mM PMSF. After sonication, the resulting soluble

chromatin was diluted 1:10 with dilution buffer and immunoprecipitated by incubation with the AR antibody overnight at 4℃ with rotation. The following day, chromatin-antibody complexes were isolated from solution by incubation with protein G-Agarose/Salmon Sperm DNA beads for 2 hr at 4 ℃. The sepharose-bound immune complexes were washed two times with high salt buffer, for two times, LiCl buffer for one time and rinse with TE for two times. The immune complexes were eluted from beads with an elution buffer (1% SDS and 0.1 M NaHCO$_3$) followed by DNA extraction. DNA samples from chromatin immunoprecipitation preparations were analyzed by real-time PCR using an iCycler iQ™ Real-Time PCR Detection System as described previously. The primers and probes were as following: human PSA enhancer forward (5´-GCCTGGATCTGAGAGAGATATCATC-3´), reverse (5´-ACACCTTTTTTTTTCTGGATTGTTG-3´); human PSA promoter forward (5´-CCTAGATGAAGTCTCCATGAGCTACA-3´), reverse (5´-GGGAGGGAGA-GCTAGCACTTG-3´); human GSTP1 promoter forward (5´-GACCTGGGAAAGAGGGAAAG-3´), reverse (5´-CCCCAGTGCTGAGTCACG-3´).

3.7.4 Quantification of PSA levels by ELISA (performed and provided by Dr. Achim Bub, MRI Karlsruhe)

For the determination of PSA secretion, 25 ul of mouse serum was subjected to the PSA Total Elisa Assay according to the manufacturer's instructions.

3.7.5 Measurement of Hb concentration in tumor xenografts

15 mg of xenograft was homogenized with 1 ml PBS. Hemoglobin (Hb) concentration was measured by using Elisa Spectramax at a wave length of 410 nm. Hb standard curve was used for the calculation.

3.7.6 Immunohistochemistry-CD31$^+$, α-SMA, AR (performed and provided by Mattthias Wieland, DKFZ)

LNCap xenograft cryosections (8 µm) were fixed for 10 min in ice-cold methanol and washed afterwards two times in PBS. In case of the CD31-α Desmin co-staining, sections were blocked with Avidin solution for 10 min at RT, washed 3 times in TBS-T, 0.1 % for 3

min, blocked with Biotin solution for 10 min at RT, and washed again. All sections were blocked using the Zymed Blocking Solution. Primary antibody incubation with rat anti-mouse CD31, diluted 1:100 in Blocking Solution alone, or in case of the CD31-α Desmin co-staining together with a 1:200 diluted rabbit anti-mouse αDesmin antibody, was performed over night at 4 °C. Sections were washed twice with TBS-T 0.1% for 5 min followed by incubation with 1:500 diluted rabbit anti-rat-Alexa488 antibody alone, or for the CD31-α Desmin staining together with 1:200 diluted biotinylated goat anti-rabbit antibody, for 45 min at RT. After three washing steps with TBS-T 0,1 % for 5 min, sections for the CD31-α SMA staining were stained using a 1:100 dilution of the directly labeled anti-SMA-Cy3 antibody for 1 h at room temperature. In case of the CD31-α Desmin staining sections were incubated with 1:250 diluted Streptavidin-Alexa546 in PBS for 30 min at RT. After the antibody incubations sections were washed in TBS-T 0.1 % and nuclei were counterstained by Hoechst dye in a 1:5000 dilution. Finally, sections were mounted with fluoro-mount medium.

3.7.7 Immunohistochemistry- androgen receptor

Paraffin embedded sections were irrigated with xylol and ethanol. Endogenous peroxidase was inactivated by incubation in 0.3 % H_2O_2. 50 µl of blocking serum added to 5 ml TBS was used for blocking. Incubation with AR antibody was performed overnight (1:200, Santa Cruz Biotechnology, Heidelberg, Germany). After washing three times with TBS-T, VECTASTAIN ABC Kit for rabbit IgG was added for 30 min. Development was carried out by diaminobenzidine tetrahydrochloride (DAB) and H_2O_2. For H&E staining, paraffin embedded tissue sections were stained with basic dye hematoxylin and alcohol based acidic eosin.

3.7.8 Gelatin zymography

100 µg of total tumor cell lysate was mixed with sample buffer and incubated for 10 min at room temperature. Samples were loaded to 8 % SDS-PAGE containing 1 mg/ml gelatin. After electrophoresis, gels were washed and rinsed with renaturing buffer (2.5 % Triton X-100 in water) for 1 hr at room temperature followed by incubation with developing buffer (containing 50 mM Tris base, 50 mM Tris-HCl, 0.2 mM NaCl, 5 mM $CaCl_2$, 0.02 % Brij 35) for 48 hrs at 37 °C. After staining with 0.5 % Coomassie blue R-250, gels were washed with

destaining solution containing 50 % methanol and 10 % acetic acid. Areas of gelatinase activity were detected as clear bands against blue-stained gelatin background.

3.8 Methods- Histone modification by kale sprouts

3.8.1 Determination of mitotic cells by immunohistochemistry

Paraffin embedded sections were irrigated with xylol and ethanol. Endogenous peroxidase was inactivated by incubation in 0.3 % H_2O_2. After 1 hr blocking with serum, posphoH3 antibody (1:200 dilution in TBS) was incubated overnight. After washing three times with TBS-T, 1:200 diluted VECTASTAIN ABC Kit for rabbit (PK-6102) was added for 30 min. Development was carried out by diaminobenzidine tetrahydrochloride (DAB) and H_2O_2.

3.8.2 Immunoblotting

The same method to prepare samples was used as previously described in Chapter 3.7.2. About 20-30 µg of total cell lysates were used for the western blot analysis, as described previously (chapter 3.7.2). Primary antibodies against phospho-H3 (1:2000), p21 (1:1000), HDACs (1:1000) and Sirt-1 (1:1000) were incubated over night at 4 ℃ followed by secondary antibodies (1:5000) incubation at room temperature for 2 hrs. ECL was used for protein detection by standard methods.

3.8.3 Detection of histone acetylation

Acid extracted histone samples, as described previously (161), were separated by electrophoresis. Ac-H3, Ac-H4 antibody from Upstate was blotted to detect histone acetylation and total H4 was used as a loading control in the same membrane. Membranes were incubated with primary antibodies (1:1000 diluted in PBS) over-night at 4 ℃ followed by secondary antibody incubation for 2 hrs at room temperature. ECL was used for detection by standard methods.

3.8.4 Nuclear protein extraction and PACF expression assay

About 20 mg of tumors were homogenized using a Tissue lyser II with buffer A, containing 10 mM HEPES (pH 7.9), 1.5 mM $MgCl_2$ 10 mM KCl, 0.5 mM DTT and 0.2 mM phenylmethylsulfonyl fluoride (PMSF). After incubation for 10 min on ice, the lysates were centrifuged and pellets were re-suspended in cold buffer C, containing 20 mM HEPES (pH 7.9), 20 % glycerol, 420 mM NaCl, 1.5 mM $MgCl_2$, 0.2 mM EDTA, 0.5 mM DTT, and 0.2 mM PMSF and incubated for 20 min on ice. After a vigorous vortex, nuclear fractions were centrifuged and collected. 30 µg of nuclear protein was used for Western blotting. Anti-PCAF antibody was used to detect nuclear PCAF protein expression. Membranes were incubated over-night at 4°C with PCAF antibody (1:1000 dilution) followed by secondary antibody incubation for 2 hrs at room temperature. ECL was used for detection by standard methods.

3.8.5 HDAC activity measurement (performed and provided by Julia Wagner, University of Freiburg)

HDAC activity was determined using the Fluor-de-Lys substrate. Incubations were performed at 37°C for 10 min with tumor nuclear extracts, and the HDAC reaction was initiated by the addition of Fluor-de-Lys substrate (162). After 10 min, Fluor-de-Lys Developer was added, and the mixture was incubated for another 10 min at room temperature. Fluorescence was measured using a Spectra Max Gemini XS fluorescent plate reader (Molecular Devices), with excitation at 360 nm and emission at 460 nm.

3.8.6 RNA isolation, reverse transcription and quantitative real time PCR

Isolation of RNA and PCR conditions were as described previously in Chapter 3.7.1. Primer sequences are listed below.

Gene	Species		Sequence 5'- 3'	Temp. (°C)	Size (bp)
HAT1	Human	For	ggt tga ttc gtc ctt cct ca	61	150
		Rev	tta gtt caa ttg ctg tgt tgg tg		
CBP	Human	For	cag agc gga tca tcc atg act	61	348
		Rev	gct tct cca tgg tgg cat ac		
P300	Human	For	cct gag tag ggg caa caa ga	60	353
		Rev	gtg tct cca cat ggt gct tg		

PCAF	Human	For	gcc tcc tcc aga aca tga ga	61	69
		Rev	ctc ttc tgg act tga ggc aaa		
p21	Human	For	ctc cgt cag aac cca tgc	62	155
		Rev	agt ggt gtc tcg gtg aca aa		
HPRT-1	Human	For	tgaccttgatttattttgcatacc	60	102
		Rev	cgagcaagacgttcagtcct		
β-Actin	Human	For	ccatcatgaagtgtgacgtgg	62	293
		Rev	gtccgcctagaagcatttgcg		

3.8.7 Chromatin Immunoprecipitation – p21, PCAF promoter

The procedure of ChIP assay was performed as previously described in Chapter 3.7.3. The primers and probes were as following: human p21 promoter (forward primer, 5'-GGTGTCTAGGTGCTCCAGGT-3'; reverse primer, 5'- GCACTCTCCAGGAGGACACA-3'), PCAF promoter (forward primer, 5'-CACCCAGAAACGAATCCTGT-3'; reverse primer, 5'-TGTTTGAAAGTGCTGGTTGC-3').

4 RESULTS

4.1 Se-enriched broccoli as a functional food for prostate cancer prevention (Induction of detoxifying and antioxidant enzymes)

Since previous publications demonstrated chemopreventive effects of broccoli and selenium in prostate cancer by induction of antioxidant and Phase 2 enzymes, our first aim was to investigate the effects of Se-enriched broccoli on these mechanisms in prostate cancer cells *in vitro* and *in vivo*.

We first compared the spectrum of bioactivities of experimental broccoli extracts in combination with selenium *in vitro* in cultured prostate (cancer) cell lines in comparison to SFN and in/organic selenium. We further performed an *in vivo* intervention study with Se-fertilized broccoli in various preparations in nude mice bearing human prostate cancer xenografts. Enzyme activities were analyzed in liver and tumor samples and compared to selected metabolite levels in plasma, urine and feces samples determined by collaboration partners (described in 3.6.7).

4.1.1 Combination of Se and broccoli extract *in vitro*

Before we investigated the effects of Se-fertilized broccoli preparations, we first investigated the effects of SFN, Na_2SeO_3, Na_2SeO_4 and SeMSC as reference compounds and a special broccoli extract (containing free SFN) alone and in combination with SeMSC, as indicated in Table 3. An immortalized prostate cell line (BPH-1) and two prostate cancer cell lines (LNCaP, PC-3) were treated with SFN in comparison to selected Se sources for 5 days. SFN induced both QR and Trx-R activity in all three cell lines, with similar potential to induced QR and Trx-R activity in BPH-1 and LNCaP cells. In comparison to the two other cell lines, PC-3 cells were less responsive to SFN with respect to Trx-R induction. Both inorganic and organic Se sources at a dose of 25 nM potently induced Trx-R activity by 1.5 to 4.9 fold in all three cell lines, but had no effect on QR activity. Trx-R inducing potential increased in the order of Na_2SeO_3 > SeMSC > Na_2SeO_4.

RESULTS

Table 3. Induction of QR and Trx-R in prostate cancer cell lines by single and combined treatment with SFN/broccoli extract and organic/anorganic selenium

	BPH-1		LNCaP		PC-3	
	QR[a] (fold ind.)	Trx-R (fold ind.)	QR (fold ind.)	Trx-R (fold ind.)	QR (fold ind.)	Trx-R (fold ind.)
Control	1.0 ± 0.02	1.0 ± 0.02	1.0 ± 0.02	1.0 ± 0.02	1.0 ± 0.01	1.0 ± 0.02
Pure compounds						
SFN (1 µM)	$1.4 \pm 0.01^{\dagger}$	$1.5 \pm 0.03^{\dagger}$	$1.6 \pm 0.07^{\dagger}$	$1.5 \pm 0.04^{\dagger}$	$1.4 \pm 0.04^{\dagger}$	$1.1 \pm 0.03^{\dagger}$
SFN (4 µM)	$2.1 \pm 0.01^{\dagger}$	$2.5 \pm 0.1^{\dagger}$	$2.2 \pm 0.07^{\dagger}$	$1.9 \pm 0.04^{\dagger}$	2.1 ± 0.01	$1.3 \pm 0.1^{\dagger}$
Na_2SeO_3 (25 nM)[b]	1.1 ± 0.1	$4.9 \pm 0.05^{\dagger}$	1.1 ± 0.04	$4.1 \pm 0.1^{\dagger}$	1.0 ± 0.1	$3.5 \pm 0.1^{\dagger}$
Na_2SeO_4 (25 nM)	1.1 ± 0.05	$2.6 \pm 0.3^{\dagger}$	1.1 ± 0.05	$1.7 \pm 0.05^{\dagger}$	1.0 ± 0.05	$1.5 \pm 0.05^{\dagger}$
SeMSC (25 nM)	1.1 ± 0.07	$4.1 \pm 0.1^{\dagger}$	1.0 ± 0.04	$2.6 \pm 0.1^{\dagger}$	1.0 ± 0.07	$1.8 \pm 0.04^{\dagger}$
Combination of Broccoli extract with SeMSC (Se)						
Br-Ex[c]	$1.9 \pm 0.04^{\ddagger}$	$1.3 \pm 0.02^{\ddagger}$	$2.5 \pm 0.05^{\ddagger}$	$1.7 \pm 0.06^{\ddagger}$	$2.1 \pm 0.05^{\ddagger}$	$1.1 \pm 0.02^{\ddagger}$
Br-Ex+Se (2 nM)	$1.9 \pm 0.09^{\ddagger}$	$2.4 \pm 0.03^{\ddagger}$	$2.4 \pm 0.12^{\ddagger}$	$1.7 \pm 0.07^{\ddagger}$	$2.0 \pm 0.1^{\ddagger}$	$1.5 \pm 0.02^{\ddagger}$
Br-Ex+Se (20 nM)	$1.8 \pm 0.05^{\ddagger}$	$5.6 \pm 0.08^{\ddagger}$	$2.1 \pm 0.06^{\ddagger}$	$2.4 \pm 0.09^{\ddagger}$	$1.7 \pm 0.07^{\ddagger\S}$	$1.3 \pm 0.02^{\ddagger}$
Br-Ex+Se (100 nM)	$1.7 \pm 0.03^{\ddagger\S}$	$8.9 \pm 0.12^{\ddagger\S}$	$2.2 \pm 0.11^{\ddagger}$	$4.6 \pm 0.18^{\ddagger\S}$	$1.6 \pm 0.08^{\ddagger\S}$	$2.1 \pm 0.03^{\ddagger}$

[a] Specific activities of solvent control: BPH-1 QR 25.2 ± 0.2 nmol/min/mg; Trx-R 2.6 ± 0.2 nmol/min/mg; LNCaP QR 23.1 ± 0.6 nmol/min/mg, Trx-R 6.2 ± 0.3 nmol/min/mg; PC-3 QR 1.9 ± 0.2 nmol/min/mg, Trx-R 3.1 ± 0.2 nmol/min/mg
[b] Se intervention at 25 nM is equivalent to 4.3 ng/ml of Na_2SeO_3, 4.7 ng/ml of Na_2SeO_4 and 5.4 ng/ml of SeMSC
[c] Br-Ex: broccoli extract (625 µg/ml, equivalent to 2.8 µM SFN), Se: SeMSC, 2 , 20, 100 nM are equivalent to 0.4, 4, 20 ng/ml SeMSC
Data indicate mean $\pm$ SD, $^{\ddagger}p<0.001$ vs. control, $^{\S}p<0.05$ vs. Br-Ex. Statistical significance was tested by one way ANOVA, followed by Tukey test for multiple comparisons.

Next, we analyzed the inducing potential of broccoli extract alone and in combination with SeSMC as a source of Se. The broccoli extract was tested at a concentration of 625 µg/ml (equivalent to 2.8 µM SFN) and induced QR activity in all cell lines. Interestingly, co-treatment with increasing concentrations of SeMSC in a range of 2-100 nM weakly, but dose-dependently reduced QR enzyme activity (p<0.01) compared to treatment with broccoli extract alone. Induction of TRx-R activity in the immortalized BPH-1 cell line was higher by the combined treatment with extract and 20 nM SeMSC than by the individual treatments (although tested concentrations were not identical), indicating an additive effect on Trx-R induction by Se and SFN. In the cancer cell lines, the additive effect was less prominent, but SeMSC still dose-dependently induced Trx-R activity in the presence of the broccoli extract (Table 3).

In line with the increase in Trx-R enzyme activity, incubation with increasing concentrations

of SeMSC in combination with broccoli extract induced Trx-R protein expression in a dose dependent manner. Induction was most prominent in the BPH-1 cell line (Fig. 9).
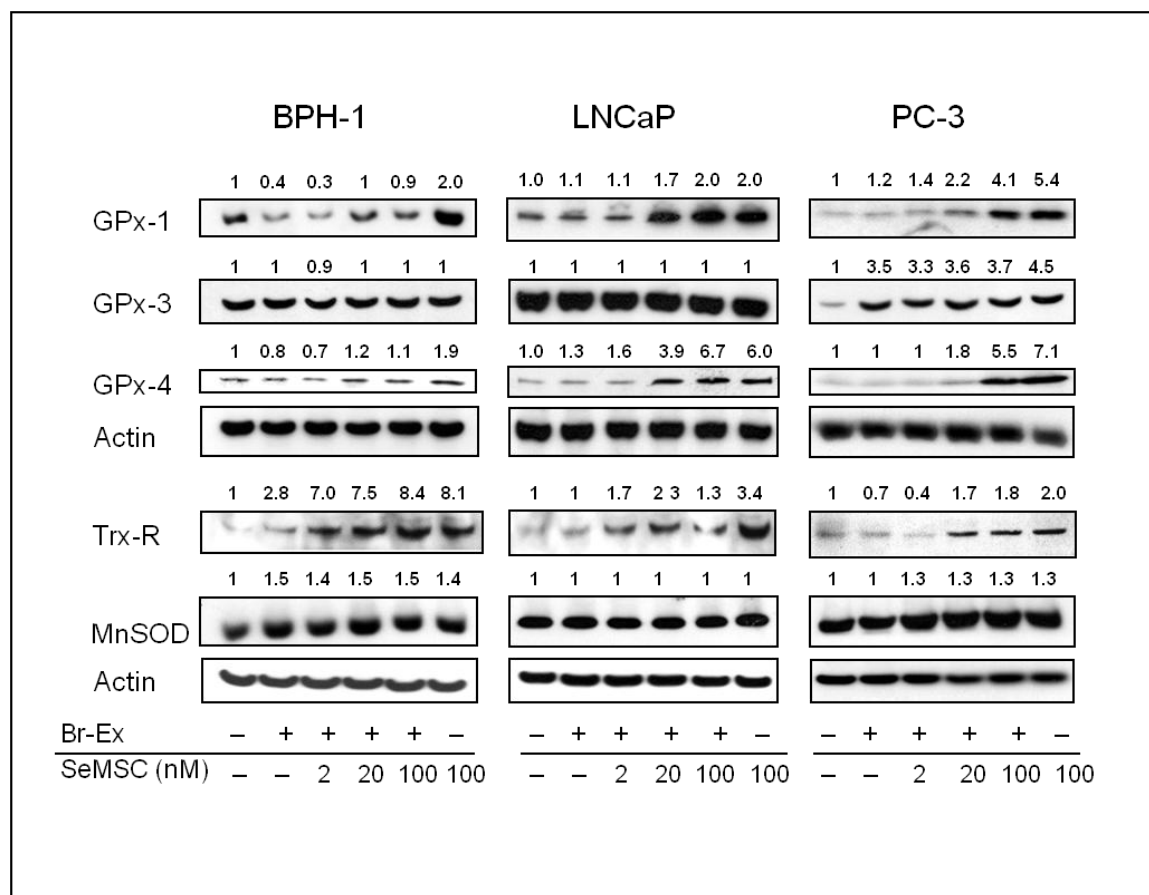

Fig. 9: Effects of broccoli extract, selenium and their combination on expression levels of selenoproteins and antioxidant enzymes in prostate (cancer) cell lines. BPH-1, LNCaP and PC-3 cells were treated with broccoli extract 625 μg/ml (eq. 2.8 μM SFN), co-treated with SeMSC and SeMSC alone for 72hr. After incubation, total cell lysates were used to detect expression of the indicated selenoproteins and antioxidant enzymes by Western blotting. β-Actin was used as a loading control. The numbers above the immuno-reactive bands represent fold changes relative to the corresponding vehicle control. Each experiment was repeated three times and representative data from one such experiment are shown.

In addition to TRx-R expression, the expression of GPx as a selenium-containing antioxidant enzyme family was analyzed. Treatment with SeMSC induced GPx-1 and GPx-4 protein expressions in cancer cell lines in dose dependent manner (Fig. 9). However, broccoli extract alone had no effect on the expression of GPx-1 and -4. Different from the prostate cancer cell lines, the BPH-1 cell line was sensitive to extract treatment in a way that GPx-1 expression was down-regulated, although SeMSC treatment alone induced GPx-1 and -4 expression. Reasons for this discrepancy need to be further explored. Another GPx family member, GPx-3, was not responsive to both extract and SeMSC treatment in BPH-1 and LNCaP cell lines, but was induced by both treatments in the PC-3 cell line. We also analyzed the

expression of the antioxidant enzyme MnSOD that inactivates superoxide anion radicals. This enzyme was only weakly induced in BPH-1 and PC-3 cells by broccoli extract or SeMSC, but there was no enhancement of induction by the combination.

4.1.2 Effects of Se-enriched broccoli sprouts *in vitro*

The effects of broccoli extract in combination with SeMSC on QR and Trx-R enzyme activity in prostate (cancer) cell lines indicated that it may be possible to maximize dual bioactive components in a single broccoli plant for beneficial effects on prostate cancer prevention. As a first approach to test this strategy, we cultured broccoli sprouts in a liquid culture system containing Na_2SeO_3 or Na_2SeO_4.

Without changing the glucoraphanin contents, broccoli sprouts accumulated selenium in the plants in two to three weeks. Uptake of selenium was more efficient by inoculation with selenite compared to selenate. Selenium fertilization induced Se accumulation about 44 and 5 fold, respectively, in 2 weeks, and the accumulation was higher after 2 weeks culture that after 3 weeks culture (Table 4).

Table 4. Antioxidant enzyme induction by Se-enriched broccoli sprouts in prostate (cancer) cell lines

Sample	Total Se* (ng/ml)	Gluco-raphanin* (µM)	BPH-1		LNCaP	
			QR[a] (fold ind.)	Trx-R (fold ind.)	QR (fold ind.)	Trx-R (fold ind.)
Solvent control	-	-	1.0 ± 0.02	1.0 ± 0.02	1.0 ± 0.02	1.0 ± 0.02
2w control	0.3 ± 0.01	0.3 ± 0.04	$1.6 \pm 0.01^{\dagger}$	1.0 ± 0.04	$1.2 \pm 0.01^{\dagger}$	$1.5 \pm 0.01^{\dagger}$
2w SeO_3^{2-}	13.2 ± 0.2	0.3 ± 0.06	$1.7 \pm 0.03^{\dagger}$	$4.2 \pm 0.03^{\dagger\S}$	$1.2 \pm 0.02^{\dagger}$	$4.8 \pm 0.02^{\dagger\S}$
2w SeO_4^{2-}	2.7 ± 0.5	0.3 ± 0.04	$1.6 \pm 0.1^{\dagger}$	$2.3 \pm 0.11^{\dagger\S}$	$1.1 \pm 0.03^{\dagger}$	$2.5 \pm 0.04^{\dagger\S}$
3w control	0.7 ± 0.3	0.2 ± 0.04	$2.2 \pm 0.05^{\dagger}$	$1.7 \pm 0.07^{\dagger}$	$1.5 \pm 0.02^{\dagger}$	$1.5 \pm 0.01^{\dagger}$
3w SeO_3^{2-}	7.8 ± 0.5	0.2 ± 0.04	$1.8 \pm 0.04^{\dagger\S}$	$7.0 \pm 0.06^{\dagger\S}$	$1.2 \pm 0.02^{\dagger\S}$	$5.0 \pm 0.08^{\dagger\S}$
3w SeO_4^{2-}	5.3 ± 0.4	0.2 ± 0.04	$2.1 \pm 0.1^{\dagger}$	$4.5 \pm 0.06^{\dagger\S}$	$1.7 \pm 0.01^{\dagger\S}$	$2.5 \pm 0.02^{\dagger\S}$

Data indicate mean ± SD; w: culture period in weeks.
* Concentration: This is the content in Se and glucoraphanin in the final cell culture incubation when 6.25 µg/ml of the sprouts were used to prepare an extract
[a] Specific activities of solvent control: BPH-1 QR 21.6 ± 0.5 nmol/min/mg; Trx-R 3.75 ± 0.3 nmol/min/mg, LNCaP QR 26.4 ± 0.8 nmol/min/mg, Trx-R 5.6 ± 0.3 nmol/min/mg
Statistical significance was tested by one way ANOVA, followed by Tukey test for multiple comparisons. [†]$p<0.05$ vs solvent control, [§]$p<0.05$ vs. control sprouts, respectively.

QR activity

Treatment with Se-enriched or standard broccoli sprouts at a concentration of 6.25 µg/ml for 5 days induced QR enzyme activity in BPH-1 and LNCaP cell lines (Table 4). Sprouts

cultured for 2 weeks induced QR activity approximately 1.6 fold. Interestingly, potential to induce QR enzyme activity by sprouts cultured with selenate for 3 weeks was about 20% less efficient than that of standard sprouts in both the BPH-1 and LNCaP cell line ($p<0.05$, ANOVA) (Table 4). Taken together, QR activity was mainly induced by SFN and little, or even negatively, influenced by culturing the sprouts with selenium.

TRx-R activity

Incubation of BPH-1 and LNCaP cell lines with Se-fertilized or standard broccoli sprouts at a concentration of 6.25 µg/ml for 5 days also induced Trx-R enzyme activity (Table 4). Treatment with untreated sprouts weakly induced TRx-R activity in both cell lines by 1.5- to 2.2-fold. The increase in Se-content by culture of the sprouts with selenite or selenate resulted in a significant increase in TRx-R induction, with a maximum 7-fold increase after incubation of BPH-1 cells with sprouts cultured for 3 weeks with selenite. These data indicate that both broccoli components as well as Se contribute to the induction of TRx-R, with selenium having a more prominent effect than SFN.

GPx expression

Treatment of BPH-1 and LNCaP cells with Se-enriched sprouts at a concentration of 6.25 µg/ml for 5 days also induced GPx-1 and -4 expression compared to control, as indicated in Fig. 10.

Especially sprouts cultivated with selenite for 2 or 3 weeks resulted in a strong induction of GPx-1 and -4 expression in both the BPH-1 and LNCaP cell line. Cultivation with selenate resulted in lower Se-levels in the sprouts in comparison with selenite culture (as indicated in Table 4), and this was also reflected in a lower potential to induced GPx proteins. Treatment with standard sprouts also resulted in the induction of GPX-1 and -4 expression, especially in the BPH-1 cell line. This was different from our observations with the broccoli extract, which rather reduced GPx-1 and -4 expression in BPH-1 cells (Fig. 9).
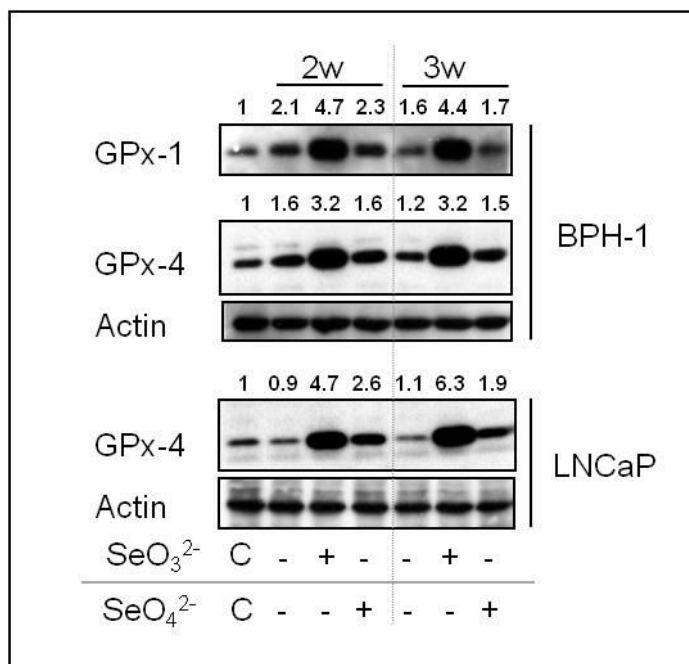
Fig. 10: Induction of GPx expression in BPH-1 and LNCaP cell lines by broccoli sprouts which were cultivated in selenium-contained media. Freeze-dried broccoli sprouts which cultured for 2 or 3 weeks in the presence of water, 50 μM of selenate or selenite were homogenized with water (detailed description in Materials and Methods). BPH-1 and LNCaP cells were treated with broccoli sprouts for 72 hrs and total cell lysates were used to detect GPx protein expression. The numbers above the immuno-reactive bands represent fold changes relative to the corresponding vehicle control, quantified by Image J software.

Similar to TRx-R activity and total selenium contents, inducing potential of GPx expression increased in the order of sprouts cultivated with standard conditions < selenate < selenite in BPH-1 and LNCaP cell lines. Compared to the reference compound SeMSC at 100 nM, GPx induction by treatment with 6.25 μg/ml of Se-enriched sprouts which contains about 25 nM of SeMSC was more efficient in BPH-1 and LNCaP cells (compare Fig. 9 and Fig. 10). However, only total Se-levels were determined in the sprouts, it is presently unclear whether Se is contained in organic or anorganic form.

4.1.3 Activity of Se-enriched broccoli florets *in vitro*

Next, we investigated the chemopreventive potential of Se-enriched broccoli florets. Mature broccoli has previously been reported as a Se accumulator (88).To avoid competition between sulfur and selenium by sharing the same enzymes for uptake and further synthesis of glucoraphanin and organic selenium in the plant, as previously described (89, 163), we sprayed 0, 2, 20 mg of Na_2SeO_4 on to the broccoli leaves instead of inoculation into the soil. Direct contact of Se with soil and florets was avoided by coverage with aluminum foil.

RESULTS

The consequence of Se spraying was accumulation of Se in the broccoli florets without altering of glucoraphanin contents, as indicated in Table 5. Total Se content was increased in a dose-dependent manner. Spraying with 20 mg of selenate per broccoli head induced a 35-fold accumulation of Se in the florets.

Table 5. Antioxidant enzyme induction by Se-enriched broccoli florets in prostate (cancer) cell lines

Sample	Total Se[*] (ng/ml)	Gluco-raphanin[*] (µM)	BPH-1		LNCaP	
			QR[a] (fold ind.)	Trx-R (fold ind.)	QR (fold ind.)	Trx-R (fold ind.)
Solvent control	-	-	1.0 ± 0.02	1.0 ± 0.02	1.0 ± 0.02	1.0 ± 0.02
0 mg	0.1 ± 0.3	1.3 ± 0.2	$1.9 \pm 0.03^{\dagger}$	$2.4 \pm 0.1^{\dagger}$	$1.5 \pm 0.07^{\dagger}$	$1.6 \pm 0.05^{\dagger}$
2 mg SeO$_4^{2-}$	0.8 ± 0.5	1.4 ± 0.1	$1.9 \pm 0.2^{\dagger}$	$3.5 \pm 0.3^{\dagger\S}$	$1.5 \pm 0.09^{\dagger}$	$2.1 \pm 0.05^{\dagger\S}$
20 mg SeO$_4^{2-}$	3.5 ± 0.9	1.3 ± 0.2	$1.8 \pm 0.1^{\dagger}$	$3.3 \pm 0.2^{\dagger\S}$	$1.4 \pm 0.07^{\dagger}$	$4.1 \pm 0.2^{\dagger\S}$

Data indicate mean $\pm$ SD.
[*] Concentration: This is the content in Se and glucoraphanin in the final cell culture incubation when 625 µg/ml of the sprouts were used to prepare an extract
[a] Specific activities of solvent control: BPH-1 QR 21.6 ± 0.5 nmol/min/mg; Trx-R 3.75 ± 0.3 nmol/min/mg, LNCaP QR 26.4 ± 0.8 nmol/min/mg, Trx-R 5.6 ± 0.3 nmol/min/mg
Statistical significance was tested by one way ANOVA, followed by Tukey test for multiple comparisons.
[†] $p<0.05$ vs solvent control, [§] $p<0.05$ vs. control florets, respectively.

Treatment BPH-1 and LNCaP cells with homogenates of both Se-enriched broccoli florets (Se-florets) and standard broccoli florets at a concentration of 625 µg/ml for 3 days induced QR enzyme activity 1.4 to 1.9 fold (Table 5).

Compared to LNCaP cells, BPH-1 cells were more sensitive to induce QR enzyme activity after treatment with broccoli florets. As Se-fertilization accumulate Se in the broccoli florets, treatment with Se-florets induced Se-containing antioxidant enzymes in the cells. TRx-R enzyme activity was increased by 1.6- to 4.1-fold in a Se dose-dependent manner (0 mg florets < 2 mg florets < 20 mg florets), especially in the LNCaP cell line.
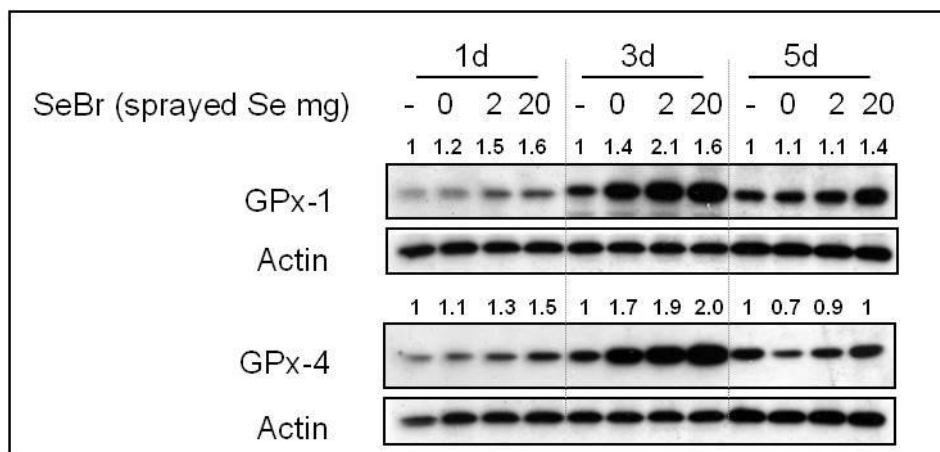
Fig. 11: Induction of GPx expression by Se-enriched broccoli florets in LNCaP cells. Freeze-dried broccoli florets of plants sprayed on to the leaves with water, 2 mg or 20 mg selenate once before harvesting (described in Materials and Methods) were homogenized with water. After the indicated incubation times, cells were harvested and GPx protein expression was analyzed by Western blotting. The numbers above the immuno-reactive bands represent fold changes relative to the corresponding vehicle control, quantified by Image J software.

Elevated total Se levels in the broccoli florets were also correlated with induction of GPx-1 and GPx-4 protein expression in LNCaP cells after treatment with floret homogenates at a concentration of 625 µg/ml for 1 to 5 days, evaluated by Western blot analysis (Fig.11). Interestingly, highest induction was observed after incubation for 3 days, whereas relative expression levels declined after further treatment up to 5 days. Although spraying with 20 mg selenate resulted in more that 4-fold higher Se levels than spraying with 2 mg selenate, the inducing potential of both preparations was similar and weaker than that observed with broccoli sprouts enriched with selenium (compare Fig. 10).

4.1.4 Se-enriched broccoli and food preparations in the LNCaP xenograft model

After we optimized the Se fertilization conditions for Se-enriched broccoli and evaluated their effects on the induction of phase II and antioxidant enzymes in prostate (cancer) cell lines, we further tested these effects *in vivo* in the LNCaP xenograft model. In this animal experiment, we compared the effects of standard broccoli (broccoli), Se-enriched broccoli (Se-enriched broccoli), Se-enriched broccoli extract (extract), Se-enriched broccoli puree (puree), and kale sprouts (sprouts) used as a commercially available control product with a high content in glucosinolates (detailed described in chapter 3.5.2).

RESULTS

Description of experimental broccoli food preparations

Extract and puree were prepared from Se-enriched broccoli. The aim was to test these preparations as food supplement or functional food. Glucosinolate and total Se contents in the various broccoli preparations are summarized in Table 6.

Table 6. Glucosinolate contents in broccoli preparations and kale sprouts

	Broccoli	Se-enriched broccoli	Se-broccoli [*]extract	Se-br	Kale sprouts
Glucosinolates /SFN (µmol/g DW)					
Glucoiberin	0.7 ± 0.02	1.1 ± 0.04	0	0.2 ± 0.0003	18.1 ± 0.4
Progoitrin	0	0	0	0	9.8 ± 0.5
Sinigrin	0	0	0	0	22.3 ± 0.9
Glucoraphanin	5.3 ± 0.4	6.6 ± 0.08	0	2.1 ± 0.01	9.2 ± 0.5
Glucoalyssin	0.1 ± 0.01	0.1 ± 0.01	0	0	0
Gluconapsin	0	0	0	0	2.4 ± 0.1
4OH-Glucobrassicin	0.2 ±0.02	0.1 ± 0.01	0	0	5.7 ± 0.6
Glucoiberverin	0	0	0	0	7.0 ± 0.4
Glucoerucin	0	0	0	0	2.5 ± 2.5
Glucobrassicin	3.1 ± 0.03	3.6 ± 0.05	0	0.5 ± 0.002	0.7 ± 0.03
4OCH$_3$-Glucobrassicin	0.7 ± 0.01	0.6 ± 0.01	0	0.06 ± 0.0004	0
Neo-Glucobrassicin	3.9 ± 0.04	6.7 ±0.1	0	1.3 ± 0.04	0
SFN	3.2 ± 0.3	1.2 ± 0.03	2.5 ± 0.08	0.7 ± 0.01	1.3 ± 0.01
SFN-nitrile	1.7 ± 0.01	1.0 ± 0.01	1.4 ± 0.06	0	0
Indol-3-acetonitril	0	0	0	20.9 ± 0.71	
Total	**18.7 ± 0.8**	**21.1 ± 0.3**	**3.9 ± 0.1**	**25. 7 ± 0.7**	**79 ± 5.9**
Total Se (µg/g DW)	0.1 ± 0.0	3.9 ± 1.4	4.4	2.6 ± 0.2	-

Data indicate mean ± SD of three determinations
[*]Se-brocoli extract: Se-enriched broccoli extract, Se-broccoli puree: Se-enriched broccoli puree.

Standard broccoli and Se-enriched broccoli contained similar total amounts of glucosinolates in the range of 20 µmol/g DW. Also, the composition was relatively similar. The most prevalent glucosinolate in both standard broccoli and Se-enriched broccoli was glucoraphanin, which is the precursor of SFN. Neo-Glucobrassicin was detected at an about 1.7-fold higher level in the Se-enriched sample in comparison to standard broccoli. The extract was produced following a specialized protocol to convert glucoraphanin to free SFN, in contrast to the broccoli products which contained glucosinolates. Consequently, glucosinolates were no longer detectable in the final extract, which mainly contained free SFN and SFN-nitrile. Interestingly, the puree contained large quantities of indole-3-acetonitrile, whereas the levels of glucosinolates and SFN were reduced during production (Table 6). As described before, kale sprouts are very rich in glucosinolates, mainly glucoiberin and sinigrin. Kale sprouts also

contained active myrosinase, whereas we expected that myrosinase activity of broccoli and its preparation would be destroyed during blanching and sterilization.

For the preparation of experimental diets for the animal experiment, freeze-dried broccoli, Se-enriched broccoli, puree and kale sprout powder was weighed, grinded, and mixed with powdered control diet in a 1:5 ratio. The extract was mixed with the control diet in a 1:10 ratio. After addition of a defined amount of water, the diet preparations were compacted using a plastic syringe and the resulting pellets were dried at 37 ℃ over night. A control diet was prepared accordingly without addition of any broccoli source.

Effect on xenograft growth

Balb-c nude mice (n=10 per group) were inoculated with LNCaP cells mixed with matrigel in both flanks as described in Chapter 3.5.3. After randomization, feeding with broccoli diets started one day after the injection of LNCaP cells. After seven to eight weeks intervention with the experimental diets, LNCaP tumor xenografts were isolated, weighed and stored at -80 ℃ until further use.

Unexpectedly, none of the preparations reduced xenograft growth (Fig. 12). In the intervention study testing broccoli and SE-enriched broccoli preparations, tumor weights were in the range 10 to 600 mg wet weight with an average of about 200 mg in all groups (Fig. 12 left panel). In the kale sprout experiment, tumor weights in both the control and the kale sprout group were higher, with an average tumor wet weight of about 500 mg (Fig. 12, right panel). Independent of the tumor size, which may be due to differences in cell proliferation rate in both experiments none of the interventions significantly reduced tumor growth.
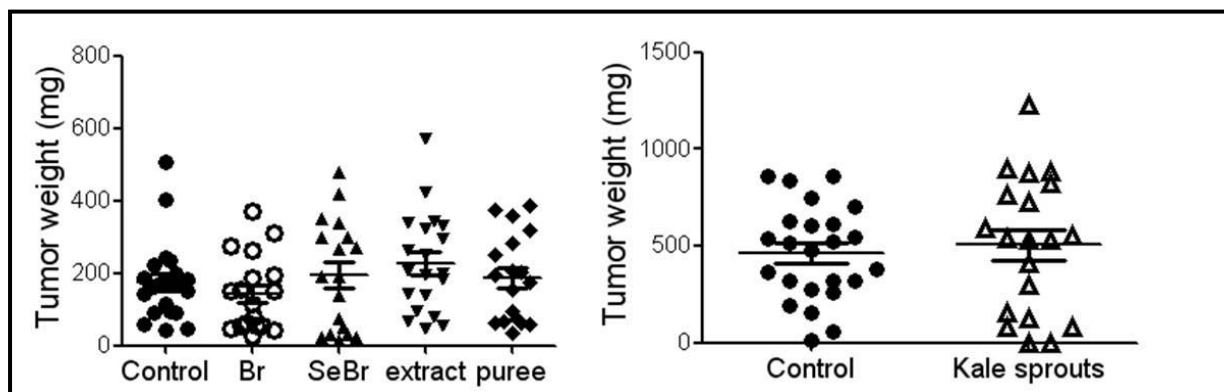

Fig. 12: Tumor weight. Wet weight of tumors were measured. Each point indicates a single tumor; Horizontal bars indicate the mean ± standard error with n= 17-24. Control (●), broccoli (○), Se-enriched broccoli (▲), extract (▼), puree (♦), kale sprouts (△).

RESULTS

Induction of Phase II and antioxidant enzymes in tumor tissue

To get an impression whether the interventions had any biological effect in the animal model, we analyzed the activity and expression of Phase II and antioxidant enzymes in tumor xenograft samples, in analogy with our *in vitro* investigations. Tumor samples (four per group) were homogenized, and homogenates were used to measure QR and TRx-R activities. Results are expressed relative to the activities of the control group and summarized in Table 7.

None of the broccoli-based dietary interventions significantly induced QR or TRx-R enzymatic activity. Only intervention with kale sprouts resulted in a significant 2.2-fold induction of QR activity (p <0.05) in comparison to the control group.

Table 7 Relative QR and Trx-R activities in LNCaP xenografts

Group	QR (fold ind.)	Trx-R (fold ind.)
Control[a]	1.0 ± 0.1[b]	1.0 ± 0.1
Broccoli	1.0 ± 0.06	1.1 ± 0.2
Se-enriched broccoli	1.2 ± 0.04	1.3 ± 0.2
Se-enriched broccoli extract	1.1 ± 0.06	1.3 ± 0.2
Se-enriched broccoli puree	1.0 ± 0.1	1.4 ± 0.1
Kale sprouts	2.2 ± 0.3[†]	1.2 ± 0.4

[a] Data are mean ± SE of four xenografts
[b] Enzyme activities in the control: QR, 42 ± 1.2 nmol/min/mg; Trx-R, 6.7 ± 0.6 nmol/min/mg.
Statistical significance was tested by one way Anova with post-hoc multiple comparison test by Tukey. [†]$p<0.01$ vs. dietary control.

We attributed this effect to the high content in glucosinolates, which was in total about 4-fold higher than that of the broccoli, Se-enriched broccoli and puree preparation, and to the fact that kale sprouts contain active myrosinase necessary for the conversion of glucosinolates to bioavailable ITCs. Although the extract contained free SFN, total levels of broccoli components were lowest in comparison to the other preparations, and the extract was even used at a lower ratio in the diet as the other broccoli preparations. We therefore concluded that levels of bioactive compounds were too low to cause significant induction of enzyme activities in xenograft samples.

This was further confirmed when the effects of broccoli and Se-enriched broccoli on GPx-1 expression in LNCaP xenograft were analyzed by Western blotting. Similar to the effects on QR and TRx-R activities, GPx-1 protein expression was not influenced by dietary intervention with these two diets *in vivo* in LNCaP xenograft samples (Fig. 13).
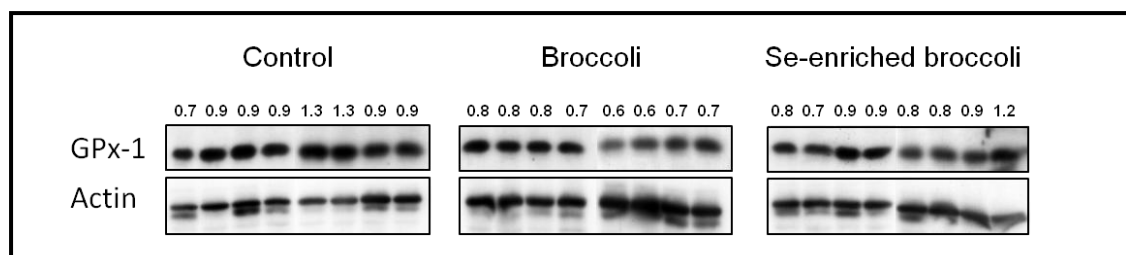
Fig. 13 GPx expression in LNCaP xenograft samples after intervention with dietary broccoli or Se-enriched broccoli preparation. Results of 8 individual xenograft samples of the control, broccoli and Se-enriched broccoli group are depicted. The numbers above the immuno-reactive bands represent fold changes of GPx-1 expression relative to the actin expression, quantified by Image J software.

Determination of Phase I and Phase II metabolizing and antioxidant enzymes in murine liver

Liver is the major organ of drug and xenobiotic metabolism. SFN and other ITCs have been shown to modulate the activities of hepatic enzymes of drug metabolism and antioxidant enzymes *in vivo* in many previous studies (24, 50). Therefore we further analyzed the effect of dietary broccoli and kale sprout interventions on mouse liver antioxidant enzymes. Livers were homogenized and fractionated by centrifugation in microsomal and cytosolic fractions, as described in Chapter 3.6.2.

Table 8 Induction of Phase I and II enzymes and GSH in mouse liver

Group	Phase I		Phase II			
	Cyp1A1[b] (fold ind.)	Cyp2B1 (fold ind.)	QR (fold ind.)	GST (fold ind.)	Trx-R (fold ind.)	GSH (fold ind.)
Control[a]	1.0 ± 0.1	1.0 ± 0.1	1.0 ± 0.1	1.0 ± 0.1	1.0 ± 0.1	1.0 ± 0.1
Broccoli	1.1 ± 0.1	0.8 ± 0.2	$2.5 \pm 0.2^{\dagger}$	1.3 ± 0.2	1.3 ± 0.2	0.8 ± 0.1
Se-enriched broccoli	1.1 ± 0.1	1.0 ± 0.2	$3.1 \pm 0.3^{\dagger}$	$1.5 \pm 0.2^{\dagger}$	$1.7 \pm 0.2^{\dagger}$	1.0 ± 0.1
Extract	1.0 ± 0.1	0.8 ± 0.3	$1.9 \pm 0.3^{\dagger*}$	1.1 ± 0.2	1.3 ± 0.1	0.8 ± 0.2
Puree	1.1 ± 0.1	0.7 ± 0.2	$1.4 \pm 0.3^{*}$	1.1 ± 0.2	$1.2 \pm 0.1^{*}$	1.0 ± 0.1
Kale sprouts	0.9 ± 0.1	0.8 ± 0.1	$5.9 \pm 0.7^{\dagger}$	$2.2 \pm 0.2^{\dagger}$	$1.5 \pm 0.1^{\dagger*}$	$1.5 \pm 0.1^{\dagger}$

[a] Data are mean $\pm$ SE of 8 animals per group
[b] Enzyme activities in control groups (1. intervention study, 2. intervention study, mean $\pm$ SE): EROD: 32.1 ± 2.3, 40.3 ± 5.1 pmol/min/mg; PROD: 9.1 ± 0.4, 6.2 ± 0.5 pmol/min/mg; QR: 101.4 ± 6.7, 119.6 ± 8.6 nmol/min/mg; GST 830 ± 73, 677 ± 29 nmol/min/mg; TRx-R 16.1 ± 1.3, 14.0 ± 0.9 nmol/min/mg; GSH 53.1 ± 3.9, 60.1 ± 3.2 nmol/min/mg.
Group comparison was tested by Wilcoxon Rank sum-Test, significant under multiple comparisons by Bonferoni-Holm test $^{\dagger}p < 0.05$ vs. dietary control, $^{*}p < 0.05$ vs. Se-enriched broccoli.

As representatives of phase I drug metabolizing enzymes, enzyme activities of Cyp1A1 and Cyp2B1 were analyzed in microsomal fractions by the EROD and PROD activity assay. The

results are summarized in Table 8. None of the dietary interventions significantly inhibited or induced these activities in liver microsomes in comparison to the control group.

We further investigated the effect of the dietary intervention on QR, GST, and TRx-R activities in cytosolic fractions, as well as on GSH levels. As indicated in Table 8, intervention with broccoli, Se-enriched broccoli, extract and kale sprouts significantly induced QR activities in the cytosolic fraction of liver tissue by 1.9- to 5.9-fold ($p<0.01$, Wilcoxon Rank sum-Test). Inducing potential of QR activity in the liver was correlated with glucoraphanin content and total glucosinolates contents of each dietary preparation in the order of kale sprouts > Se-enriched broccoli > standard broccoli > Se-enriched broccoli extract. Although the extract and puree were made from Se-enriched broccoli, potential to induce QR activity was significantly lower than that of Se-enriched broccoli. This indicates again that the processes to produce extract and puree reduces important glucosinolates or ITCs, respectively, with potential to induce QR activity.

GST, another phase II enzyme regulated by transcription factors Nrf-2, was less efficiently induced by the broccoli preparations. Only interventions with Se-enriched broccoli and kale sprouts resulted in a significant induction of GST enzyme activity in the liver cytosolic fraction ($p<0.05$, Wilcoxon Rank sum-test).

The antioxidant enzyme TRx-R is regulated by Nrf-2 and Se-dependant. Again, only intervention with Se-enriched broccoli and kale sprouts significantly induced hepatic TRx-R activity by 1.7- and 1.5-fold. Although kale sprouts contained higher glucosinolate levels than Se-enriched broccoli, potential to induce TRx-R of Se-enriched broccoli was higher than that of the kale sprout intervention (Table 8). Also, TRx-R activity was higher in the dietary Se-enriched broccoli group than in the standard broccoli group. These data further confirm that Se contributes to the induction of TRx-R activity.

Similar to the activities of QR, GST and TRx-R, levels of the important intracellular antioxidant GSH are regulated in a Nrf-2 dependent manner. However, of all factors analyzed, the effect on GSH synthesis was weakest by all interventions. Only kale sprout intervention resulted in a significant 1.5-fold induction.

While we could detect elevated TRx-R activity by Se-enriched broccoli, protein expression of the other selenium-dependant antioxidant enzymes GPx -1 and -4 was not influenced by dietary Se-enriched broccoli (Fig. 14).
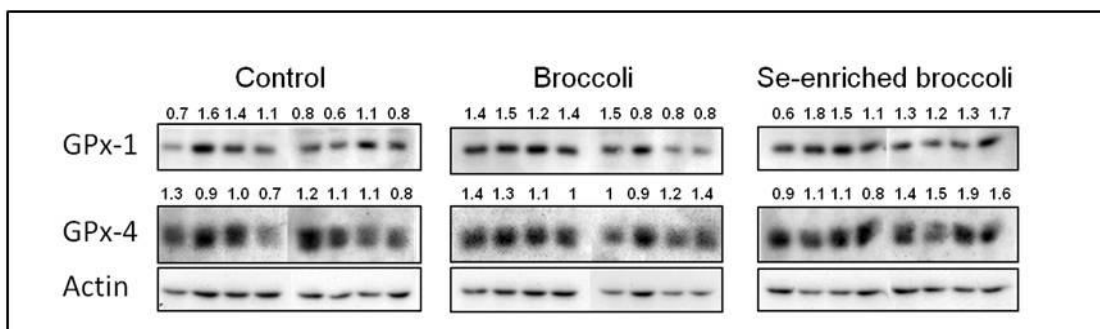
Fig. 14: Effects of dietary broccoli and Se- enriched broccoli on GPx expression in mouse liver. Animals were fed with dietary broccoli and Se-enriched broccoli for 8 week (details were described in Materials and Methods). After sacrifice, livers (n=8) were homogenized. Liver cytosolic fractions were used to detect GPx protein expression by Western blotting. Four samples per group were directly compared on one gel. Representative Western blot images of GPx-1 and GPx-4 were normalized to actin expression. The numbers above the immuno-reactive bands represent fold changes of GPX-1 and -4 expression relative to the actin expression, quantified by Image J software.

4.1.5 Sulforaphane metabolites in mouse plasma, urine and feces after the interventions.

To identify and quantify the major glucosinolate metabolites as suitable biomarkers of broccoli intake and to find a correlation with antioxidant enzymes activity, we measured sulforaphane metabolites in mouse plasma, urine and feces obtained from our dietary intervention study with broccoli preparations and kale sprouts. After release of ITCs from glucosinolates by plant myrosinase or myrosinase activity of the gut microflora, they are absorbed and conjugated by GST activity with GSH or proteins bearing free sulfur groups. ITC-GSH conjugates are further processed *via* the mercapturic acid pathway, resulting in -cysteine-glycine (-Cys-Gly), -cysteine (-Cys), and -N-acetyl cysteine (NAC) conjugates as intermediates (164). We analyzed free SFN, SFN-GSH, SFN-Cys-Gly, SFN-Cys, and SFN-NAC by HPLC coupled with mass spectrometry, as described in Chapter 3.6.4.

As summarized in Table 9, plasma concentrations of free sulforaphane and sulforaphane metabolites in the control group were below 1 nmol/L or below the detection range. Levels of free SFN were elevated in all plasma samples of dietary broccoli and kale sprouts intervention groups, with the exception of the extract group. Among the sulforaphane metabolites, SFN-NAC was the most abundant metabolite circulating in the plasma after intervention with the broccoli preparations (about 70% of the total amount of free SFN and all metabolites), followed by free SFN (about 20%), SFN-Cys-Gly, SFN-GSH and SFN-Csy. One exception was the relatively high level of SFN-Cys-Gly in plasma from mice that were fed with the Se-enriched broccoli extract. As mentioned above, this extract contains free STN

and SFN-nitrile. Therefore uptake, metabolism and excretion might follow a different kinetic that that of the other broccoli preparations.

Table 9 Sulforaphane metabolites in mouse plasma, urine and feces

	SFN	SFN-NAC	SFN-Cys-Gly	SFN-Cys	SFN-GSH
Plasma concentration [nmol/L]					
Control	0.6 ± 0.3	0.6 ± 0.3	n.d.	0.2 ± 0.2	n.d.
Broccoli	$54 \pm 4.7^\dagger$	$208 \pm 28^\dagger$	$16 \pm 4.9^\dagger$	$1.7 \pm 0.4^\dagger$	$4.1 \pm 0.9^\dagger$
Se-enriched broccoli	$43 \pm 7.4^\dagger$	$164 \pm 42^\dagger$	$11 \pm 2.6^{\dagger\S}$	0.9 ± 0.3	$2.9 \pm 0.9^\dagger$
Extract[a]	23 ± 3.5	63 ± 16	$46 \pm 20^\dagger$	5.3 ± 2.9	$5.1 \pm 1.4^\dagger$
Puree	$35 \pm 7.0^\dagger$	$88 \pm 17^\dagger$	$9.9 \pm 3.1^\dagger$	$1.3 \pm 0.6^\dagger$	$3.5 \pm 0.8^\dagger$
Kale sprouts	$55 \pm 16^\dagger$	$116 \pm 32^\dagger$	1.1 ± 0.3	3.9 ± 2.3	5.0 ± 2.4
Urine concentration [nmol/µmol creatinine]					
Control	0.1 ± 0.01	0.04 ± 0.03	0.01 ± 0.01	0.04 ± 0.02	n.d.
Broccoli	15.6 ± 8.9	57 ± 9.2	0.1 ± 0.04	0.8 ± 0.4	0.03 ± 0.03
Se-enriched broccoli	$15.3 \pm 3.0^\dagger$	$73 \pm 21^\dagger$	0.2 ± 0.1	1.2 ± 0.8	n.d.
Extract	6.8 ± 2.0	23 ± 0.5	0.1 ± 0.1	0.3 ± 0.2	n.d
Puree	6.4 ± 1.5	51 ± 6.3	0.1 ± 0.1	0.4 ± 0.1	n.d.
Kale sprouts	1.5	11	0.02	0.8	n.d.
Feces concentration [nmol/g dry weight]					
Control	n.d.	n.d.	n.d.	n.d.	n.d.
Broccoli	$4.3 \pm 0.6^\dagger$	$1.1 \pm 0.3^\dagger$	$0.7 \pm 0.05^\dagger$	$0.4 \pm 0.04^\dagger$	n.d.
Se-enriched broccoli	$5.6 \pm 0.8^\dagger$	0.8 ± 0.1	0.9 ± 0.2	$0.4 \pm 0.01^\dagger$	n.d.
Extract	$3.4 \pm 0.5^{\dagger*}$	1.1 ± 0.4	0.6 ± 0.2	$0.4 \pm 0.05^\dagger$	n.d.
Puree	$5.3 \pm 0.4^\dagger$	$2.4 \pm 1.8^\dagger$	$0.6 \pm 0.07^\dagger$	$0.6 \pm 0.04^{\dagger*}$	n.d.
Kale sprouts	1.9	2.6	n.d.	0.4	n.d.

n.d. not detectable
[a] Extract: Se-enriched broccoli extract, Puree: Se-enriched broccoli puree.
Data indicate mean $\pm$ SE, $^\dagger p<0.05$ vs. dietary control, $^\S p<0.05$ vs. Br, $*p<0.05$ vs. Se-enriched broccoli. Statistical significance was tested by one way Anova followed by Tukey post-hoc multiple comparison test.

Overall, plasma concentrations of SFN and metabolites correlated with the concentrations of glucoraphanin and free SFN in the broccoli preparations. Those broccoli products which contained higher concentrations resulted in higher plasma levels of SFN and metabolites (broccoli > Se-enriched broccoli > extract > puree).

In urine samples, the major SFN-metabolite was also SFN-NAC in all intervention groups (about 80% of the total amount of free SFN and metabolites in urine). Similar to plasma SFN metabolites, about 15% of free SFN was detected as the second leading SFN metabolite in the urine samples. The other three metabolites were detectable only at very low concentrations $\leq$ 1 nmol/µmol creatinine. In comparison to the dietary glucosinolate uptake provided by broccoli preparations and kale sprouts, dietary excretion of SFN and metabolites was lower in the kale sprout group than in the broccoli intervention groups.

Different from plasma and urine samples, free SFN was the major form of SFN metabolites in feces samples. There were no significant differences in fecal levels of SFN metabolites between the dietary intervention groups, despite differences in uptake.

Since induction of antioxidant and phase II enzymes can be affected by additional components of the broccoli preparations except glucoraphanin/SFN, it is statistically not 'correct' to calculate a correlation between SFN metabolites in the plasma samples and enzyme activities in liver samples after intervention. However, when comparing individual animals, we could still observe a linear trend of free SFN concentrations in mouse plasma and hepatic QR enzyme activities by using the Jump® statistical calculation software.

4.1.6 Summary

The present study aimed to investigate the effects of Se-enriched broccoli preparations in prostate cancer prevention *in vitro* and *in vivo*. These studies were based on earlier reports on the anti-prostate cancer properties of selenium and broccoli as chemopreventive agents. We first tested the combination effects of Se and broccoli components at various concentrations *in vitro* in prostate (cancer) cell lines on the activities of antioxidant and detoxifying enzymes. In continuation, we analyzed broccoli sprouts cultivated in selenium-containing medium as well as broccoli florets Se-enriched by leaf fertilization to optimize the conditions of Se-enrichment in broccoli. As expected, broccoli extract induced phase II detoxifying enzymes, such as QR activity, whereas Se-dependent antioxidant enzymes, such as TRx-R and GPx, were increased by treatment with Se in a dose-dependent manner. Interestingly, co-treatment of broccoli and selenium showed a competitive effect to induced QR activity. We found that Se-enriched broccoli florets increased both Nrf-2 dependent phase II enzymes and Se-containing antioxidant enzymes *in vitro*. Furthermore, Se-enriched broccoli and preparations of it were tested in a mouse LNCaP xenograft study. After 8 weeks of dietary Se-enriched

broccoli intervention at a dose of 20% in the diet, none of the preparations had an effect on xenograft growth as well as phase II and anti-oxidant enzymes activities in LNCaP xenograft samples. However, they induced hepatic phase II metabolic enzyme activities such as QR, TRx-R, and GST. Although selenium concentration in the Se-enriched broccoli was elevated enough to induced Se-dependant antioxidant enzymes *in vitro*, Se-enriched broccoli did not induced GPx expression in xenograft or liver samples.

To compare the different preparations in terms of bioavailability, SFN as the major ITC of broccoli and its metabolites were measured in mouse plasma, urine and feces samples after intervention for 7-8 weeks. The major form of SFN metabolites in the plasma and urine samples was SFN-NAC, which showed a linear correlation with the glucoraphanin content in the different broccoli preparations, as well as with QR enzyme induction in the liver. In summary, although selenium fertilization increased selenium contents in the broccoli preparations, these elevated levels did not induce antioxidant enzymes above control levels in mouse xenografts.

4.2 Anti-angiogenic potential of kale sprouts

Angiogenesis (formation of new blood vessels) is implicated in cancer including prostate cancer. It permits the growth and invasiveness of cancer cells leading to metastasis to distant organs (165). Evidence is accumulating to indicate that ITCs potently inhibit tumor angiogenesis in *in vitro* models. In this second part of the thesis, we aimed to test the anti-angiogenic potential of glucosinolate-rich kale sprouts as dietary compound in the LNCaP xenograft model and to further evaluate detailed underlying mechanisms.

4.2.1 Influence on tumor growth, necrosis and hemorrhage

In the present study, dietary intervention with kale sprouts (20% in the diet) was started one week before tumor injection in both sides of the flank of mal nude Balb/c mice (n=10-12). During the duration of the study we monitored tumor growth two times per week for 6.5 weeks by measuring tumor dimensions using a Vernier caliper. Tumor size was then calculated using the following formula: $4.16 \times a^2 \times b$ (a length < b width), as described in Chapter 3.5.3.

As a first results of this study, we observed that dietary intervention with glucosinolate-rich kale sprouts did not inhibit tumor growth in LNCaP xenograft model (Fig. 15) (compare Chapter 4.1.4).
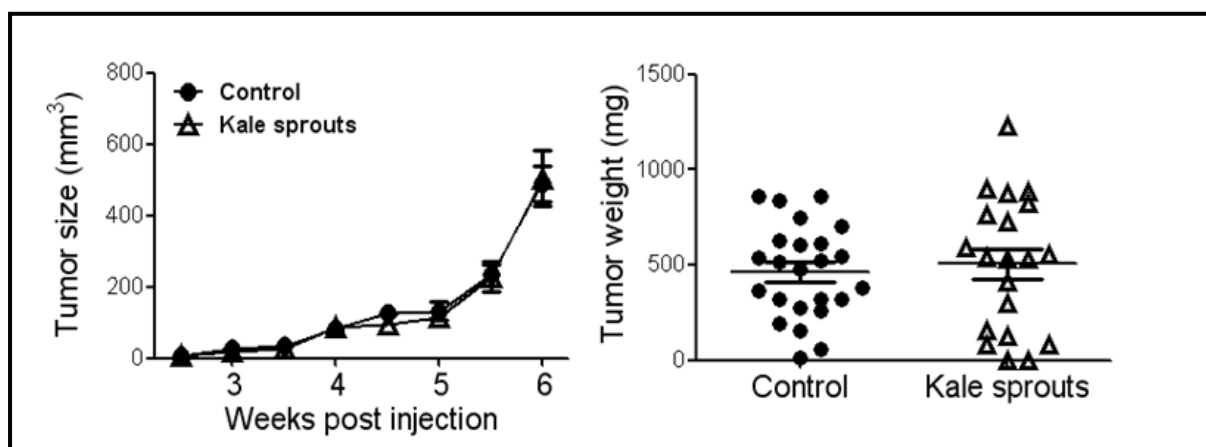
Fig. 15: Influence of kale sprouts on LNCaP xenograft growth. Average tumor size $\pm$ SE (n=20-24) in dietary kale sprouts ($\triangle$) and control ($\bullet$) group is indicated in the left panel. Tumor weights in dietary kale sprouts ($\triangle$) and control ($\bullet$) groups are indicated in the right panel.

Cell growth is controlled by cell proliferation and cell death. To further analyze cell

proliferation in tumor xenografts, slices of paraffin-embedded tumor tissue were immunohistochemically stained to detect levels of proliferating cell nuclear antigen (PCNA), a maker of proliferating cells. To detect cells undergoing apoptosis, we analyzed cleaved PARP levels (cPARP) as a marker of caspase activation. As indicated in Fig. 16A, we did not observe any difference in PCNA staining in the tumor xenografts of both groups when PCNA positive cells were quantified by cell counting in tumor sections. Western blot analysis of PCNA protein expression confirmed the staining results of PCNA (Fig. 16B).
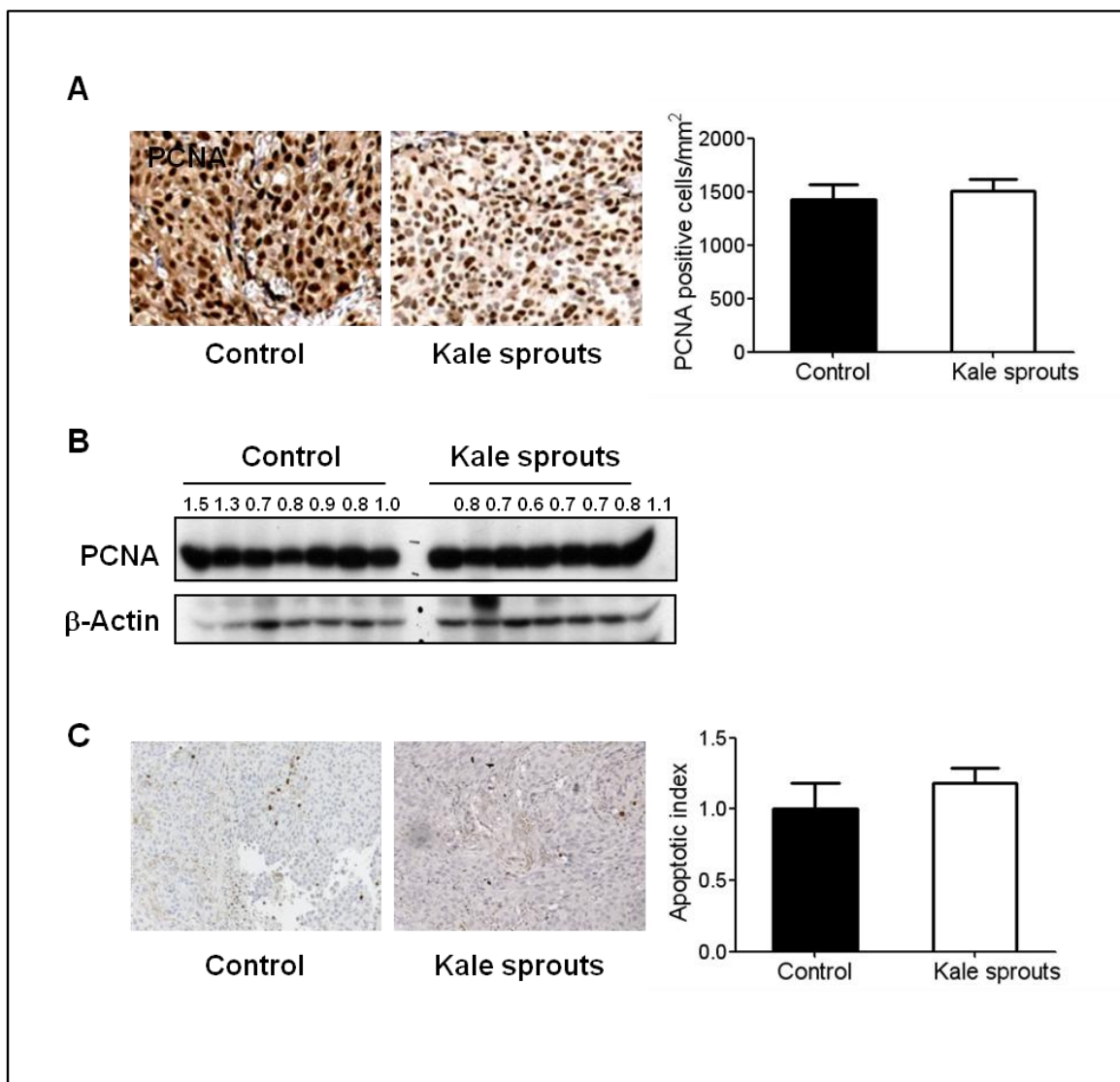
Fig. 16: Kale sprouts has no effect on cell proliferation and apoptosis in LNCaP xenograft model A, PCNA expression in representative LNCaP xenograft sections of control and kale sprout intervention groups (magnification, 100x). The bar graph represents quantitative analysis of PCNA expression. *Columns;* mean (n=8), *bars;* SD. B, Western blotting of PCNA protein expression in LNCaP xenografts of control and kale sprouts intervention groups. The relative band intensity was normalized to β-actin levels and is indicated above the immuno-reactive bands. C, IHC of cleaved PARP in paraffin-embedded LNCaP xenograft of control and kale sprout intervention groups. *Columns;* mean (n=8), *bars;* SD

As indicated in Fig. 16C, the percentage of cells undergoing apoptosis was very low, with an apoptotic index of about 1 in both intervention groups. We did not detect an increase in cleaved PARP staining in the kale sprout group. From this data we conclude that tumors of both groups have a high proliferation rate and low rate of apoptosis.

Further evaluation of the tumor tissue included histolopathological analyses of H&E stained tumor sections by a trained pathologist. A quantitative summary of histological features is given in Table 10.

Table 10. Main histological features kale sprout intervention group vs. control tumors

Sample	Necrosis * (in %)	Stroma (in %)	Inflammation[a]	Hemorrhage[a] *
control tumors				
1L	45	5	1	1
2R	50	5	1	2
3L	55	5	1.5	2
5L	50	15	2	2
6R	47.5	3	1.5	2
8L	40	12.5	1.5	2
11L	35	10	1.25	2
12L	40	15	1	2
kale sprout				
1R	15	5	1	0
2L	5	1	2	0
3L	10	5	1	0
4L	10	10	1	0
4R	5	15	1	1
5L	10	10	1	0
6L	10	5	1.5	0
7R	15	5	1	1

[a]: 0 = none; 1 = low; 2 = high
*: Indicated significant difference between the groups. $p < 0.0001$, *Student`t test* , analysed by sigma plot version 10.

Interestingly, control tumors showed a high percentage of necrosis in 35 to 55% of the tumor mass (median 46.25%, mean $\pm$ SE: 45 $\pm$ 2%) and (moderate to) severe hemorrhage in all samples (compare Fig. 17). Mild inflammation was also present. In contrast, tumors of the kale sprout-treated group showed significantly less necrotic areas (5 to 15 % of tumor mass; median 10%, mean 10% $\pm$ 1%, p< 0.0001, Student's *t*-test with n=8, in comparison to the control group) and almost no detectable hemorrhage (Table 10). Control tumor cells were less differentiated with highly pleomorphic nuclei and abnormal nucleus-plasma-relation, and displayed several mitotic figures and unsharply demarcated borders to the surrounding non-tumorous tissue, representing a highly invasive tumor phenotype (Fig. 17). In contrast,

tumors of the kale sprout group were demarcated more sharply with a thin, partial fibrous capsule in some cases. Nevertheless, the tumor cells themselves presented much more homogenously with only slight pleomorphic nuclei.
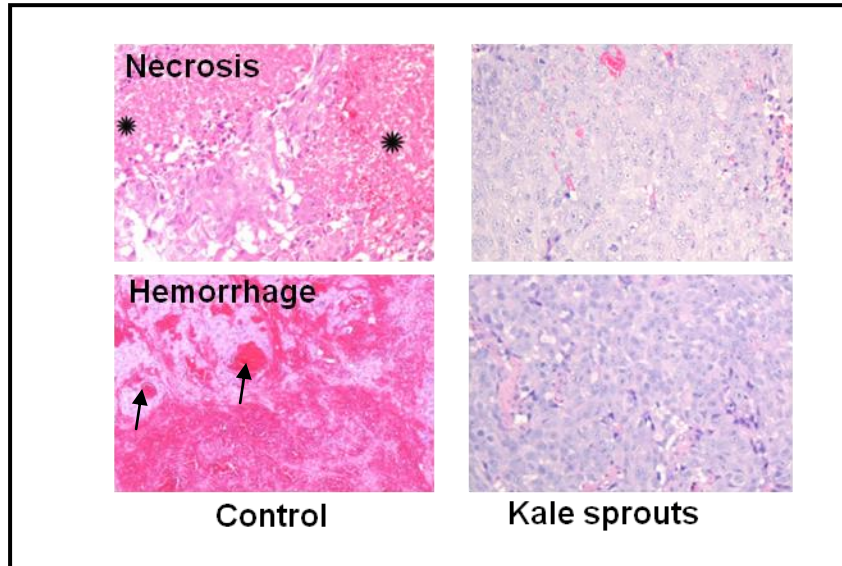

Fig. 17: Dietary kale sprout intervention inhibits tumor necrosis and hemorrhage. H&E staining of LNCaP xenografts of both dietary control and kale sprouts groups. Necrotic areas are indicate by asterisks in the upper panel. Arrows indicated hemorrhagic areas in the lower panel (magnification, 100x)

Taken together, ^{o}ne of the most significant effects of kale sprout intervention was to prevent hemorrhage in LNCaP xenografts and consequently to prevent tumor necrosis.

Hemorrhage is known to be caused by defective angiogenesis, while inhibition of angiogenesis reduces hemorrhage (166). Since LNCaP cells are of human origin, whereas the host, and consequently any new blood vessels, lymph vessels or inflammatory cells near necrotic areas, is of mouse origin, we next stained mouse tissue with mouse IgG to detect any cells invading the tumor tissue. As shown in Fig. 18A and quantified by the pathologist, the area of mouse invading tissue in tumor sections was 23 ± 1 % in control tumors and significantly reduced to 4 ± 0.2 % ($p < 0.01$, tested by Student's t-test) in tumors of kale sprout group.

These results were confirmed by an additional method. We measured mRNA expression levels of mouse housekeeping genes and normalized them with human housekeeping genes. As can be seen in Fig. 18B, the relative expressions of mouse GAPDH and HPRT-1 were 3.8 and 4-fold lower in the kale sprout intervention group compared with the control group ($p < 0.01$, Student's t-test with n=7).
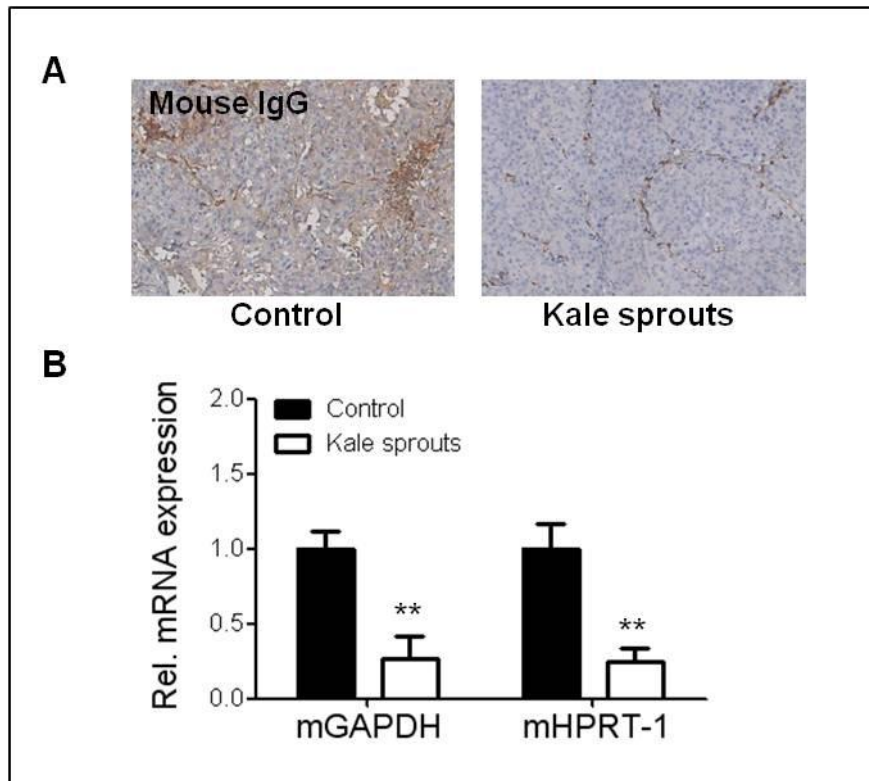
Fig. 18: Dietary kale sprout intervention inhibits invasion of mouse host cells into the human LNCaP tumor xenograft. A, Immuno-histochemistry (IHC) staining of mouse IgG in human LNCaP xenograft of control and kale sprout intervention groups (magnification, 100x). B, Relative mRNA expression of mouse housekeeping genes, GAPDH and HPRT-1 of control and kale sprouts group (n=7). Data are means ± SD, **$p<$ 0.01 tested by Student's t-test from sigma plot software version 10.

To sum up, dietary kale sprout intervention had no direct influence on the tumor growth, but the tumors demonstrated dramatically reduced hemorrhage and necrosis, and fewer invasions of murine cell types.

4.2.2 Induction of vascular maturation

Macroscopic comparison of the tumors indicated striking differences between the two groups: Tumors of the control groups showed a blood-red color, whereas tumors of the kale sprout group tumors were pale (Fig. 19, left panel). We thus measured the hemoglobin content in the xenografts and found a significantly lower Hb level in the kale sprout intervention group (mean ± SE: 5.5 ± 2.3 µg/mg) in comparison with the control group (32.7 ± 3.7 µg/mg, $p<0.01$, *Student's t-test* with n=8).
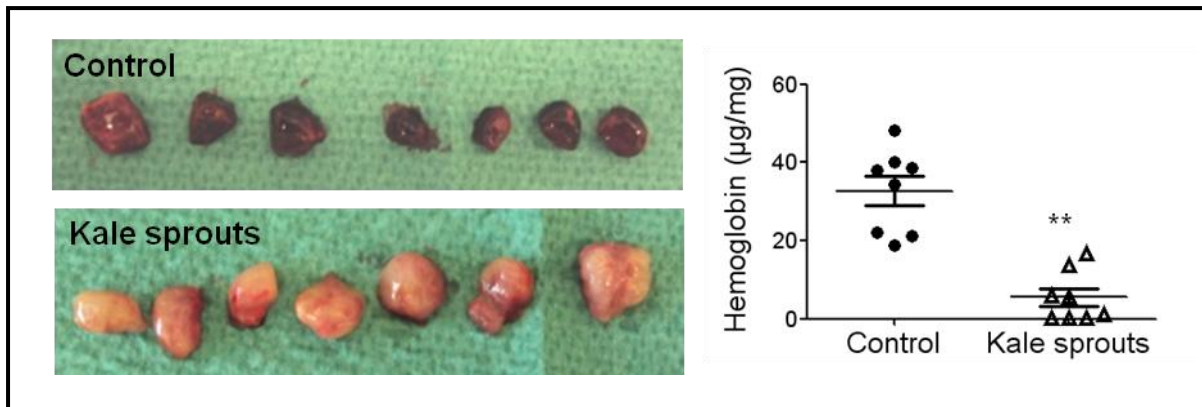
Fig. 19: Kale sprouts intervention reduces hemoglobin content in tumors. Total hemoglobin concentration in the tumor xenograft was measured in tumor homogenates. (●) hemoglobin content in a single tumor of control group, (△) hemoglobin level in a single tumor of dietary kale sprouts. Horizontal lines indicate mean values from eight tumors; bars, SE. ** $p < 0.01$, Student's *t*-test.

The tumor vasculature often contains non-functional and not properly covered, immature and leaky blood vessels (124). To address the question whether the massive hemorrhage and increased murine cell infiltrations in the control group were due to uncontrolled angiogenesis, we investigated the blood vessel density by staining of the blood vessel marker, CD31 (green). Unexpectedly, the vessel density was not different between the groups (Fig. 20A). However, when we co-stained CD31 with α–smooth muscle actin (αSMA, red), which is an early pericyte marker (167), we found significantly more covered vessels (86 ± 1.2%) in the kale sprout group compared to the control group (65 ± 3.2%, $p < 0.001$ Student's *t*-test with n=10) (Fig. 20B). To confirm the result, we additionally performed a co-staining of CD31 (green) and α–desmin (red), which is an another marker for pericytes when the vessels are more in a more mature state (167). The quantification of the α–desmin positively covered vessels yielded an even more significant difference between the two groups with a higher number of covered vessels (96 ± 2.8%) when the mice received kale sprout (Fig. 20C) compared with control diet group (64 ± 2.9%; $p < 0.01$, Student's *t*-test with n=5). These findings strongly suggest that kale sprout diet promotes vessel normalization. Since tumor vessel density was not different between the control and the kale sprout group but the vessel coverage was higher in the kale sprout intervention group, the huge amount of hemoglobin in the control tumors is probably resulting from hemorrhagic vessels.
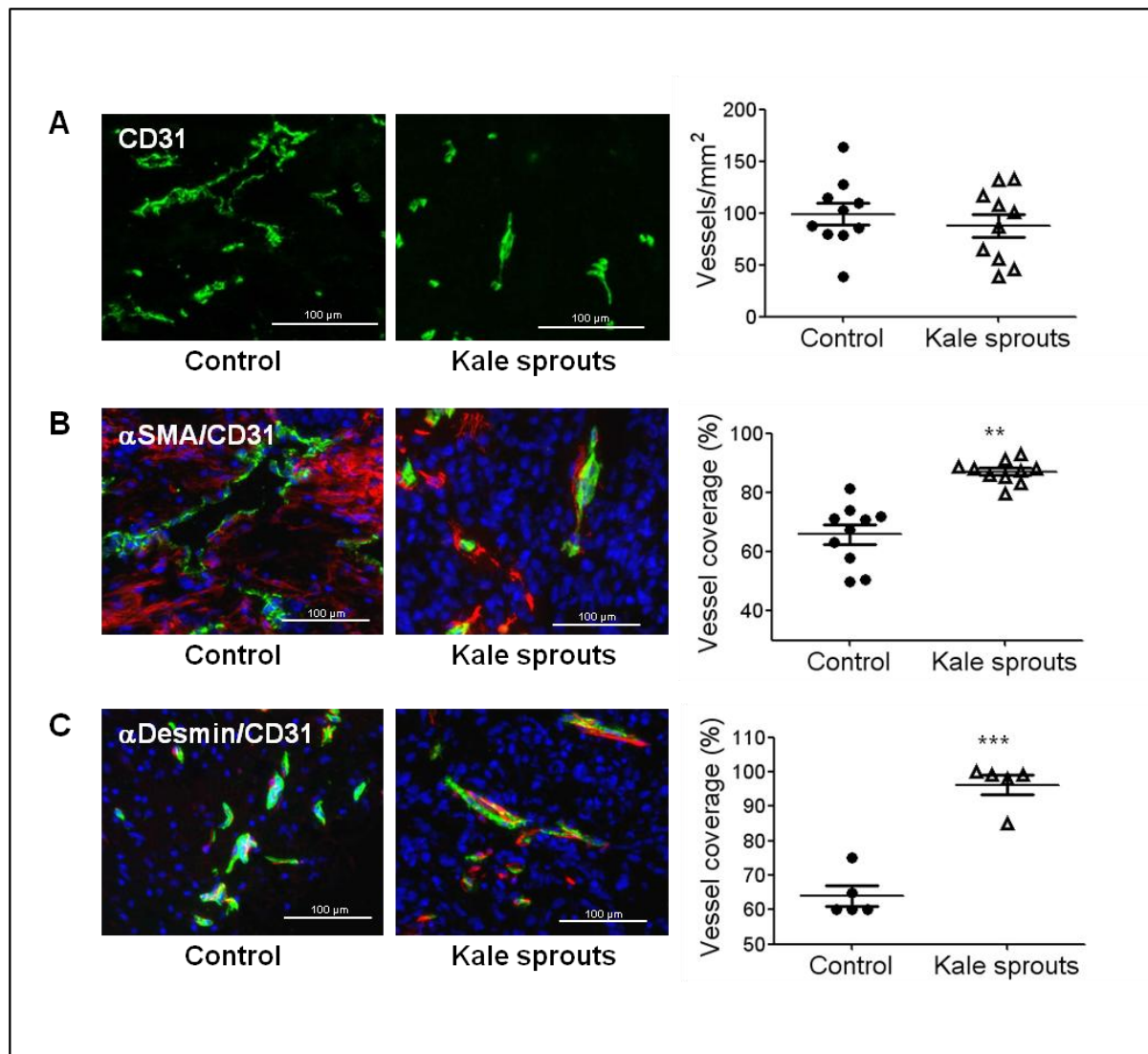
Fig. 20: Dietary kale sprouts induce vascular maturation by coverage of mural cells. A, Total micro vessel density was measured by immunohistochemistry. CD31 (green) antibody was used to stain two sections per tumor sample in five tumors of each group. CD31 positive endothelial cells were counted by image J, total number of vessels were normalized to the area of the photograf (left), each point means 'number of vessels/ area' in each section of tumors. Mean values are presented with horizontal lines, bar means SE. B,C αSMA or α−Desmin positive cells (indicative of early and mature pericytes, respectively) were counted and the percent of covered vessels of total vessel were computed. Mean values are indicated by horizontal lines, bar: SEM. **, ***p<0.01, 0.001, Student's *t*-test.

4.2.3 Inhibition of pro-angiogenic factors and induction of anti-angiogenic factors

In the next set of experiments we addressed the question how kale sprout intervention could induce vessel maturation and prevent hemorrhage. According to a previous report of Jain *et al*, who described that anti-angiogenic therapy can normalize the tumor vasculature by pruning the immature and inefficient vessels and remodel the remaining ones (166), we measured pro-

and anti-angiogenic factors to check weather kale sprout feeding had a similar effect. A well-known target of anti-angiogenic therapy, vascular endothelial growth factor (VEGF), was not altered upon kale sprout diet (Fig. 21).
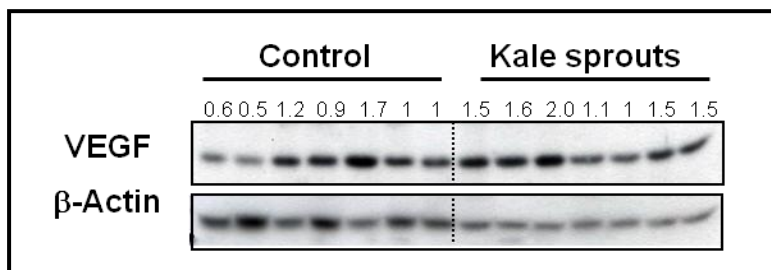
Fig. 21: Kale sprout intervention does not inhibit VEGF protein expression. Western blot evaluation of VEGF protein expression in LNCaP xenograft. Total cell lysates of seven tumors of the control and kale sprout group were used. Numbers indicated band intensity normalized to β-actin levels.

However, other growth factors like placenta growth factor (PlGF) and fibroblast growth factor β (FGFβ) demonstrated reduced mRNA levels by kale sprout intervention (Fig. 22A). We determined a significant 50% reduction of human PlGF mRNA expression, 60% reduction in mouse PlGF mRNA expression and a 75% reduction in mouse FGFβ by kale sprout intervention in comparison to the control group (*,**p< 0.05, 0.01; Student's *t-* test with n=7).
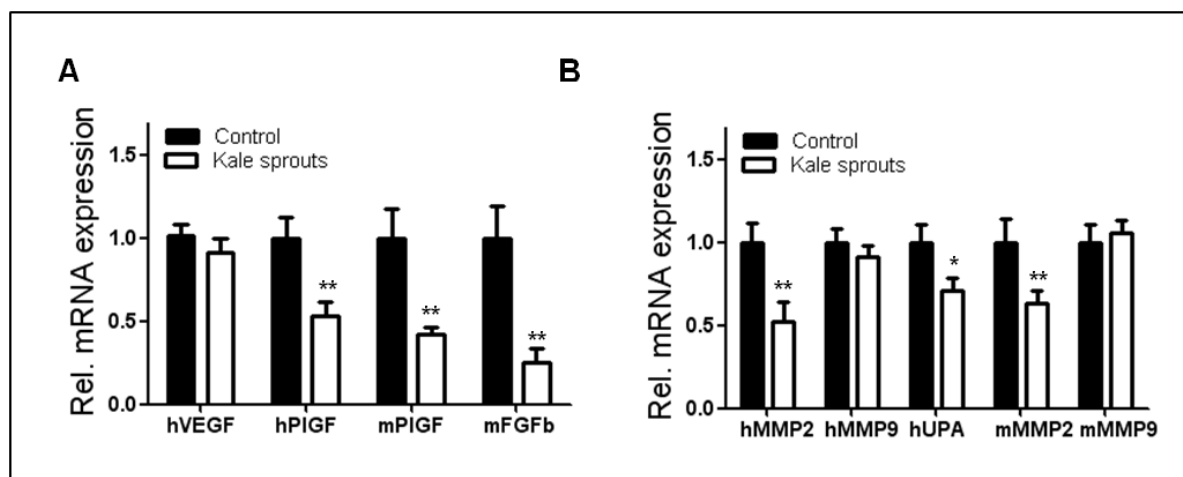
Fig. 22: The effects of kale sprout intervention on pro-angiogenic factors. Relative mRNA expression of human (h) and mouse (m) pro-angiogenic factors (A) and pro-invasive factors (B) were quantified by real-time PCR. Gene expression was normalize to human human β- actin as a housekeeping gene. *Columns*, mean: *bars*, SD, *,**p<0.05, 0.01, Student's *t*-test with n=7).

Similar with our findings a previous study by Fischer and colleagues demonstrated that anti-VEGF treatment reduced vessel density, whereas anti-PlGF therapy promotes vascular normalization rather than reducing vessel density (168). Among the tested pro-angiogenic

factors, mFGFb was the most significantly down regulated by kale sprout diet (Fig. 22A), which is not produced from LNCaP cells (169). One of the most prominent sources of FGFβ are myofibroblasts. Thus, the reduced mFGFb mRNA levels possibly result from a reduced or prevented fibroblast activation or infiltration to the xenografts by in the kale sprout intervention (Fig. 18B).

Next, we analysed mRNA expression levels of factors promoting invarsion. Both mouse and human MMP2 mRNA expression was significantly inhibited by 50% and 40% by kale sprout intervention (**$p<0.01$, Student's *t*-test with n=7) (Fig. 22B). In addition to MMP2, expression of human urokinase plasminogen activator (uPA), a serine protease, was significantly down-regulated by kale sprouts by 30% (*$p<0.05$, Student's *t*-test with n=7) . However, MMP-9 mRNA level was not changed between the two groups. To check the MMP enzyme activity, we performed a gelatin zymography. The amount of catalytically active MMP2 and MMP9 was strongly reduced in the kale sprout group (Fig. 23).
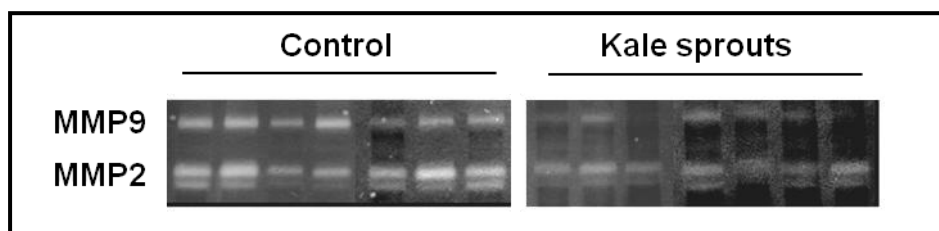
Fig. 23: Enzyme activity of MMP-2 and MMP-9 in tumor cell lysate. The digested band indicating MMP2 and MMP9 enzyme activity was measured by using gelatin zymography.

After checking pro-angiogenic factors, we further investigated the effect of kale sprout intervention on the anti-angiogenic factor angiostatin. The angiostatin protein level, as shown by immunoblotting, was significantly higher in the kale sprout intervention group than in tumors of the control group (Fig. 24). The average of relative band intensity in tumors of the kale sprout group was 2-fold higher than that of control tumors ($p<0.05$).
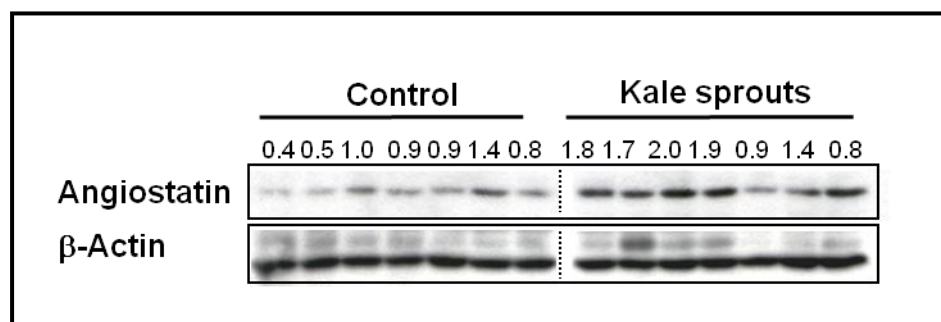

Fig. 24: Induction of angiostatin by kale sprouts intervention. Protein expression of angiostatin was analysed by western blot and normalized by β-actin expression in total tumor cell lysates.

Taken together, regarding the molecular targets of kale sprouts to promote vascular normalization, we found that mRNA expression of mouse FGFβ and PlGF was inhibited rather than VEGF expression. Furthermore kale sprouts induced an anti-angiogenic factor, angiostatin. Antiostatin has been investigated as a cleaveage product of plasminogen by PSA (170). Therefore we further tested PSA secretion.

4.2.4 Influence of kale sprouts on PSA secretion and AR expression

PSA is not only a proliferation marker of hormone-responsive prostate cancer cells such as LNCaP cells, but also a proteinase, which targets plasminogen with angiostatin as a byproduct (170). Since angiostatin levels were elevated in tumors of the kale sprout group, we next tested whether this was related to altered PSA levels. As shown in Fig. 25, dietary kale sprout intervention resulted in significantly 6.5-fold elevated PSA mRNA levels in tumor tissue and 2.2-fold higher PSA protein secretion in mouse serum (p<0.01 and p<0.05 tested by Student's t-test (Fig. 25A) .
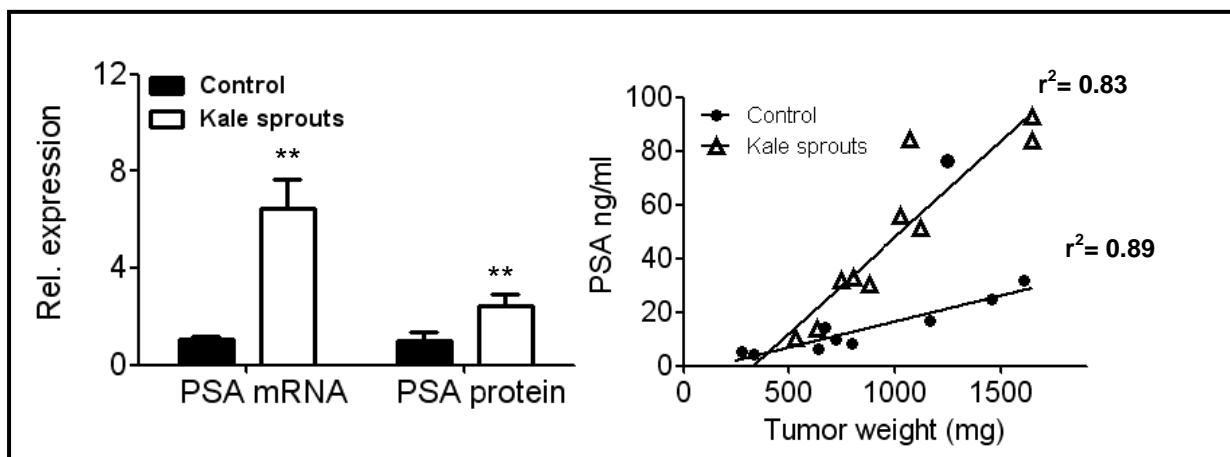

Fig. 25: PSA mRNA and protein levels (A) in relation to tumor weights (B). (A) Relative PSA mRNA and protein levels in tumor material of each group were analyzed by real-time RT-PCR and ELISA (n=7). Means ± SD, **p < 0.01 (Student's *t*-test). (B), Linear correlation of secreted PSA levels in mouse serum and the sum of tumor weights per mouse. (△) kale sprouts group, (●) control group; r²; squared correlation coefficient.

PSA is produced and secreted from LNCaP tumor cells in the xenografts and has therefore been used as a marker of tumor proliferation (171). We found that the serum PSA concentration correlated very well with tumor weights in both the control and the kale sprout group (r^2=0.83-0.89) (Fig. 25B). Interestingly, the slope of the kale sprout group was 2.2-fold

higher than that of control group (Fig. 25B). This indicated that, although the tumor sizes were not different, the tumors of the kale sprout group produced more PSA than control tumors. To understand the mechanisms how kale sprouts induced PSA, we focused on AR signaling because the androgen receptor (AR) is a key transcription factor to induced PSA (12).

Thus, we next analyzed the AR protein levels in the two groups by immunoblotting and immunostaining.
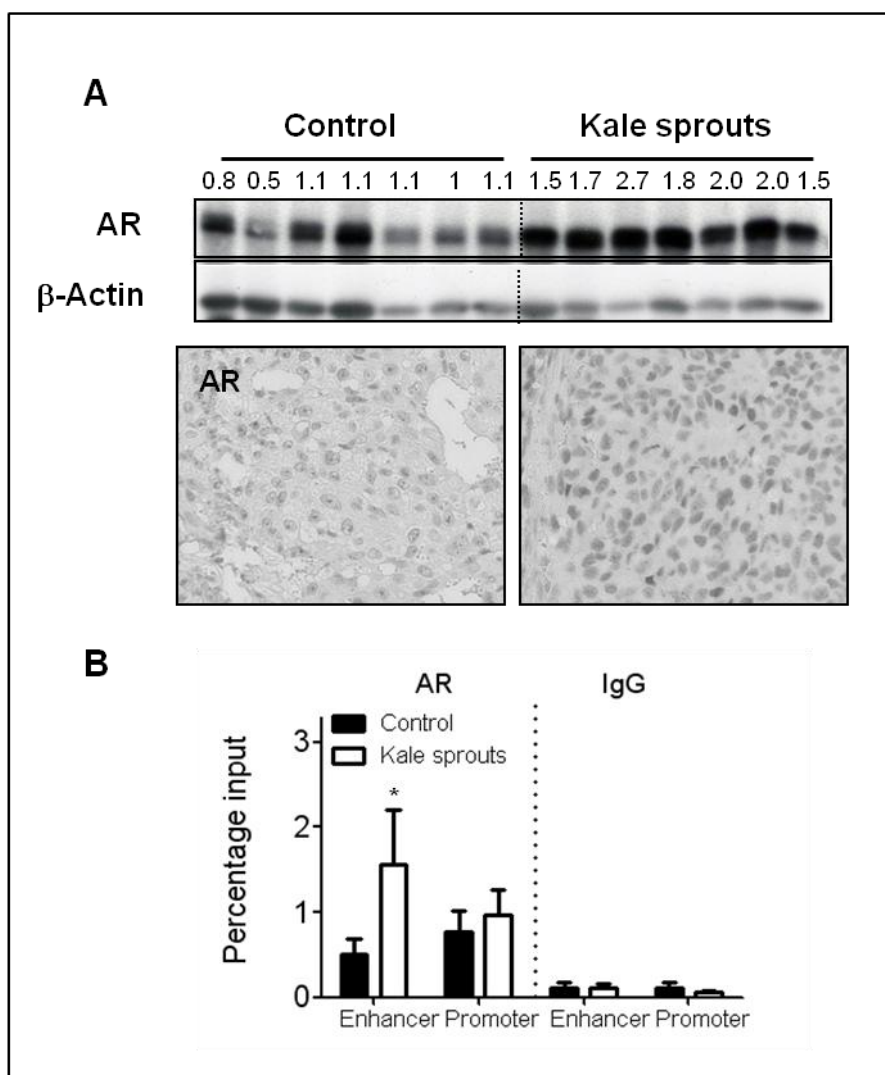
Fig. 26: Kale sprout intervention prevents down-regulation of AR protein expression and binding to PSA promoter. A, Western blotting of AR protein expression (upper panel) of seven tumors in each group. Numbers indicated band intensity normalized to β-actin expression. AR protein was stained by IHC (lower panel). Ten sections of each tumor were stained and positive cells per area was counted. B, Androgen receptor occupancy (using AR antibody) of the androgen response element (ARE) in the PSA enhancer and promoter area was examined by ChIP analyses in four tumors of each group. Input values were obtained from samples treated in the same way as the experimental ones, except immunoprecipitation steps. *p<0.05, Student's *t*-test.

By Western blotting of tumor lysates of both intervention groups, we found significantly higher levels of AR protein expression in the tumors of mice fed with kale sprouts, compared to the control group ($p < 0.001$, Mann-Whitney Rank Sum test). The mean $\pm$ SE of relative band intensities of control vs. kale sprout group is 1.0 ± 0.1, 1.9 ± 0.2).

To proof a direct interaction of AR with the promoter and enhancer sequences of PSA, we conducted a ChIP assay. There we could demonstrate that the binding affinity of AR to the enhancer area of PSA was significantly 3-fold elevated in tumors of the kale sprout group compared to the control group tumors (*$p < 0.05$, Student's t-test with n=4) (Fig. 26B).

One possible explanation of these findings was that kale sprout intervention might induce androgen receptor protein expression in the LNCaP xenografts. However, when we treated LNCaP cells *in vitro* with kale sprout extract at different doses and different time points we could neither observe any induction of the androgen receptor, nor increased PSA secretion (data not shown).

Gastric condensation products of indole-based glucosinolate-derived compounds such as I3C have been reported to modulate the metabolism of estrogen by inducing phase I metabolizing enzymes (172). Since similar mechanisms might be involved in our observations, we performed an *in vitro* digestion experiment with kale sprouts.
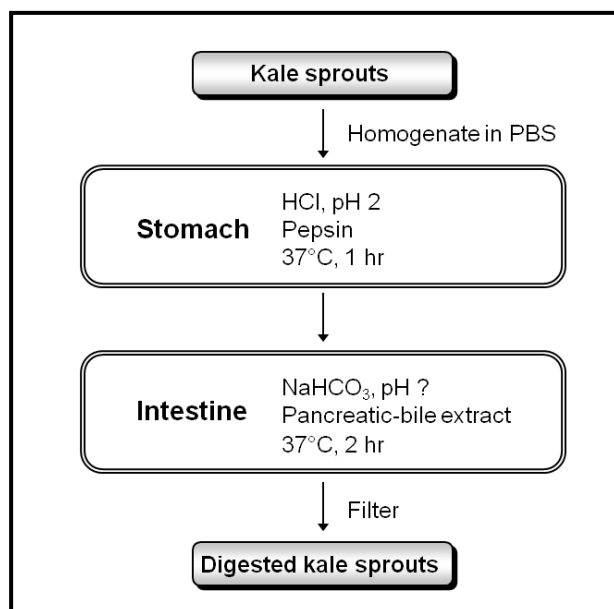

Fig. 27: *In-vitro* digestion of kale sprouts. Kale sprouts or vehicle (PBS) were homogenized in PBS by using a dismembrator at 3000 rpm for 2 x 30 sec. By adding HCl, the pH was adjusted to 2, and pepsin was added. After 1 hr incubation at 37℃, NaHCO₃ and bovine pancreatic–bile extract was added. After 2 hr incubation at 37℃, extract or vehicle was filtered.

To mimic the *in vivo* situation including gastric and intestinal digestion of kale sprouts more

closely in our *in vitro* experiment, we performed an *in vitro* digestion with the kale sprouts (scheme in Fig. 27). Kale sprouts were first homogenized in PBS by using a dismembrator to mimic chewing and to activate myrosinase. Next, by adjusting the pH to 2 and addition of pepsin, gastric conditions were mimicked. After 1 hr incubation at 37 ℃, $NaHCO_3$ and bovine pancreatic–bile extract was added to mimic intestinal conditions. After 2 hr incubation at 37 ℃, extract or vehicle was filtered. LNCaP cells were treated with both 'non-digested' and 'digested' kale sprouts for 24 hr in a concentration range of 0 – 200 µg/ml. However, even under these more 'in vivo' adjusted incubation conditions, AR expression in the total cell lysate as well as PSA secretion in the conditioned media were not induced by kale sprouts treatment (Fig. 28 A, B)
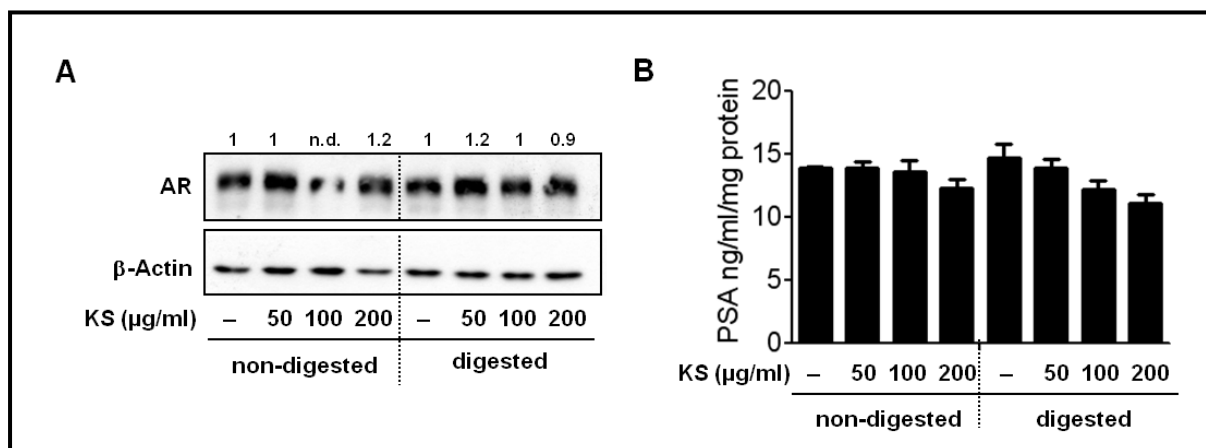

Fig. 28: Kale sprouts do not induced androgen receptor protein expression and PSA secretion in LNCaP cells *in vitro*. A, Androgen receptor protein expression analyzed by Western blotting. Numbers above immunoreactive bands indicate band intensity normalized to β-actin. LNCaP cells were treated with native or *in vitro* digested kale sprout extracts for 24 hrs at the indicated concentration. For the vehicle control, cells were treated with PBS or digested PBS for 24 hrs. B, Secreted PSA concentrations in conditioned media after treatment of with native or digested kale sprouts extract.

As a last test to explain elevated AR levels, we treated LNCaP cells with mouse serum, which was obtained from mice receiving kale sprouts diet. Again, the AR protein expression was not changed compared to treatment with control serum (data not shown). We conclude from these experiments that kale sprout did not directly induce AR signaling, although higher AR levels were detectable in tumors of the kale sprout group, which correlated with the higher PSA levels.

4.2.5 Expression of AR mediated by TNFα

Since neither native nor digested kale sprouts as well as mouse serum which was obtained from the *in vivo* kale sprout intervention study did not induce AR protein expression in LNCaP cells *in vitro*, we hypothesized that kale sprout intervention may alternatively block down-regulation of AR expression in control tumors.

Mizokami *et al.* reported previously that TNFα treatment down-regulates AR protein expression in LNCaP cells (173). When repeating these experiments, we could indeed confirm that LNCaP cells showed reduced AR protein expression upon TNFα stimulation in a dose- and time-dependent manner (Fig. 29).
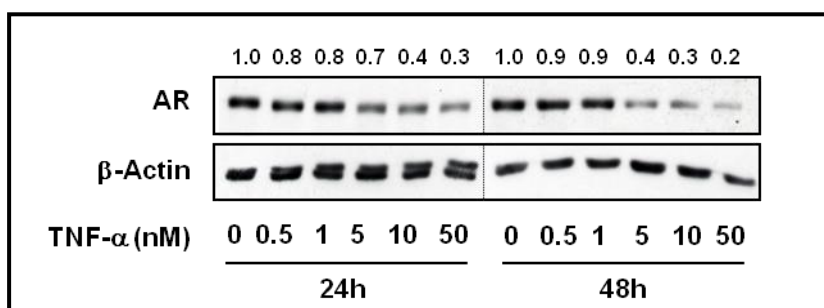

Fig. 29: TNFα treatment down-regulates androgen receptor protein expression. Immunoblotting of AR protein expression after treatment with TNFα at the indicated doses and times in LNCaP cells *in vitro*.

Therefore we hypothesized that kale sprouts intervention blocks TNFα expression as a potential mechanisms to inhibit AR protein expression. To check whether dietary kale sprout had an influence on the TNFα protein levels, we analyzed the protein expression of this cytokine in LNCaP tumor xenograft by western blot analysis. Interestingly, TNFα expression was completely blocked by kale sprout intervention in the tumors (Fig. 30A). Moreover, murine TNFα mRNA levels were significantly inhibited in tumors of the kale sprout fed animals (3.7-fold reduction, $p < 0.05$, Student's t–test with n=7), whereas human TNFα mRNA levels were not affected (Fig. 30B).
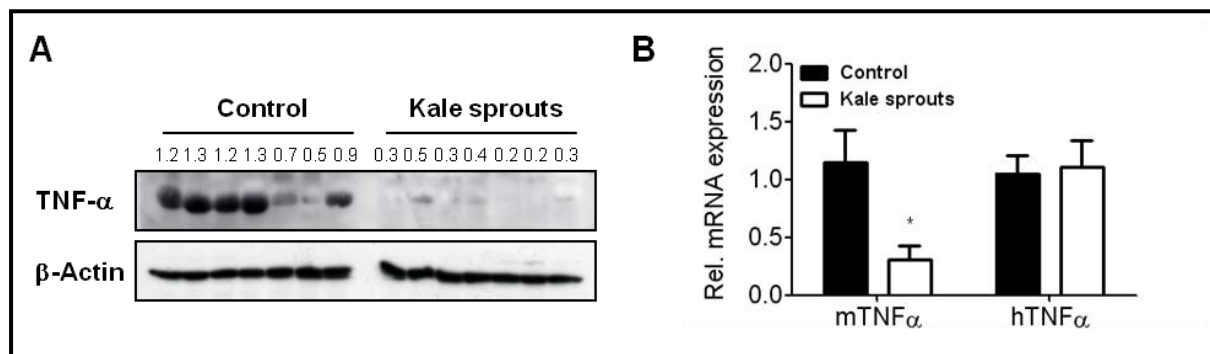
Fig. 30: Kale sprouts block TNFα protein and mRNA expression. A, Immunoblotting of TNFα protein expression using total cell lysates from seven tumors of the control and kale sprout intervention group. B, Relative mRNA expression of human and mouse TNFα was analyzed by quantitative RT-PCR. Means ± SD, *p<0.05, Student's *t*–test with n=7.

Heiss and colleagues described earlier that SFN inhibits LPS-induced TNFα secretion in mouse macrophages (49). Kale sprouts contain relatively high amount of glucoraphanin, the precursor of SFN, and structurally related glucosinolates, which maybe inhibit TNFα secretion in the LNCaP xenograft. Therefore we next tested whether TNFα mediated down-regulation of AR expression is prevented by kale sprouts. Treatment of LNCaP cells with 5 nM TNFα for 24 hrs reduced AR protein expression by 40%. This down-regulation was blocked by co-treatment with kale sprout (Fig. 31A). Furthermore, the significant reduction in PSA secretion by LNCaP cells upon stimulation with 5 nM TNFα for 36 hrs was potently inhibited by co-treatment with kale sprouts in a dose dependent manner (Fig. 31B).
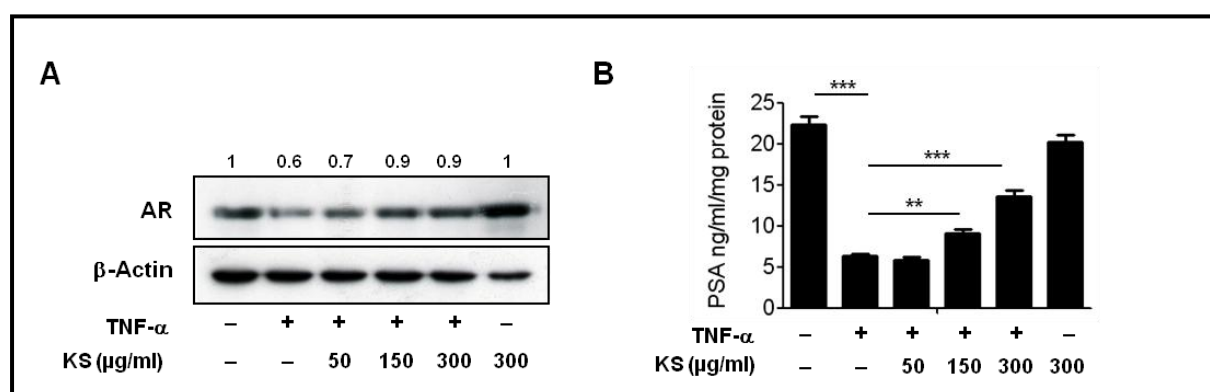

Fig. 31: Kale sprouts prevent TNFα–mediated AR down-regulation in LNCaP cells. A, AR protein expression. Cells were treated with TNFα alone or co-treated with kale sprout (KS) extract at the indicated concentrations. After 24 hrs incubation total protein was harvested and AR protein expression was measured by Western blotting. Numbers above the immuno-reactive bands indicate expression intensity of AR normalized to β-actin levels. B, Secreted PSA in conditioned media after treatment of TNFα alone or in combination with kale sprouts. *Columns*, mean; *bars*, SD, **,***p<0.01, 0.001 analyzed by AVOVA with Tukey post-hoc test for multiple comparisons.

Finally, we were curious whether we could link the elevated PSA levels in the kale sprout group in the *in vivo* xenograft model to the induction of angiostasis. Therefore, we correlated the PSA levels with the hemoglobin concentration which stands for angiostasis in both groups. Interestingly, we observed an inverse correlation both between PSA mRNA levels and secreted PSA with the Hb concentration ($r^2 = 0.75$ and $r^2 = 0.62$) (Fig. 32).
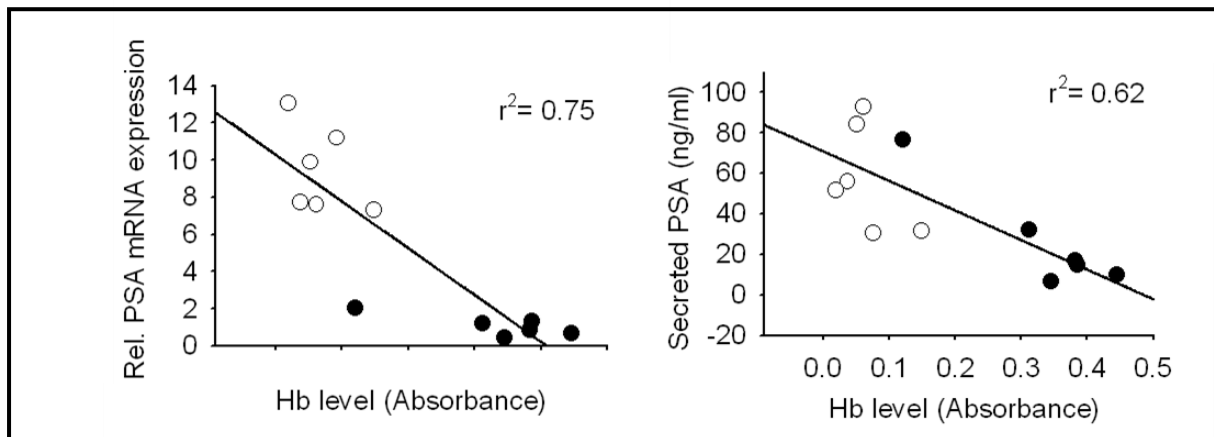

Fig. 32: Inverse correlation between Hb concentration and PSA in LNCaP xenograft model. (A) PSA relative mRNA expression and Hb concentration of each tumor of the control and kale sprout group was correlated, r^2 squared correlation coefficient, tested by Sigma plot version 10. (B) Secreted PSA level in mouse serum and Hb concentration in tumors of control and kale sprouts group was correlated, r^2 squared correlation coefficient, tested by Sigma plot version 10.

4.2.6 Summary

The angiogenic potential of cancer cells is regulated by several pro- and anti-angiogenic factors as well as growth factors, cytokines and MMPs. We here could demonstrate that kale sprout intervention inhibited the expression of pro-angiogenic factors, like FGFb and PlGF, and MMPs, and induced the anti-angiogenic factors angiostatin and PSA via inhibition of TNFα. The combination of these factors led to vascular normalization, thus prevented the leakage of blood and thereby reduced tumor necrosis (Fig. 33).
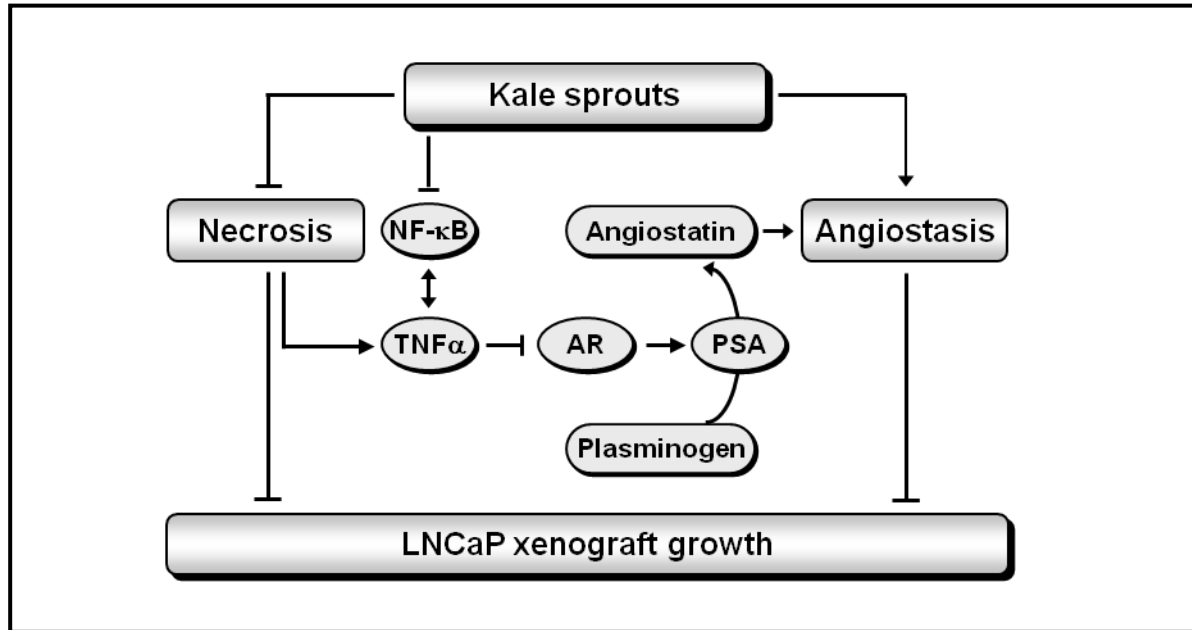
Fig. 33: Scheme of anti-necrotic and angiostatic potential of kale sprouts in LNCaP xenograft model. Based on our results we propose:1) Kale sprouts inhibit tumor necrosis. 2) TNFα secretion is blocked by kale sprouts which leads to maintained AR protein expression and PSA secretion. PSA has been studied as an anti-angiogenic factor in prostate cancer because it promotes angiostatin production by degradation of plasminogen. 3) Induced blood vessel maturation (angiostasis) by inhibition of pro-angiogenic factors and induction of anti-angiogenic factors by dietary kale sprouts may block hemorrhage and tumor necrosis. Dietary kale sprouts play a dual role with respect to tumor growth, on the one hand blocking of necrosis may induced tumor growth but in the other hand angiostasis inhibits tumor growth. Overall tumor growth is not changed even though many factors inside of the tumors are changed.

4.3 Epigenetic modifications by kale sprout intervention in LNCaP xenografts

Since several ITCs have been identified as HDAC inhibitors in various cancer cell lines including prostate cancer cell lines, the last part of this thesis sought to verify whether dietary kale sprouts, rich in glucosinolates, also acts as an HDAC inhibitor in the prostate cancer xenograft model.

4.3.1 Induction of histone acetylation but no inhibition of HDAC activity

As a first approach to analyze the effect of kale sprout intervention on histone acetylation, we isolated histones from xenograft samples and determined their acetylation status by Western blotting using pan specific antibodies for acetylated histones H3 and H4. As shown in Fig. 34, daily intervention with kale sprouts for 7.5 weeks induced histone acetylation at H4 rather than at H3 (Fig. 34 A) in LNCaP xenografts. The immunoblotting confirmed that level of acetylated H4 was 2-fold increased in the kale sprout dietary group compared to the control group. This was in line with earlier findings that oral administration of SFN for 21 day induced 50 % of acetylation at histone H4 in a PC-3 xenograft model (174).
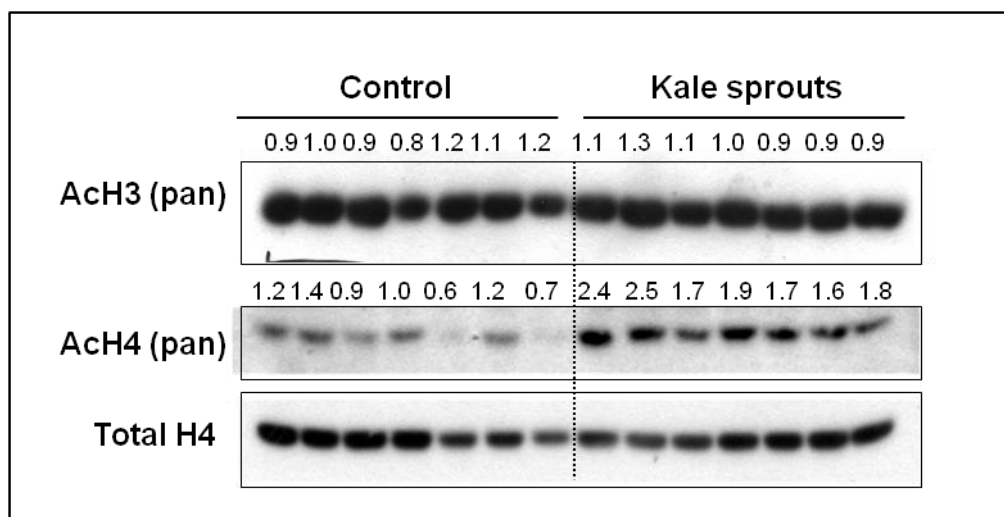
Fig. 34: Increased global histone acetylation at histone H4 after intervention of kale sprouts. Acetylation of histones H3 and H4 was measured in acid-extracted histone samples from seven tumors of each group. Total H4 was used as a loading control.

Since we could confirm that histone acetylation was induced by kale sprout intervention, we further determined the enzymatic activity of HDAC, which is the key enzyme to modulate

histone acetylation status. Interestingly, when nuclear fractions of tumor samples were analyzed for HDAC activity using the Fluor-de-Lys assay, no change in HDAC activity by kale sprout intervention could be observed (Fig. 34B).
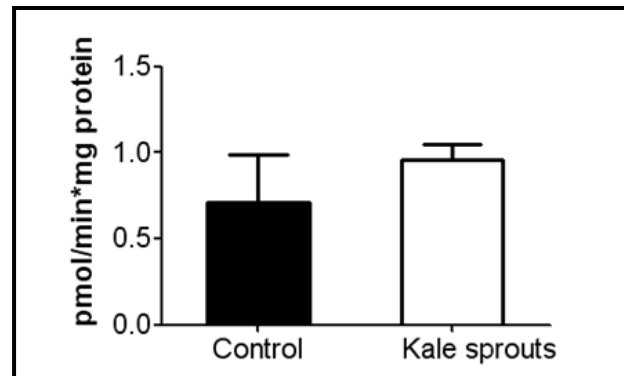

Fig. 34: Kale sprout intervention does not inhibit HDAC activity. HDAC activity in nuclear fraction of eight tumors in each groups was measured by the Fluor-de Lys assay and normalized to protein concentration. *Columns:* Means, *bars:* SD.

4.3.2 Acetylation on each lysine residue and HDACs expression

After demonstrating up-regulated global histone acetylation, but lack of inhibition of HDAC activity by kale sprout intervention in the LNCaP xenograft model, we decided to next determine the acetylation status at each individual lysine residue on histone H4 to identify whether selected lysines were particularly acetylated.
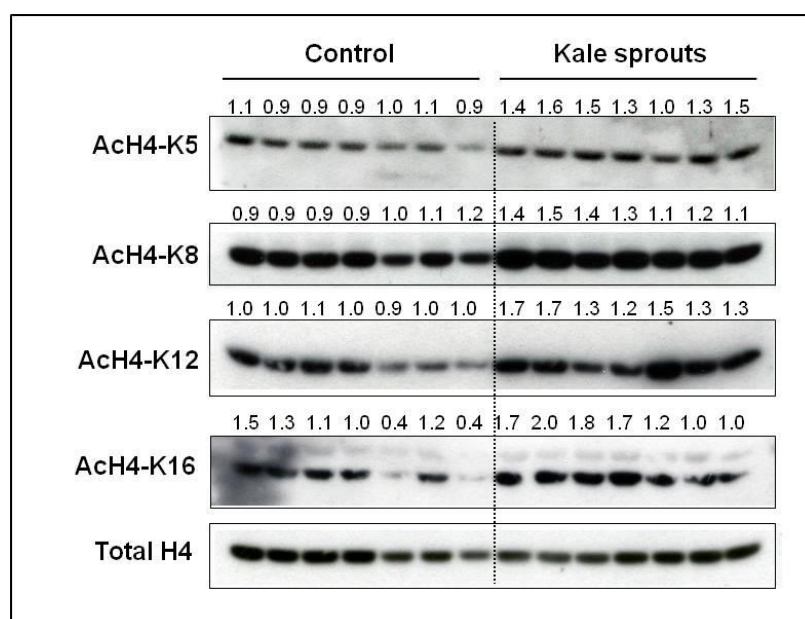

Fig. 35: Histone aceylation at each H4 lysine group in tumors after kale sprouts intervention. Acid-

extracted histone samples of seven tumors of the control and kale sprout intervention groups were used to detect acetylation at each lysine group K5, K8, K12 and K16 of histone H4. Total H4 was used as a loading control.

Acetylation at H4-K12, preferentially acetylated at newly synthesized histones, was mostly induced in tumors of mice fed the kale sprout diet. However, increased acetylation was also detected at all other the lysine residue of H4 in LNCaP xenograft samples after kale sprout intervention (Fig. 35).

As outlined in Chapter 1.6, HDACs are a large enzyme family with several subclasses. Since kale sprout intervention induced histone acetylation, but did not inhibit total nuclear HDAC activity, we further investigated the influence of kale sprout intervention on the expression of individual classes of HDACs, using whole cell lysates of xenografts of both intervention groups.
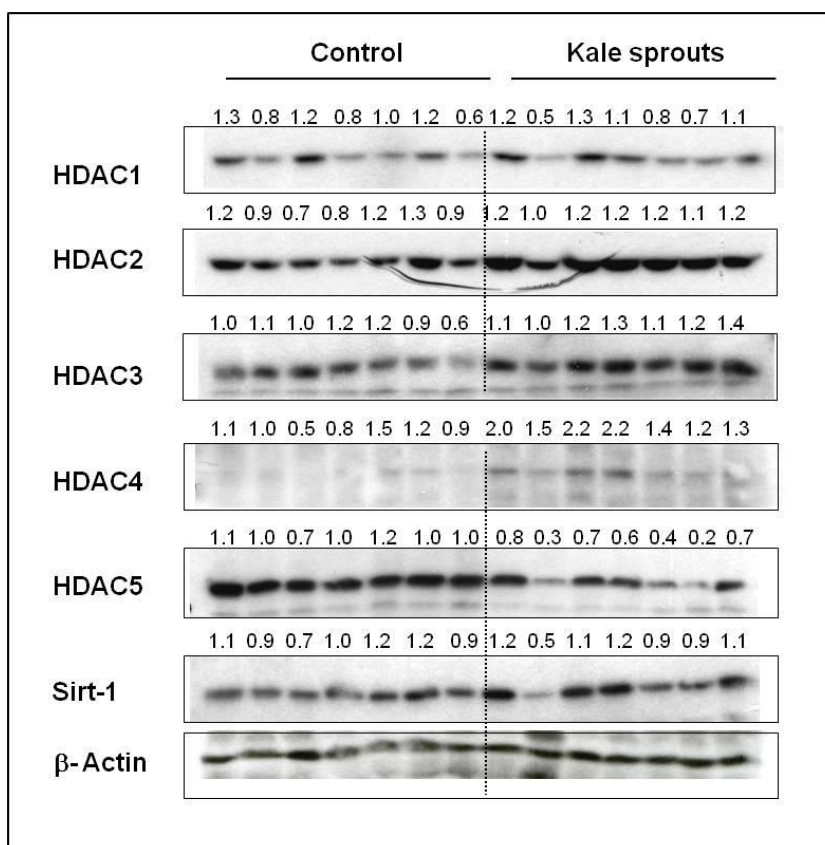
Fig. 36: HDAC expression in tumors after kale sprouts intervention. Expression of HDAC 1-5 and Sirt 1 in seven tumors of each group was determined by Western blot analysis using specific antibodies.

Interestingly, kale sprout intervention differentially influenced expression of individual HDACs (Fig. 36). Of the class I HDACs, HDAC1 expression was not influenced, whereas HDAC 2 and 3 were weakly induced by the kale sprout intervention. Of the class II HDACS,

HDAC4 was almost undetectable in tumors of the control group, and was also weakly induced in the kale sprout group. Only HDAC5 expression was reduced by kale sprout intervention. Sirt1 was analyzed as an example of a class III HDAC. There was no difference in expression detectable between both intervention groups. These data did not help to understand why lysines at histone H4 were consistently hyperacetylated in tumors of the kale sprout group.

4.3.3 Induction of HAT expression

The histone acetylation status is balanced by the opposing activities of HDACs removing acetyl groups and HATs (histone acetyl transferases) adding acetyl groups. Since we could not detect any inhibitory effect of the kale sprout intervention on the activity or protein expression of selected HDACs, we next investigated the influence of kale sprouts on the expression of selected HATs.
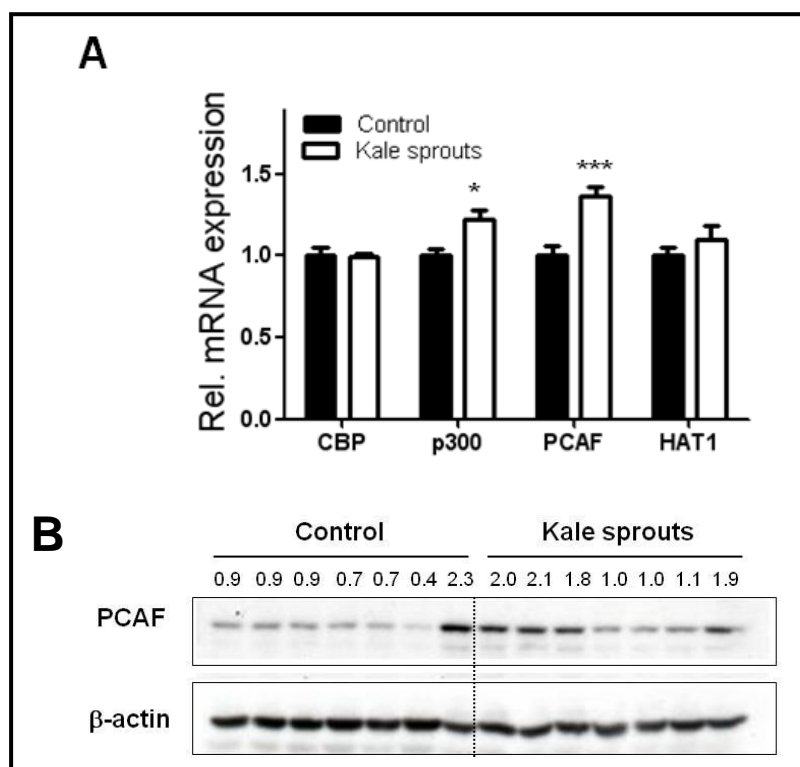
Fig. 37: Kale sprouts intervention increases PCAF mRNA and protein expression. (A) Relative mRNA expression of four HATs in LNCaP xenografts, measured by quantitative RT-PCR. Data gene expression of HATs were normalized to human β-actin and calibrated to levels in control samples (n=7). *Columns*: mean; *bars*, SD, *, ***$p<0.05$, 0.001, Student's *t*-test. **(B)** PCAF protein levels in nuclear fractions of seven individual tumors in each group were detected by Western blotting. β-Actin was used as a loading control.

Certain transcriptional co-activators, including CREB-binding protein (CBP), p300, and p300/CBP-associated factor (PCAF) possess intrinsic HAT activity. As shown in Fig. 37A, relative mRNA expression of p300 and PCAF was significantly increased by dietary kale sprouts by 20% and 40% in xenograft samples (*,***p< 0.05, 0.001, Student's *t*-test with n=7), whereas mRNA levels of CBP and HAT1 were not influenced. We could confirm the induction of PCAF by kale sprout intervention also at the protein level in nuclear extracts of LNCaP xenografts (Fig. 37B).

To investigate the possible mechanism why PCAF mRNA and protein expression was induced, we analyzed the acetylation status at the PCAF promoter area by chromatin immunoprecipitation (ChIP). Interestingly, acetylation at H4 at the PCAF promoter was increased 2-fold in tumors of the kale sprout group compared to samples from the control group (**p<0.01, Student's *t*–test with n=4) (Fig. 38). IgG served as a negative control with samples processed by the same protocol except immunoprecipitation with Ac-H4 antibody. These results indicated that increased histone acetylation was associated with increased PCAF mRNA expression.
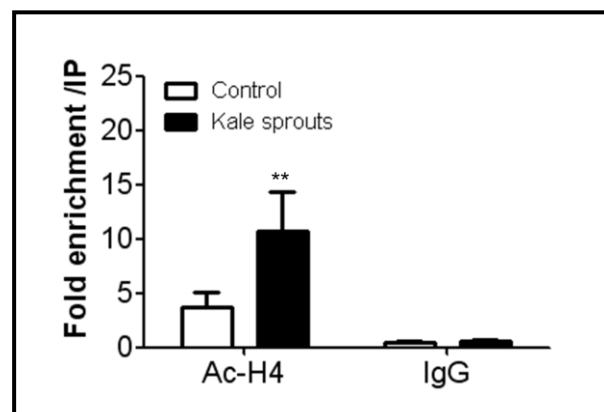
Fig. 38: Increased association of acetylated H4 at the promoter region of PCAF by kale sprout intervention. Fold enrichment of acetylated histone H4 at the PCAF promoter area was measured in four tumors of each group. IgG was used as negative control with the same tumor samples of each group. *Columns*: mean; *bars*, SD, **p< 0.01, Student's *t*–test with n=4.

4.3.4 Influence on cell cycle inhibitor p21 expression

It is well established that the expression of the cyclin-dependent kinase inhibitor and cell cycle regulator p21 is induced by HDAC inhibitors (175). To further determine functional consequences of increased histone acetylation in tumors of mice on a kale sprout diet, we measured p21 mRNA and protein expression and acetylated histone enrichment in the

promoter region of the p21 gene. The relative mRNA expression of p21 was significantly 2-fold induced by kale sprout intervention in LNCaP xenografts (**p<0.01, Student's *t*–test with n=7) (Fig. 39A) and this was in line with enhanced protein expression (Fig. 39B).
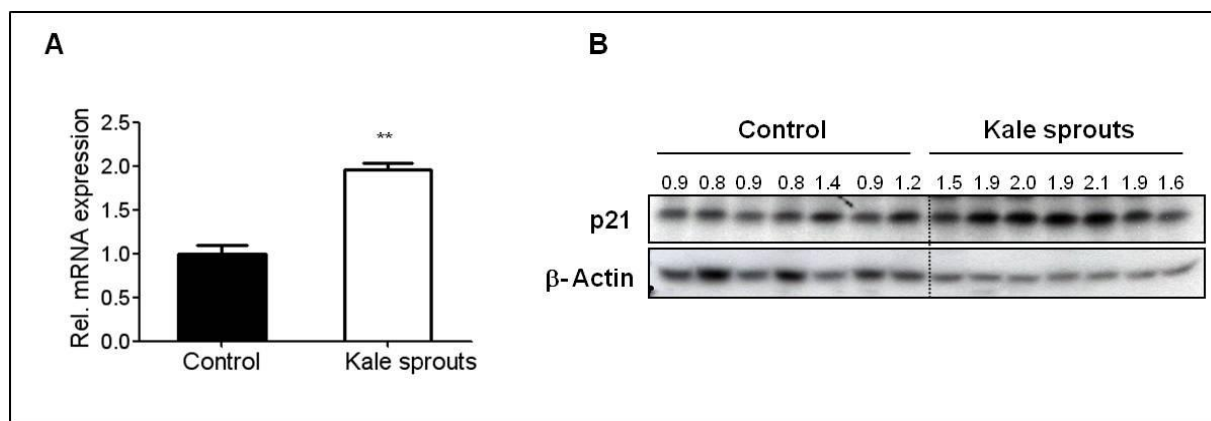

Fig. 39: p21 expression is elevated in xenografts by kale sprout intervention. (A) Relative mRNA expression of p21 in LNCaP xenograft was measured by quantitative RT-PCR. *Column*: mean, *bar:* SD, **p<0.01, Student's *t*–test with n=7. (B) p21 protein expression was measured by Western blot analysis.

To clarify whether p21 gene expression in xenografts of the kale sprout group was due to the increased histone acetylation, we further measured binding of acetylated H4 in the promoter region of p21 by chromatin immunoprecipitation. Kale sprout intervention significantly increased the association of acetylated histone H4 at the promoter area of p21 gene compared to samples of mice on the control diet (*p<0.05, Student's *t*–test with n=4) (Fig. 40).
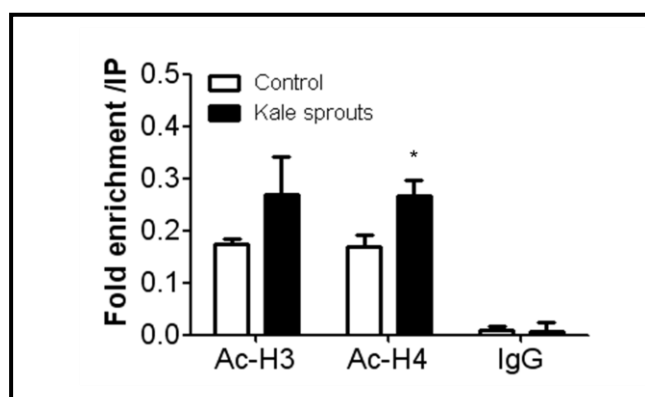
Fig. 40: p21 expression is associated with increased histone acetylation at H4. Relative enrichment of acetylated histone H3 and H4 versus IP control at the p21 promoter area was measured in four tumors of each group. IgG was used as negative control using the same tumor samples. *Columns*: mean, *bars*: SD, *p< 0.05, Student's *t*–test with n=4.

4.3.5 Mitotic arrest

To determine the downstream effects of histone acetylation and p21 induction by kale sprouts,

mitotic arrest was examined by immunohistochemistry and immunoblotting, using the mitotic cell marker, phospho-H3 (p-H3). We could demonstrate that kale sprout intervention induced mitotic cell cycle arrest in LNCaP xenografts. Immunohistochemical detection of p-H3 in paraffin-embedded xenograft sections indicated that in tumors of the kale sprout group, the number of p-H3 positive cells was increased (Fig. 41A). When we counted the number of positive cells per 1000 cells which indicates the mitotic index, tumors of the kale sprout group had a significantly 30% increased mitotic index compared with control tumors (***p<0.001, Student's *t*–test with n=6) (Fig. 41B).
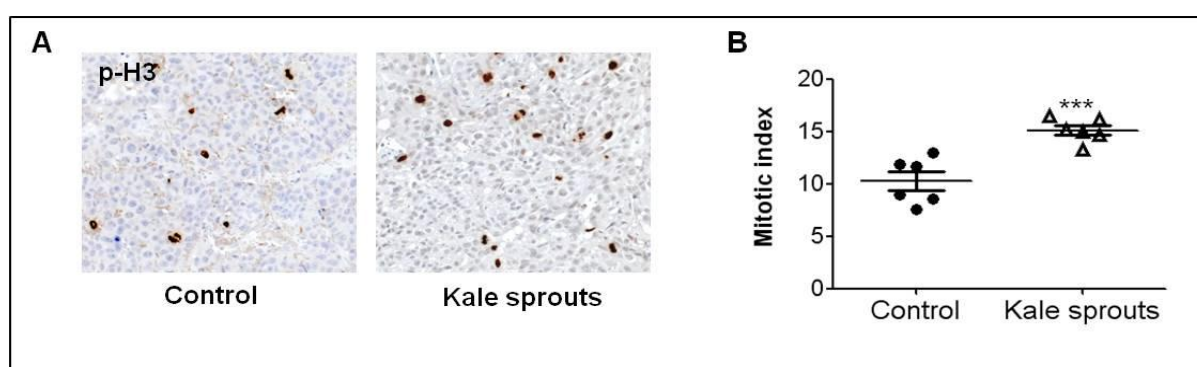
Fig. 41: Evidence of mitotic arrest in tumors by kale sprout intervention. (A) Phospho-H3 was detected by immunohistochemistry in paraffin-embedded tumor sections. 10 slides from each tumor were stained with phospho-H3 and counterstained. (B) Phospho-H3 positive cells in each slide were counted by image J. Mitotic index indicates numbers of positive cells in 1000 cells. ***p<0.001, Student's *t*–test with n=6

Increased histone H3 protein phosphorylation was also shown in total cell lysate of tumor tissue of the kale sprout group compared with control by Western blotting, confirming our immunohistochemistry data (Fig. 42).
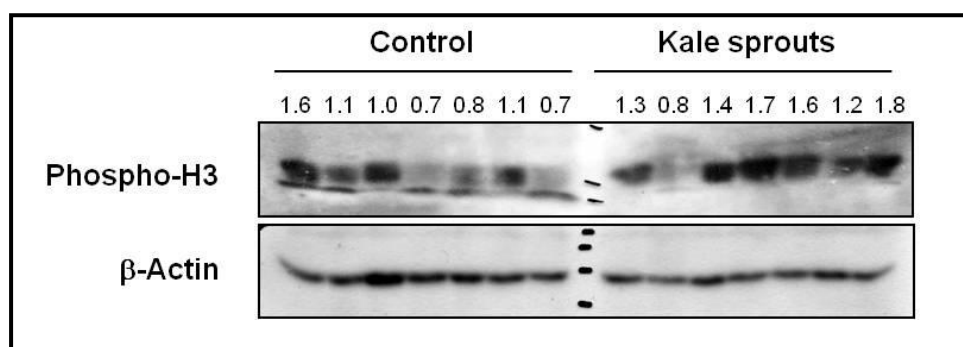
Fig. 42: Increased histone H3 phosphorylation, a mitotic marker, by kale sprout intervention. Phospho-H3 levels were measured by Western blot analysis. 30 µg of total protein from seven tumors in each group were analyzed. Actin was blotted after stripping the membrane as a loading control.

In summary, although average tumor weights in both intervention groups were not

significantly different (as shown in Chapter 4.2.1) we could demonstrate that control tumors contained significantly larger necrotic areas than tumors of the kale sprout group (Fig. 17). Also, kale sprout intervention causes histone hyperacetylation, resulting in PCAF and p21 upregulation and mitotic arrest. Overall, these mechanisms may lead to a reduction of tumor growth or of tumor-associated death in more long term carcinogenesis models.

4.3.6 Human intervention study- induction of histone acetylation in PBMC

Although efficacy in animal models gives a good indication whether an intervention might be relevant for the human situation, ultimately effects need to be demonstrated in humans. As a first test to address the question whether kale sprouts affect histone acetylation in humans, we performed a small pilot study with five female subjects. We decided to analyze H4 acetylation in peripheral blood mononuclear cells (PBMC) as a surrogate biomaterial after kale sprout intervention. Healthy women volunteers in the age range 20-50 years, with no history of non-nutritional supplement use, refrained from cruciferous vegetable intake for 24 hr. They consumed 10 g of kale sprouts, containing approximately 800 µmol of total glucosinolates, with some water. After a light lunch, blood was drawn 1.5 and 3 hrs after kale sprout consumption. PBMCs were isolated, lysed, and whole cell lysates were used for Western blotting. In comparison to ac-H4 levels before intervention (time 0h), a time-dependent increase in histone H4 acetylation was detected in PBMCs of all volunteers (Fig. 43). Induction was already detectable 1.5 h after kale sprout consumption, and further increased up to 3 h. Maximum induction differed between individuals. This was partly due to differences in basal levels, and might additionally depend on differences in bodyweight-adjusted doses. This data indicate that histone acetylation is regulated very rapidly. Also, we could demonstrate that it is possible to consume biological effective doses by dietary consumption. So far we have no further information on organ-specific histone modifications.
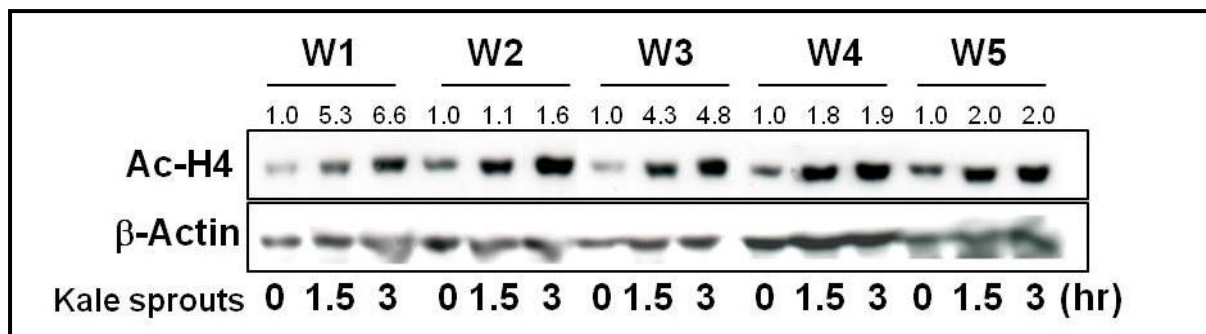
Fig. 43: Induction of histone acetylation by kale sprout intervention in human volunteers. Five healthy female volunteers (W1-W5) consumed 10 g kale sprouts with water. Blood was collected at the indicated times. Acetyl-H4 was detected in total PBMC lysates by immuno-blotting, using β-actin as a loading control.

4.3.7 Summary – histone modifications by kale sprouts

Recently the potential of various isothiocyanates to inhibit HDAC activity was investigated. The present investigation has shown that dietary kale sprouts, rich in isothiocyanate precursors, increased histone acetylation associated with increased HAT rather than inhibition of HDAC activity in the LNCaP xenograft model. The changing balance between HAT and HDAC activity and expression by kale sprouts was associated with increased histone acetylation at the promoter of p21 and gene expression in the LNCaP xenograft model. Mitotic arrest was observed as a consequence.
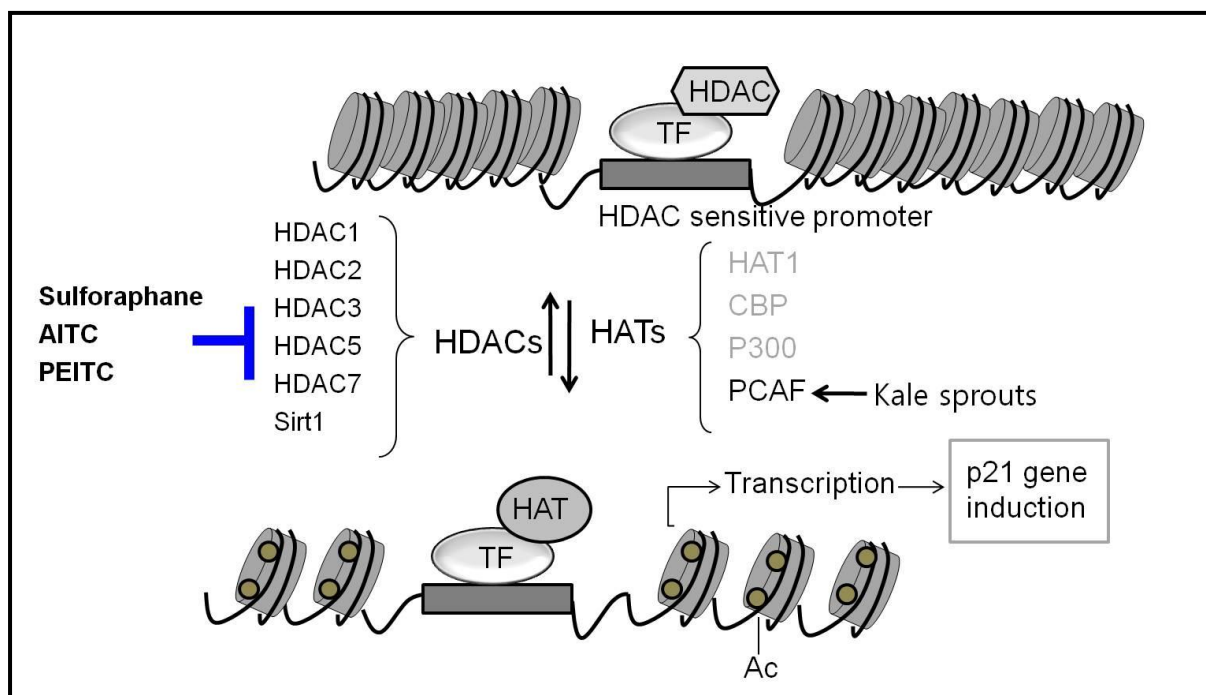
Fig. 44: Summary - histone modifications by kale sprouts. Dietary consumption of kale sprouts increased global acetylation of histone H4 in tumor xenografts even though it had no effect on tumor growth. Hyper-acetylation of histone is possibly due to induction of HAT expression rather than inhibition of HDAC activity.

5 DISCUSSION

Dietary factors are major elements accounting for international and interethnic differences in prostate cancer rates (176). Chemoprevention is defined as the use of pharmaceutical agents, dietary components, natural products, food supplements (vitamins, selenium) or other agents in order to reduce the risk, delay the development, or prevent the recurrence of cancer (19). Prostate cancer is believed to be a suitable candidate for chemopreventive strategies as it develops in a multistep process with involvement of genetic mutations, inflammation, impaired differentiation, proliferation, hormone dependence and metastasis as important factors during prostate cancer development (Chapter 1.1.2).

Various agents have been evaluated for their primary and secondary chemopreventive potential targeting different stages and molecular signaling pathways of prostate cancer, which include selenium and cruciferous vegetables.

Selenium, a macronutrient exists naturally in food predominantly in the an organic form. It has the potential to reduce prostate cancer risk by targeting aspects of prostate cancer carcinogenesis including proliferation and the redox status (previously described in Chapter 1.2.2.1).

Cruciferous vegetables include the *Brassicaceae* family with most prominent members such as broccoli, cauliflower, and kale. As a family they have the unique feature to contain large amounts of glucosinolates. The metabolic product of glucosinolates, isothiocyanates (ITCs), exerts a very broad spectrum of chemopreventive activities in prostate cancer development (described in Chapter 1.2.2.2).

Combination of potential agents to prevent prostate cancer may synergistically reduce prostate cancer development. Following this approach, the first aim of the present thesis was to investigate potential synergistic effects of selenium and broccoli constituents as an even better chemopreventive agent in prostate cancer when they are combined as selenium-enriched broccoli.

In a second approach we aimed to reduce prostate cancer risk efficiently using cruciferous vegetables that are especially rich in glucosinolates. The young seedlings or sprouts of cruciferous vegetables contain about 10-100 times more glucosinolates when compared to corresponding mature vegetables (98). The second aim of the present thesis was therefore to investigate the chemopreventive potential of glucosinolate–rich kale sprouts with regard to anti-angiogenic effects and its capability to modulate histone acetylation.

5.1 Potential of Se-enriched broccoli as a chemopreventive agent in prostate cancer

A series of studies examined how Se-enrichment in broccoli affects plant physiology and the physiology of broccoli consuming animals. In the plant physiology Se fertilization has been described to cause a modest decrease of indole-based and aliphatic glucosinolates (177). Robbins and co-workers previously reported that fertilization with Se increased Se concentration in broccoli in a dose-dependent manner (178). However, increasing Se concentration led at the same time to a dramatic reduction of glucoraphanin and sulforaphane content down to 41% and 82% respectively (178). This limitation may be attributed to the fact that Se and sulfur share the same transporter during the initial route of uptake (89, 163). To avoid this expected competition, a different fertilization method to enhance selenium levels was been considered.

One method has been developed by our collaboration partner (group of Prof. T. Rausch, Heidelberg Institute of Plant Science) (179). The procedure is based on spraying Se onto the broccoli leaves, while the broccoli florets and soil were protected in order to avoid a direct inpact of Se (179). Spraying sodium selenate in a concentration of 2 mg or 20 mg/plant increased the total Se concentration in the broccoli florets without changing glucoraphanin contents in the broccoli florets compared to plants that were not sprayed upon.

Another possible method is to develop Se fertilization in the broccoli young sprouts. It has been reported that glucoraphanin contents does not change during two or three weeks of culturing time (92). This is mainly because broccoli seed do not synthesize glucoraphanin per se, highly concentrated glucosinolates in the seed are distributed while they grow to sprouts (180). Therefore using selenium fertilization in young broccoli sprouts may be a promising method to avoid competition.

With respect to the animal physiology, Se-enriched broccoli was considered to have greater chemopreventive potential than that contributed to the two single agents, broccoli or Se.

The primary chemopreventive mechanism of broccoli is attributed to the alteration of phase I and II enzyme detoxification pathways (50). Sulforaphane, which is a major glucosinolate hydrolysis product, activates phase II enzymes through thiol modification of Keap-1. This leads to translocation of the Nrf-2 transcription factor to the nucleus where it interacts with transcriptional regulatory elements, which are common to multiple genes involved in redox signaling, such as QR, GST and Trx-R (181, 182). On the other hand, the primary mechanism

of Se is modulating redox signaling by induction of selenoproteins such as GPx and Trx-R (183). The combination of selenium and broccoli can be hypothesized to target both mechanisms in a synergistic manner. However, it has been reported that QR activity was highest in low-Se broccoli extract treatment compare to high-Se broccoli extract treatment in murine hepatoma cells. These previous findings were explained by reduced contents of glucoraphanin in high-Se broccoli compared to low-Se broccoli (184).

In our present study, we found that although the glucoraphanin contents was similar in the selenium fertilized broccoli (or sprouts) compare with standard broccoli (or sprouts), the induction of QR activity was lower by treatment of selenium-fertilized broccoli than standard broccoli in both BPH-1 and LNCaP cell lines. In addition, treatment of prostate (cancer) cells with SeMSC as a selenium source together with broccoli extract showed moderately reduced QR activity compared with treatment of the same concentration of broccoli extract, although treatment with selenium alone had no influence on QR enzyme activity. It is possible that a competitive mechanism between ITCs and Se is not only presented in plant physiology but also in cell physiology. The induction of phase II detoxifying enzymes by SFN may be interfered by co-treatment with Se in the cells. Detailed underlying mechanisms have to be the subject of further investigations.

Besides the competitive effect or antagonistic effect on QR induction, we found that there was a synergistic effect between broccoli and Se with respect to the induction of TRx-R. Both Se and broccoli contributed to Trx-R activity induction. The inducing potential of Se-enriched broccoli was higher than standard broccoli. In addition, Se-fertilized broccoli sprouts also had higher potential to induce TRx-R activity compared with standard sprouts, although the glucoraphanin contents were similar in both sprout types. There are two possible mechanisms to induce Trx-R expression. The primary mechanism is Nrf-2-dependent expression of the Trx-R gene (181, 182). As described previously, ITCs contain an electrophilic carbon moiety which actively interacts with thiol groups. Keap-1 is one of the candidate molecules which are targeted by the electrophilic moiety of ITCs, since it contains a cysteine thiol group (50). The interaction of ITCs with Keap-1 results in a release of the Nrf-2 transcription factor from Keap-1 and translocation to the nucleus. Binding of Nrf-2 to the antioxidant responsive element (ARE) leads to the transactivation of TRx-R gene expression (50). The secondary mechanism to increase TRx-R activity is by Se-cysteine (SeCys) incorporation during Trx-R protein synthesis. SeCys incorporation into selenoproteins is encoded by a UGA codon which is more frequently the signal for the

termination of protein synthesis (185, 186). The reading of UGA during translation as a SeCys codon occurs in the presence of specific 3'-untranslated region (UTR) mRNA secondary structures termed SECIS (selenocysteine insertion sequence) elements. Potential SECIS elements have been identified in the 3'-UTR of Trx-R [28, 29]. Similarly, the 3'-UTR of GPx contains SECIS elements, therefore GPx protein synthesis is induced in the presence of Se (187). Se-enriched broccoli contains active compounds to induce TRx-R activity by both mechanisms. This explains why induction of TRx-R activity by Se-enriched broccoli was higher than after treatment with standard broccoli.

Different plants contain different amounts and different chemical forms of Se (29). As listed in Table 2 and described in Chapter 1.2.2.1, various chemical forms of Se have been reported to target diverse mechanisms and possess varying potential to protect against prostate cancer development. In addition, two recent clinical trials, that is the NPC and SELECT trials, showed dramatically opposite results of two forms of selenium. NPC reported an inverse correlation between Se consumption and prostate cancer risk, whereas the SELECT study could not find any relationship (27, 28). This might be due to the fact that the NPC study used selenized yeast, whereas in the SELECT trial, selenomethionine was used for intervention. Considering these previous reports, it is reasonable to assume that different chemical forms of Se which accumulated in broccoli might lead to diverse biological effects in the cells. Presently, we could only compare total amounts of Se after fertilization of sprouts, florets or broccoli. Further investigations are required to identify which forms of Se are predominant incorporated by selenium fertilization in the sprouts and broccoli florets. As a preliminary result, we observed that treatment of cultured prostate cancer cells with selenite, selenate or SeMSC at identical concentrations induced seleno-enzymes to different degrees, with selenite treatment being most potent. In addition, we observed that broccoli sprouts cultured in media containing selenite and selenate differentially accumulate Se in the plant, and also differed in their potential to induce Se-containing enzymes in cell culture. Cultivation with selenite resulted in a higher accumulation of Se compared to selenate cultivation in broccoli sprouts. Also, sprouts cultivated with selenite more potently induced GPx expression and TRx-R activity in the prostate cancer cells. Although we found that total selenium concentration was higher after selenite fertilization than after selenate fertilization, to better understand differences in biological response in the sprouts the major form of Se needs to be determined. One of our major interests in the present study was to compare the effect of Se-enriched broccoli *in vitro* and in an *in vivo* prostate cancer model. Induction of phase II enzymes and

selenoproteins by Se-enriched broccoli could not reproduced *in vivo* in the LNCaP xenograft model. However, although the tested broccoli preparations failed to induce antioxidant enzymes in the tumor tissue, liver antioxidant enzymes were significantly induced. Moreover, inducted of liver enzyme activities such as QR activity linearly correlated with glucoraphanin metabolites in mouse serum as well as glucosinolates contents in broccoli samples. However, selenoproteins were not induced by Se-enriched broccoli preparations both in tumor and liver samples. This was surprising since the animals received 6.2 µg Se per day, which was five-fold more than the Se-content in the control diet group or standard broccoli group. Limited work in our study has been conducted to determine the chemical form of Se in our Se-enriched broccoli and biological samples. It has been reported that broccoli contains large amounts of SeMSC, and that SeMSC in the broccoli does not accumulate in the rat or human to the same extent as other forms of Se do (188-190), presumably because SeMSC is metabolized directly to methylselenol and enters the excretory pathway. We still need to determine the percentage of SeMSC within the total selenium content in our Se-enriched experimental broccoli and derived products.

The dose of selenium in clinical trials and bench experiments is another the key factor relevant for biological effects (39, 40). The relationship between selenium dose and biological effect showed a U-shaped dose-response in an animal model with beagle dogs when comparing selenium status and the extent of DNA damage within the prostate (39, 40). In our present study we observed that results of our *in vitro* cell culture experiment regarding induction of selenoproteins by Se-enriched broccoli was not transferrable to the animal model. It is possible that the Se concentration in mouse serum is already high enough to maximally induce selenoproteins by the basal Se contents in the control diet. In contrast, cell culture medium without added Se containing 10% fetal-bovine serum has a Se concentration of less than 0.01 µM (191) therefore additional Se potently induces Se containing proteins.

Se-enriched food intervention may be beneficial to not with respect to cancer prevention under defined conditions, but also to Se deficiency diseases which are caused by extremely low dietary Se-intakes such as Kehan disease in humans and white muscle disease in domestic live stocks (192, 193). Se-enriched broccoli as a functional food may help to increase the uptake of Se also under these conditions. In the present study, we made Se-enriched broccoli puree. However during the food making process, some part of Se and a large percentage of glucosinolates was destroyed. It is still remains a question how we can maintain the beneficial compounds in the plant during food processing as well as improve

bioavailability of both compounds for humans in a synergistic manner.

5.2 Anti-angiogenic potential of kale sprouts

Various mechanisms have been described how ITCs interfere with prostate cancer development (24, 50). Relatively recent studies reported that tumor angiogenesis is a potential target of ITCs (100, 108, 127, 128). Sprouts of cruciferous vegetables are a good source of ITCs since they contain about 10-100 fold more of glucosinolates than the adult plant (98). Although there has not been any report regarding kale sprouts, we hypothesized that glucosinolate-rich kale sprouts may reduce prostate cancer progression *via* mechanisms related to anti-angiogenesis.

In the present thesis, we analyzed the influence of kale sprouts on angiogenesis using a LNCaP xerograph model, modeling hormone-dependent human prostate cancer. We observed that dietary kale sprout intervention induced vascular maturation and prevented tumor necrosis whereas control tumors showed massive hemorrhage, more necrosis, less mature vessels and a more aggressive tumor appearance. To our knowledge, this is the first report showing glucosinolate-rich cruciferous vegetable sprout-dependant induction of vascular maturation and the respective underlying mechanisms in a human prostate cancer model. The statistically significant inhibition of hemorrhage as a consequence of a matured blood vasculature was evident with the addition of 20% of kale sprout to the regular diet. Dose-dependent effects were not analyzed in this study.

The maturation of blood vessel vasculature is the last step of angiogenesis, which includes the specialization of the vessel wall for structural support and regulation of the recruitment of mural cells like pericytes (166). The recruitment of pericytes is one of the final but, at the same time, most important steps during angiogenesis, leading to vessel maturation and stabilization (116). Stabilized blood vessels block hemorrhage, which causes leakage of blood and causes necrosis. However, vessel stabilization also helps to deliver oxygen and nutrients to the tumors (124). Thus, it has been an important strategy of anti-cancer drug development to reduce vessel density (166). Although there is no doubt about anti-angiogenic drugs having success in cancer therapy regarding some tumor types, there are some cancers that do not respond well to anti-angiogenic therapy (194, 195). It has recently been reported that the main cause of resistance to anti-angiogenic therapy is due to reduced vessel density (166). As a result of anti-angiogenic therapy, oxygen and nutrients cannot be delivered to the tumor,

which leads to a hypoxic condition of the tumor environment (166). Hypoxia is considered to be one of the triggers to increase tumor growth through activation of hypoxia inducible factor alpha (HIF-1α)-dependent transcription (196). In addition, anti-cancer drugs, which need to be delivered inside of the tumor may not reach the cancer properly due to immature vessels. Therefore, recent studies suggested that vascular normalization is one of the next goals of anti-angiogenic therapy (124, 197).

In the present thesis we could show that supplementation of the diet with 20 % kale sprouts induces vascular normalization *via* increased pericyte attachment to the blood vessel. Although the tumor size was not reduced, our results may indicate that vascular normalization by dietary kale sprouts could increase the sensitivity to chemotherapy in co-treatment with chemotherapeutic drugs. Recent studies showed similar result by targeting PlGF, which is an pro-angiogenic factor. Treatment did not reduce tumor size but via this approach normalization of the vasculature was induced (168). However, co-treatment of the anti-PlGF drug with chemotherapeutic drugs inhibited tumor growth effectively (168).

It is now widely accepted that the 'angiogenic switch' is 'off' when the effect of pro-angiogenic molecules is balanced with anti-angiogenic molecules, and can be switched to 'on' when the net balance is tipped in favor of angiogenesis (112). It has been suggested that an abnormal vasculature arises from an imbalance of angiogenic regulators, such as VEGF, FGF, PIGF, angiopoietins, and anti-angiogenic factors like angiostatins (124). The present study revealed that dietary kale sprout intervention inhibited pro-angiogenic factors such as FGFb, PlGF and MMPs. At the same time it induced anti-angiogenic factors like angiostatin and PSA. Induction of anti-angiogenic factors and inhibition of pro-angiogenic factors upon regular kale sprout intake may favor the angiogenesis balance to the 'switched-off' state, leading to a more controlled angiogenesis. It has been reported that ITCs inhibit NF-κB mediated expression of pro-angiogenic factors such as VEGF and MMPs (198, 199). However, the detailed mechanisms by which kale sprout cause inhibition of pro-angiogenic factors such as FGFb, PlGF, and MMPs in the LNCaP xenograft model remain to be elucidated.

The anti-angiogenic factor angiostatin consists of four to five kringle domains of plasminogen and can be generated by proteolytic cleavage of plasminogen by proteases such as PSA and MMP 11 (170, 200, 201). Secretion of PSA has been used as a marker of prostate cancer and it has been shown that PSA is able to convert plasminogen into biologically active angiostatin-like fragments (170, 200, 201).

DISCUSSIONS

In the present study, we showed that dietary intake of kale sprouts induces angiostatin protein expression and PSA secretion. In addition, there was a inverse linear correlation between PSA levels and hemoglobin concentration. Although the detailed mechanisms about kale sprout-induced angiostatin expression still has to be described, we can assume that maintenance of PSA levels by dietary kale sprouts may lead to an increased production of angiostatin protein expression.

Recently, several groups showed growth inhibitory effects of SFN, PEITC or AITC in a dose range of 6-12 µmol/per mouse/day in both the PC-3 human prostate cancer xenograft model and the TRAMP mouse model (99, 174, 202-204). Taking these published findings into consideration, our findings suggest that glucosinolates-rich kale sprouts have a potential to inhibit cancer growth in the prostate cancer xenograft model. However, in the present study we could not observe an anti-proliferation effect using dietary kale sprouts. There are some possible reasons for these controversial results. First of all, the explanation might be the hormone-dependency of the LNCaP xenograft prostate cancer model. To our knowledge, most of the previously used animal models to investigate effects of ITCs were hormone-independent prostate cancer xenograft or (allograft) tumor models (108, 127, 174) such as PC-3 and TRAMP-1C. These xenografts do not lead to a secretion of PSA and less expression of AR and they are growth hormone independent. Therefore, the mechanisms of ITCs-mediated anti-proliferation were related to cell cycle arrest and apoptosis rather than anti-hormonal effects (99, 174, 202-204). In contrast, the LNCaP xenograft model is a hormone dependent, AR-sensitive prostate cancer model. Although kale sprouts induced cell cycle arrest in the mitotic phase, AR protein expression was maintained as well as PSA secretion. The balance between these effects may result in inhibition of cell proliferation.

Secondly, the explanation might be found in the different population of cancer stem cells which contribute to cancer initiation and progression in hormone-dependent LNCaP cells and hormone-independent PC-3 cells. Patrawala *et al.* showed that prostate stem cell markers were detectable in PC-3 cells but not in LNCaP cells (205). Similarly, another recent report demonstrated that ALDH1A1, a marker for malignant prostate stem cells, clonogenicity, and tumorigenicity presented higher levels in PC-3 than LNCaP cells (206). Recently, the effects of SFN to inhibit proliferation by abolishing cancer stem cell characteristics have been identified (207, 208). Anti-proliferative potential of SFN on cancer stem cells may lead to differences in the response of PC-3 and LNCaP cells.

Thirdly, a possible explanation could be tumor necrosis. We found that kale sprouts inhibited

tumor necrosis which is a key mechanism to reduce cancer cell proliferation in the LNCaP xenograft model. Inhibition of necrosis may set off an anti-proliferative potential of dietary kale sprouts by inhibition of the cell cycle and angiostasis.

Induction of tumor necrosis is associated with tumor necrosis factor α (TNFα), which is a potent pro-inflammatory cytokine and plays an important role in angiogenesis (209). It exists both in a membrane-bound and a soluble form, and is secreted by macrophages, monocytes, neutrophils, T cells, natural killer cells and other cell types after stimulation, for example by lipopolysaccharide (LPS) (210). Certain stimulated cells and a number of transformed cell lines, like astrocytes, microglia, smooth muscle cells, and fibroblasts also secrete TNFα (210). Based on the stimuli, TNFα can function both as a pro-survival, or a pro-apoptotic factor thereby leading either to cell survival, or cell death (210). Elevated levels of TNFα and increased expression of TNFα have been found in tumor tissues and in the serum of cancer patients, which implies that TNFα plays a major role in tumor progression (211). High expression of TNFα alpha has been correlated with proliferation and survival of malignant cells, stimulation of angiogenesis, and metastasis. In the present study, we could show that dietary kale sprout inhibits TNFα protein expression and murine TNFα mRNA levels in the xenografts. Although the mechanism by which kale sprout caused the suppression of TNFα secretion remains to be elucidated in the LNCaP xenograft model, there are possibilities to explain these effects. For instance, transcription factors, including NF-κB, bind to the TNFα promoter to initiate and activate its transcription (211, 212). It is likely that kale sprouts inhibit transcriptional activation of NF-κB to suppress TNFα expression. Suppression of NF-κB and NF-κB regulated gene expression including TNFα by ITCs has already been documented in several cell lines (50), including our own previous finding (49, 213).

Another possible explanation could be found in mouse tissue infiltrates, including macrophages and fibroblasts. Our findings indeed support this hypothesis, since we observed relatively high levels of inflammatory cells and invading fibroblast in the control tumors compared to kale sprout tumors. The inhibition of invading murine cells by kale sprout could be the possible cause of globally suppressed murine TNFα secretion.

The present study showed that glucosinolate-rich dietary kale sprout intervention led to vascular maturation and prevented hemorrhage-related tumor necrosis in the human prostate cancer LNCaP xenograft model. These results have the potential to be translated to the prevention or treatment of human prostate cancer.

5.3 Histone modification by kale sprouts

Recently the potential of various isothiocyanates to inhibit HDAC activity was investigated (60, 150, 152, 153). It has been shown that dietary kale sprouts, rich in isothiocyanates precursors, increased histone acetylation, which is associated with increased HAT rather than inhibition of HDAC activity in the LNCaP xenograft model. The changing balance between HAT and HDAC induced by kale sprouts was associated with increased acetylated histones at the promoter of p21 and elevated gene expression in the LNCaP xenograft model. In addition, mitotic arrest was observed.

Unlike a previous report that dietary SFN at a dose of about 7.5 µmol/mouse/day for 21 days inhibited HDAC activity in the PC-3 xenograft model (174), we observed that dietary kale sprout at a dose of about 70 µmoles glucosinolates/mouse/day / (9 µmoles SFN/mouse /day) for 7.5 weeks did not inhibit HDAC activity in the LNCaP xenograft model. Early findings showed that treatment with SFN had different HDAC inhibitory effects on different stages of prostate cancer cells (149). The PC-3 cell line was the cell line most sensitive to SFN with respect to HDAC inhibition. However, in LNCaP cells SFN and the HDAC inhibitor TSA showed moderate inhibitory effects at concentration required to inhibit HDAC activity in PC-3 and BPH-1 cells (149) . The authors explained that basal levels of HDAC activity in PC-3 cells are much higher than in LNCaP cells, therefore HDAC inhibitors exhibit greater effects toward PC-3 cells (149).

SFN itself has only a borderline inhibitory effect on the activity of HDAC but its metabolite, the cysteine conjugate of SFN, is more effective as an HDAC inhibitor (214, 215). After intervention with kale sprouts we found that SFN-Cys concentrations in the plasma were quite low compared to other metabolites (Table 9). Most of the SFN was presented as SNF-NAC conjugates or free SFN in the plasma. The contribution on HDAC inhibitory effects by different SFN metabolites should be further investigated in the prostate cancer cell lines.

The effect of isothiocyanates on HATs has not been well investigated, yet. Few studies showed controversial results, since different kinds of isothiocyanates have been investigated (151, 152, 216). A recent study showed the possibility of isothiocyanate to induce HAT expression. A synthetic isothiocyanate, phenhexyl isothiocyanate, increased levels of the histone acetyl transferase p300, which led to an accumulation of acetylated histones in a leukemia cell line (151). However, another study showed that BITC inhibited p300/CBP expression in pancreatic carcinoma cell lines (152). Kale sprouts contain different kinds of

glucosinolates. A major content is sinigrin, a precursor of AITC. A second one is glucoiberin, which can be metabolized to iberin. To better understand which kinds of isothiocyanate contribute to increased histone acetylation by kale sprouts, further studies with individual compounds have to be performed.

Hyperacetylation of histones, particularly at certain lysine residues of histone tails, is associated with active transcription of certain genes (130). Hypoacetylation of histones, on the other hand, is associated with the formation of heterochromatin and gene silencing (130). Although dietary kale sprouts did not inhibit HDAC activity, the action of kale sprouts on the enhancement of HAT may effectively induce acetylation of core histones. Particularly the promoter region of the p21 gene shows enrichment with acetylated histone H4 induced by dietary kale sprouts. Interestingly, we found that the increase of p21 gene expression was higher than the increase of acetylated histone enrichment by kale sprouts. Notably, induction of p21 by isothiocyanates was not only contributed to by histone acetylation. Earlier studies suggested other mechanisms to induce p21 gene expression by ITCs. has It has previously been shown that phosphorylation of the G_2/M enforcer chk2 by PEITC or BITC mediated p21 gene expression in Caco-2 cells (217). Also, increased p21 protein expression mediated by phosphorylation of chk2 and cdc25C by sulforaphane has previously been reported (58, 218). .

In summary, the present investigation has provided evidence for the induction of histone acetylation in the LNCaP xenograft model after daily application of kale sprouts as a food supplement. In this study, we suggested that increased histone acetylation may be caused by increased HAT levels. There was an increased H4 acetylation together with localized increases in acetylation histones H4 associated with the promoter region of PCAF and p21. Increased histone H4 acetylation was also detectable in human PBMC samples after a single administration of kale sprouts.

Conclusively, we have described increased histone acetylation in a prostate cancer xenograft as well as normal human PBMC. Since these activities occur rapidly after kale sprout intervention, but were not related to inhibition of tumor growth, further studies have to demonstrate the functional relevance of these findings for chemopreventive or chemotherapeutic efficacy of kale sprouts *in vivo*.

5.4 Outlook

Intervention with Se-enriched broccoli and kale sprouts resulted in the activation of several anti-cancerous and potential chemopreventive mechanisms in the LNCaP xenograft model. However, we did not observe a direct effect on the tumor size, which might be due to a variety of factors as outlined above. Regarding their biological activities, both Se-enriched broccoli as well as kale sprouts represent promising factors for prostate cancer chemoprevention. Considering the development and different stages of prostate cancer, the LNCaP xenograft model might have been not the ideal model to demonstrate preventive efficacy. Based on our results, the chemopreventive potential of Se-enriched broccoli and kale sprouts should be further investigated in more relevant models for prostate cancer development.

6. SUMMARY

Prostate cancer is the most commonly diagnosed malignancy in men in industrialized countries and the second leading cause of male cancer related death. Despite a recent increase of prostate cancer cases and related death, the prevalence of prostate cancer in Asia is much lower than in Western countries. This geographic variation reflects differences in life style and diet, which is in Western countries rich in highly saturated fat and meat, and low in vegetables. Many epidemiologic studies continue to support the idea that dietary intake of chemopreventive agents may be protective against prostate cancer.

From the several chemopreventive agents we focused on selenium and cruciferous vegetables. The first aim was to produce selenium enriched broccoli and to evaluate the effects. For optimization of selenium fertilization, we evaluated selenium and glucoraphanin contents in plants as well as antioxidant enzyme induction in prostate cancer cell lines *in vitro*. Spraying selenate onto broccoli leaves increased selenium contents in the broccoli without changing glucoraphanin contents. Se-accumulated broccoli induced phase II detoxifying enzymes such as QR, TRx-R and Se-containing antioxidant enzymes GPx-1, GPx-4 and TRx-R *in vitro*. In addition, Se-enriched broccoli increased these enzymes *in vivo* in the mouse liver. However, supplementation had no effect on LNCaP xenograft tumor growth as well as on antioxidant enzyme induction in tumor tissue although sulforaphane metabolites were detectable in the mouse plasma. In conclusion, Se-enriched broccoli potently increases phase II detoxifying enzymes and Se-containing antioxidant enzymes *in vitro*, however 20% of dietary Se-enriched broccoli and the functional foods produced from it had no influence on enzyme induction and tumor growth *in vivo* in the LNCaP xenograft model.

The second aim of this study was to investigate the effect of kale sprouts in the LNCaP xenograft model. Kale sprouts are a good source of glucosinolates, since they contain 4-fold more glucosinolates than the standard broccoli. Therefore we aimed to evaluate anti-proliferative effects of kale sprouts and underlying mechanisms in the LNCaP xenograft model. Unlike our expectation, dietary kale sprouts for 6.5 weeks did not show growth inhibitory effects in the LNCaP prostate cancer xenograft model. However, we observed much evidence that kale sprouts reduced the development of prostate cancer and aggressiveness. First of all, the tumors contained less hemorrhage and necrotic areas. Also,

invasion of mouse-derived cells into xenografts was reduced by the intervention. Although the vessel density was not different between the groups, vessel maturation in the kale sprout group was increased, which was indicated by increased pericyte coverage of endothelial cells. Vascular maturation was associated with down-regulation of the pro-angiogenic factors and up-regulation of an anti-angiogenic factor, angiostatin. According to the vascular maturation, hemorrhage could be prevented leading to prevention of necrosis. Secondly, TNFα-mediated down regulation of AR protein expression and PSA secretion was prevented by kale sprouts. TNFα-reduced AR protein expression has been considered to desensitize LNCaP cells for the binding of the ligand. In conclusion, dietary kale sprouts play a dual role in aspect of tumor growth. On the one hand they block necrosis, which may induce tumor growth but on the other hand kale sprouts induced angiostasis to inhibit tumor growth. Overall tumor sizes were not changed even though many characteristics of the tumors are influenced which would indicate anti-tumor effects of kale sprouts.

As the third part of the study, we further investigated effects of kale sprouts on epigenetic histone modifications. Histone marks have been suggested to be an important target mechanism of prostate cancer progression and ITCs have been demonstrated recently to act as HDAC inhibitors. Dietary kale sprouts increased histone acetylation associated with increased HAT levels rather than inhibition of HDAC activity in the LNCaP xenograft model. The change of balance between HAT and HDAC by kale sprouts was associated with increased histone acetylation at the promoter of p21 and its gene expression in the LNCaP xenograft model. A well known consequence of histone acetylation mediated p21 gene induction is cell cycle arrest and apoptosis. Dietary kale sprouts indeed increased mitotic arrest. Interestingly, these effects were not only limited to the xenograft model but could also be shown in human PBMC after intervention. 10 g of kale sprouts intervention increased histone H4 acetylation in human PBMC after 1.5 to 3 h. In conclusion, dietary supplement of kale sprouts may help to affect gene transcription by promotion of histone acetylation. This may contribute to cancer prevention.

In summary, the presented thesis describes novel mechanistic modes of cruciferous vegetables, which contain potent cancer chemopreventive compounds. Selenium fertilization may increase the effects of broccoli to prevent prostate cancer by inducing selenium-containing antioxidant enzymes although there is no influence on tumor growth in the models

analyzed. Kale sprouts were for the first time suggested to be used as a potential chemopreventive agent in order to increase vascular maturation and prevent hemorrhage and necrosis in tumors. Another important mechanism, which was targeted by kale spouts was histone acetylation. Importantly these effects were shown in relevant concentration that they could be used as a dietary supplement.

7 ZUSAMMENFASSUNG

Prostatakrebs ist der am häufigsten diagnostizierte bösartige Tumor in Männern in der industrialisierten Welt und die zweithäufigste Todesursache von Krebserkrankungen in Männern. Obwohl die Inzidenz- und Todesrate von Prostatakrebs in den letzten Jahren angestiegen ist, ist die Prostatakrebsprävalenz in asiatischen Ländern deutlich geringer als in westlichen Ländern. Diese geographischen Unterschiede sind auf Unterschiede im Lebensstil und in der Ernährung der westlichen Welt, das heißt viele gesättigte Fettsäuren und Fleisch und wenig Gemüse, zurückzuführen. Mehrere epidemiologische Studien haben wiederholt gezeigt, dass der Verzehr von chemopräventiven Substanzen in der täglichen Nahrung das Risiko an Prostatakrebs zu erkranken reduzieren kann.

Unter den vielen chemopräventiven Substanzen konzentriert sich die vorliegende Arbeit auf Selenium und Kreuzblütengewächse (Cruciferen). Das erste Ziel dieser Arbeit war es durch Düngung Brokkoli mit erhöhtem Selengehalt zu züchten und seine krebspräventive Wirkung zu untersuchen. Um die Selendüngung zu optimieren, ermittelten wir den Selen- und Glucoraphaningehalt in den Pflanzen, sowie die Induktion von antioxidativen Enzymen in Prostatakrebszelllinien *in vitro*. Das Aufsprühen von Selenat auf die Blätter der Brokkolipflanzen erhöhte den Selengehalt im Brokkoli, ohne den Glucoraphaningehalt zu verändern. Se-angereicherter Brokkoli induzierte die Phase II detoxifizierenden Enzyme QR, TRx-R und die Se-haltigen Enzyme GPx-1, GPx-4 und TRX-R *in vitro*. Darüber hinaus induzierte Se-angereicherter Brokkoli und daraus generierte „funktionelle Nahrungsmittel" diese Enzyme ebenfalls in Mausleber in einem *in vivo* Tiermodell. Jedoch zeigte der Brokkoli keinen hemmenden Effekt auf das Tumorwachstum, wie auch keinen induzierenden Effekt auf die antioxidativen Enzyme in den Tumoren aus dem LNCaP Tumor Xenograft-Modell, obwohl Sulforaphan-Metaboliten im Plasma der Mäuse detektiert werden konnten. Schlussfolgernd wurde gezeigt, dass Se-angereicherter Brokkoli das Potenzial hat Phase II detoxifizierende Enzyme und Se-enthaltende Enzyme *in vitro* zu induzieren, aber Futter, das zu 20% Se-angereicherten Brokkoli enthält bzw. daraus generierte „funktionelle Nahrungsmittel" keinen Einfluss auf die Enzyminduktion und das Tumorwachstum *in vivo* hatten.

Das zweite Ziel dieser Arbeit war es die Effekte von Grünkohlkeimlingen im LNCaP Tumor Xenograft-Modell zu untersuchen. Grünkohlkeimlinge sind eine reiche Quelle an Glucosinolaten und enthalten viermal so viel Glucosinolate wie gewöhnlicher Brokkoli.

Daher war es unser Ziel die anti-proliferativen Effekte von Grünkohlkeimlingen und die zugrundeliegenden Mechanismen im LNCaP Tumor Xenograft-Modell zu ermitteln. Entgegen unseren Erwartungen hatte die 6.5-wöchige Intervention mit Grünkohlkeimlingen im Futter keinen wachstumshemmenden Effekt in dem LNCaP Tumor Xenograft-Modell. Allerdings beobachteten wir Hinweise darauf, dass Grünkohlkeimlinge die Entwicklung von malignem Prostatakrebs dennoch positiv beeinflussen. Zunächst enthielten die Tumoren weniger Blut und nekrotische Zonen. Des Weitern wurde die Invasion von endogenen Mauszellen in die Xenograft-Gewebe durch die Intervention reduziert. Obwohl die Blutgefäßdichte in beiden Gruppen gleich war, war die Blutgefäß-Ausbildung in der Grünkohlgruppe deutlich erhöht, da die Endothelzellen mit einer größeren Anzahl von Pericyten bedeckt waren. Die Blutgefäßbildung wurde mit der Herunterregulierung von pro-angiongenen Faktoren und der Hochregulierung des anti-angiogenen Faktors Angiostatin korreliert. Dementsprechend waren die tumor-internen Blutungen und Nekrosen reduziert. Darüber hinaus wurde die TNFα-induzierte Herunterregulierung der AR Proteinexpression und PSA Sekretion durch Grünkohl gehemmt. Die Reduktion von AR durch TNFα wird für die Desensibilisierung von LNCaP auf Androgene verantwortlich gemacht, da die Ligandenbindung an den AR geschwächt wird. Zusammenfassend zeigt die Nahrungsergänzung mit Grünkohl zweierlei Effekte: einerseits könnte die Hemmung von Nekrosen zu vermehrtem Tumorwachstum führen, anderseits aber hemmt die Hochregulierung von Angiostatin das Tumorwachstum. Insgesamt war das Tumorwachstum nicht verändert, obwohl viele Parameter innerhalb des Tumors von Grünkohlkeimlingen beeinflusst wurden.

In einem dritten Teil dieser Arbeit untersuchten wir Effekte von Grünkohlkeimlingen auf epigenetische Veränderungen. Histonmodifikationen werden als wichtige Mediatoren der Prostatakrebsprogression gesehen und ITCs wurden kürzlich als HDAC-Inhibitoren identifiziert. Die Aufnahme von Grünkohlkeimlingen mit der Nahrung erhöhte die Histonacetylierung, was mit erhöhter HAT- und gehemmter HDAC-Aktivität im LNCaP Xenograft-Modell einherging. Die veränderte Balance zwischen HAT und HDAC durch Grünkohlkeimlinge resultierte in vermehrter Histonacetylierung in der Promoterregion von p21 und dessen Genexpression. Normalerweise führt die Induktion der p21 Expression zum Zellzyklusarrest und Apoptose. Und tatsächlich erhöhte die Grünkohlkeimling-Diät den mitotischen Arrest. Interessanterweise war die erhöhte Histon Acetylierung nicht nur im LNCaP Xenograft-Modell, sondern auch in menschlichen PBMC zu messen. Die Intervention

mit 10g Grünkohlkeimlingen erhöhte die Histon-H4-Acetylierung nach 1.5 bis 3h. Abschließend lässt sich feststellen, dass die Nahrungsergänzung mit Grünkohlkeimlingen dazu beitragen kann die Gentranskription durch Erhöhung der Histonacetylierung zu beeinflussen. Dies könnte zur Prostatakrebsprävention beitragen.

Zusammenfassend beschreibt die vorliegende Arbeit neue mechanistische Aktivitäten von Cruciferen, die sehr potente prostatachemopräventive Agenzien beinhalten. Selendüngung trägt dazu bei die Prostatakrebs-präventiven Effekte von Brokkoli zu erhöhen, indem die Selenhaltigen antioxidativen Enzyme induziert werden, allerdings ohne einen Einfluss auf das Tumorwachstum zu haben. Zum ersten Mal wurde gezeigt, dass Grünkohlkeimlinge chemopräventives Potenzial besitzen, da diese die Ausbildung von Blutgefäßen erhöhen und Blutungen sowie Nekrosen im Tumor verringern. Ein weiterer wichtiger Angriffspunkt von Grünkohlkeimlingen ist die Histonacetylierung. Erwähnenswert hierbei sind die geringen Konzentrationen der eingesetzten chemopräventiven Agenzien, die jenen Konzentrationen entsprechen, die mit Nahrungsergänzungsmitteln mit der täglichen Nahrung aufgenommen werden.

8 COLLABORATORS

8.1 Potential of Se-enriched broccoli as a chemopreventive agent in prostate cancer

Selenium fertilization of broccoli was provided by

Fu-Chou Hsu, Thomas Rausch

Heidelberger Institut für Pflanzenforschung, Heidelberg University, Heidelberg, Germany

Total selenium contents and glucoraphanin concentration in broccoli sprouts and florets were measured by

Fu-Chou Hsu, Thomas Rausch

Heidelberger Institut für Pflanzenforschung, Heidelberg University, Heidelberg, Germany

Sulforaphan metabolites from mouse plasma, urine, feces were measured by

Johanna Hauder, Veronika Somoza

German Research Center for Food Chemistry, Garching, Germany

Glucosinolates contents in the broccoli preparations and kale sprouts were measured by

[1]Corinna Rüfer, Gina De Nicola[2], Renato Iori[2]

[1]Max Rubner-Institute, Federal Research Institute of Nutrition and Food, Karlsruhe, Germany

[2]University of Bologna, Bologna, Italy

8.2 Anti-angiogenic potential of kale sprouts

Staining of blood vessels and pericytes were done by

Mattthias Wieland, Hellmut G Augustin

Joint Research Division Vascular Biology of the Medical Faculty Mannheim, University of Heidelberg, and the German Cancer Research Center (DKFZ), Vascular Oncology and Metastasis, Germany

Pathological evaluation was done by

Carolin Mogler

Institute of Pathology, university of Heidelberg

Secreted PSA was measured by

Achim Bub

Max Rubner-Institute, Federal Research Institute of Nutrition and Food, Karlsruhe, Germany

8.3 Histone modification by kale sprouts

HDAC activity was measured by

Julia M. Wagner, Manfred Jung

Institute of Pharmaceutical Science, Albert-Ludwigs-University Freiburg, Germany

9 REFERENCES

1.   Jemal A, Siegel R, Xu J, Ward E. Cancer statistics, 2010. CA Cancer J Clin; 60: 277-300.

2.   Gronberg H. Prostate cancer epidemiology. Lancet 2003; 361: 859-64.

3.   Khandrika L, Kumar B, Koul S, Maroni P, Koul HK. Oxidative stress in prostate cancer. Cancer Lett 2009; 282: 125-36.

4.   De Marzo AM, DeWeese TL, Platz EA, et al. Pathological and molecular mechanisms of prostate carcinogenesis: implications for diagnosis, detection, prevention, and treatment. J Cell Biochem 2004; 91: 459-77.

5.   Gupta S, Ahmad N, Marengo SR, MacLennan GT, Greenberg NM, Mukhtar H. Chemoprevention of prostate carcinogenesis by alpha-difluoromethylornithine in TRAMP mice. Cancer Res 2000; 60: 5125-33.

6.   Uzgare AR, Isaacs JT. Prostate cancer: potential targets of anti-proliferative and apoptotic signaling pathways. Int J Biochem Cell Biol 2005; 37: 707-14.

7.   Bookstein R, Bova GS, MacGrogan D, Levy A, Isaacs WB. Tumour-suppressor genes in prostatic oncogenesis: a positional approach. Br J Urol 1997; 79 Suppl 1: 28-36.

8.   Bertram J, Peacock JW, Fazli L, et al. Loss of PTEN is associated with progression to androgen independence. Prostate 2006; 66: 895-902.

9.   Deocampo ND, Huang H, Tindall DJ. The role of PTEN in the progression and survival of prostate cancer. Minerva Endocrinol 2003; 28: 145-53.

10.   Dong JT. Prevalent mutations in prostate cancer. J Cell Biochem 2006; 97: 433-47.

11.   DeMarzo AM, Nelson WG, Isaacs WB, Epstein JI. Pathological and molecular aspects of prostate cancer. Lancet 2003; 361: 955-64.

12.   Feldman BJ, Feldman D. The development of androgen-independent prostate cancer. Nat Rev Cancer 2001; 1: 34-45.

13.   Hayward SW, Dahiya R, Cunha GR, Bartek J, Deshpande N, Narayan P. Establishment and characterization of an immortalized but non-transformed human prostate epithelial cell line: BPH-1. In Vitro Cell Dev Biol Anim 1995; 31: 14-24.

14.   Horoszewicz JS, Leong SS, Kawinski E, et al. LNCaP model of human prostatic carcinoma. Cancer Res 1983; 43: 1809-18.

15.   Kaighn ME, Narayan KS, Ohnuki Y, Lechner JF, Jones LW. Establishment and characterization of a human prostatic carcinoma cell line (PC-3). Invest Urol 1979; 17: 16-23.

REFERENCES

16.   Stone KR, Mickey DD, Wunderli H, Mickey GH, Paulson DF. Isolation of a human prostate carcinoma cell line (DU 145). Int J Cancer 1978; 21: 274-81.

17.   Surh YJ. Cancer chemoprevention with dietary phytochemicals. Nat Rev Cancer 2003; 3: 768-80.

18.   Doll R, Peto R. The causes of cancer: quantitative estimates of avoidable risks of cancer in the United States today. J Natl Cancer Inst 1981; 66: 1191-308.

19.   Pan MH, Ho CT. Chemopreventive effects of natural dietary compounds on cancer development. Chem Soc Rev 2008; 37: 2558-74.

20.   Mehnert JM, Kelly WK. Histone deacetylase inhibitors: biology and mechanism of action. Cancer J 2007; 13: 23-9.

21.   Ho E, Clarke JD, Dashwood RH. Dietary sulforaphane, a histone deacetylase inhibitor for cancer prevention. J Nutr 2009; 139: 2393-6.

22.   Hauser AT, Jung M. Targeting epigenetic mechanisms: potential of natural products in cancer chemoprevention. Planta Med 2008; 74: 1593-601.

23.   Araldi EM, Dell'aica I, Sogno I, Lorusso G, Garbisa S, Albini A. Natural and synthetic agents targeting inflammation and angiogenesis for chemoprevention of prostate cancer. Curr Cancer Drug Targets 2008; 8: 146-55.

24.   Venkateswaran V, Klotz LH. Diet and prostate cancer: mechanisms of action and implications for chemoprevention. Nat Rev Urol; 7: 442-53.

25.   Helzlsouer KJ, Huang HY, Alberg AJ, et al. Association between alpha-tocopherol, gamma-tocopherol, selenium, and subsequent prostate cancer. J Natl Cancer Inst 2000; 92: 2018-23.

26.   Li H, Stampfer MJ, Giovannucci EL, et al. A prospective study of plasma selenium levels and prostate cancer risk. J Natl Cancer Inst 2004; 96: 696-703.

27.   Duffield-Lillico AJ, Dalkin BL, Reid ME, et al. Selenium supplementation, baseline plasma selenium status and incidence of prostate cancer: an analysis of the complete treatment period of the Nutritional Prevention of Cancer Trial. BJU Int 2003; 91: 608-12.

28.   Lippman SM, Klein EA, Goodman PJ, et al. Effect of selenium and vitamin E on risk of prostate cancer and other cancers: the Selenium and Vitamin E Cancer Prevention Trial (SELECT). JAMA 2009; 301: 39-51.

29.   Dong Y, Lee SO, Zhang H, Marshall J, Gao AC, Ip C. Prostate specific antigen expression is down-regulated by selenium through disruption of androgen receptor signaling. Cancer Res 2004; 64: 19-22.

REFERENCES

30.   Morris JD, Pramanik R, Zhang X, et al. Selenium- or quercetin-induced retardation of DNA synthesis in primary prostate cells occurs in the presence of a concomitant reduction in androgen-receptor activity. Cancer Lett 2006; 239: 111-22.

31.   Venkateswaran V, Klotz LH, Fleshner NE. Selenium modulation of cell proliferation and cell cycle biomarkers in human prostate carcinoma cell lines. Cancer Res 2002; 62: 2540-5.

32.   Hu H, Jiang C, Ip C, Rustum YM, Lu J. Methylseleninic acid potentiates apoptosis induced by chemotherapeutic drugs in androgen-independent prostate cancer cells. Clin Cancer Res 2005; 11: 2379-88.

33.   Dong Y, Zhang H, Gao AC, Marshall JR, Ip C. Androgen receptor signaling intensity is a key factor in determining the sensitivity of prostate cancer cells to selenium inhibition of growth and cancer-specific biomarkers. Mol Cancer Ther 2005; 4: 1047-55.

34.   Zhong W, Oberley TD. Redox-mediated effects of selenium on apoptosis and cell cycle in the LNCaP human prostate cancer cell line. Cancer Res 2001; 61: 7071-8.

35.   Herbette S, Roeckel-Drevet P, Drevet JR. Seleno-independent glutathione peroxidases. More than simple antioxidant scavengers. FEBS J 2007; 274: 2163-80.

36.   Steinbrenner H, Sies H. Protection against reactive oxygen species by selenoproteins. Biochim Biophys Acta 2009; 1790: 1478-85.

37.   Brigelius-Flohe R. Selenium compounds and selenoproteins in cancer. Chem Biodivers 2008; 5: 389-95.

38.   Husbeck B, Nonn L, Peehl DM, Knox SJ. Tumor-selective killing by selenite in patient-matched pairs of normal and malignant prostate cells. Prostate 2006; 66: 218-25.

39.   Waters DJ, Shen S, Glickman LT, et al. Prostate cancer risk and DNA damage: translational significance of selenium supplementation in a canine model. Carcinogenesis 2005; 26: 1256-62.

40.   Chiang EC, Shen S, Kengeri SS, et al. Defining the Optimal Selenium Dose for Prostate Cancer Risk Reduction: Insights from the U-Shaped Relationship between Selenium Status, DNA Damage, and Apoptosis. Dose Response 2009; 8: 285-300.

41.   Higdon JV, Delage B, Williams DE, Dashwood RH. Cruciferous vegetables and human cancer risk: epidemiologic evidence and mechanistic basis. Pharmacol Res 2007; 55: 224-36.

42.   Giovannucci E, Rimm EB, Liu Y, Stampfer MJ, Willett WC. A prospective study of cruciferous vegetables and prostate cancer. Cancer Epidemiol Biomarkers Prev 2003; 12:

REFERENCES

1403-9.

43.   Stram DO, Hankin JH, Wilkens LR, et al. Prostate cancer incidence and intake of fruits, vegetables and related micronutrients: the multiethnic cohort study* (United States). Cancer Causes Control 2006; 17: 1193-207.

44.   Kirsh VA, Peters U, Mayne ST, et al. Prospective study of fruit and vegetable intake and risk of prostate cancer. J Natl Cancer Inst 2007; 99: 1200-9.

45.   Steinbrecher A, Nimptsch K, Husing A, Rohrmann S, Linseisen J. Dietary glucosinolate intake and risk of prostate cancer in the EPIC-Heidelberg cohort study. Int J Cancer 2009; 125: 2179-86.

46.   Kolonel LN, Hankin JH, Whittemore AS, et al. Vegetables, fruits, legumes and prostate cancer: a multiethnic case-control study. Cancer Epidemiol Biomarkers Prev 2000; 9: 795-804.

47.   Cohen JH, Kristal AR, Stanford JL. Fruit and vegetable intakes and prostate cancer risk. J Natl Cancer Inst 2000; 92: 61-8.

48.   Hayes JD, Kelleher MO, Eggleston IM. The cancer chemopreventive actions of phytochemicals derived from glucosinolates. Eur J Nutr 2008; 47 Suppl 2: 73-88.

49.   Heiss E, Herhaus C, Klimo K, Bartsch H, Gerhauser C. Nuclear factor kappa B is a molecular target for sulforaphane-mediated anti-inflammatory mechanisms. J Biol Chem 2001; 276: 32008-15.

50.   Juge N, Mithen RF, Traka M. Molecular basis for chemoprevention by sulforaphane: a comprehensive review. Cell Mol Life Sci 2007; 64: 1105-27.

51.   Bonnesen C, Eggleston IM, Hayes JD. Dietary indoles and isothiocyanates that are generated from cruciferous vegetables can both stimulate apoptosis and confer protection against DNA damage in human colon cell lines. Cancer Res 2001; 61: 6120-30.

52.   Cheung KL, Kong AN. Molecular targets of dietary phenethyl isothiocyanate and sulforaphane for cancer chemoprevention. AAPS J; 12: 87-97.

53.   Herman-Antosiewicz A, Johnson DE, Singh SV. Sulforaphane causes autophagy to inhibit release of cytochrome C and apoptosis in human prostate cancer cells. Cancer Res 2006; 66: 5828-35.

54.   Wang M, Berthoud VM, Beyer EC. Connexin43 increases the sensitivity of prostate cancer cells to TNFalpha-induced apoptosis. J Cell Sci 2007; 120: 320-9.

55.   Singh SV, Srivastava SK, Choi S, et al. Sulforaphane-induced cell death in human prostate cancer cells is initiated by reactive oxygen species. J Biol Chem 2005; 280: 19911-

REFERENCES

24.

56.   Xiao D, Powolny AA, Moura MB, et al. Phenethyl isothiocyanate inhibits oxidative phosphorylation to trigger reactive oxygen species-mediated death of human prostate cancer cells. J Biol Chem; 285: 26558-69.

57.   Chiao JW, Wu H, Ramaswamy G, et al. Ingestion of an isothiocyanate metabolite from cruciferous vegetables inhibits growth of human prostate cancer cell xenografts by apoptosis and cell cycle arrest. Carcinogenesis 2004; 25: 1403-8.

58.   Singh SV, Herman-Antosiewicz A, Singh AV, et al. Sulforaphane-induced G2/M phase cell cycle arrest involves checkpoint kinase 2-mediated phosphorylation of cell division cycle 25C. J Biol Chem 2004; 279: 25813-22.

59.   Xiao D, Srivastava SK, Lew KL, et al. Allyl isothiocyanate, a constituent of cruciferous vegetables, inhibits proliferation of human prostate cancer cells by causing G2/M arrest and inducing apoptosis. Carcinogenesis 2003; 24: 891-7.

60.   Dashwood RH, Ho E. Dietary histone deacetylase inhibitors: from cells to mice to man. Semin Cancer Biol 2007; 17: 363-9.

61.   Wang LG, Liu XM, Fang Y, et al. De-repression of the p21 promoter in prostate cancer cells by an isothiocyanate via inhibition of HDACs and c-Myc. Int J Oncol 2008; 33: 375-80.

62.   Xiao D, Johnson CS, Trump DL, Singh SV. Proteasome-mediated degradation of cell division cycle 25C and cyclin-dependent kinase 1 in phenethyl isothiocyanate-induced G2-M-phase cell cycle arrest in PC-3 human prostate cancer cells. Mol Cancer Ther 2004; 3: 567-75.

63.   Wang LG, Liu XM, Chiao JW. Repression of androgen receptor in prostate cancer cells by phenethyl isothiocyanate. Carcinogenesis 2006; 27: 2124-32.

64.   Gibbs A, Schwartzman J, Deng V, Alumkal J. Sulforaphane destabilizes the androgen receptor in prostate cancer cells by inactivating histone deacetylase 6. Proc Natl Acad Sci U S A 2009; 106: 16663-8.

65.   Le HT, Schaldach CM, Firestone GL, Bjeldanes LF. Plant-derived 3,3'-Diindolylmethane is a strong androgen antagonist in human prostate cancer cells. J Biol Chem 2003; 278: 21136-45.

66.   Keum YS, Khor TO, Lin W, et al. Pharmacokinetics and pharmacodynamics of broccoli sprouts on the suppression of prostate cancer in transgenic adenocarcinoma of mouse prostate (TRAMP) mice: implication of induction of Nrf2, HO-1 and apoptosis and the

suppression of Akt-dependent kinase pathway. Pharm Res 2009; 26: 2324-31.

67.   Ni J, Yeh S. The roles of alpha-vitamin E and its analogues in prostate cancer. Vitam Horm 2007; 76: 493-518.

68.   Syed DN, Khan N, Afaq F, Mukhtar H. Chemoprevention of prostate cancer through dietary agents: progress and promise. Cancer Epidemiol Biomarkers Prev 2007; 16: 2193-203.

69.   The effect of vitamin E and beta carotene on the incidence of lung cancer and other cancers in male smokers. The Alpha-Tocopherol, Beta Carotene Cancer Prevention Study Group. N Engl J Med 1994; 330: 1029-35.

70.   Krupsky M, Fine A, Berk JL, Goldstein RH. Retinoic acid-induced inhibition of type I collagen gene expression by human lung fibroblasts. Biochim Biophys Acta 1994; 1219: 335-41.

71.   Israel K, Sanders BG, Kline K. RRR-alpha-tocopheryl succinate inhibits the proliferation of human prostatic tumor cells with defective cell cycle/differentiation pathways. Nutr Cancer 1995; 24: 161-9.

72.   Basu A, Imrhan V. Vitamin E and prostate cancer: is vitamin E succinate a superior chemopreventive agent? Nutr Rev 2005; 63: 247-51.

73.   van Breemen RB, Pajkovic N. Multitargeted therapy of cancer by lycopene. Cancer Lett 2008; 269: 339-51.

74.   Edinger MS, Koff WJ. Effect of the consumption of tomato paste on plasma prostate-specific antigen levels in patients with benign prostate hyperplasia. Braz J Med Biol Res 2006; 39: 1115-9.

75.   Guns ES, Cowell SP. Drug Insight: lycopene in the prevention and treatment of prostate cancer. Nat Clin Pract Urol 2005; 2: 38-43.

76.   Ivanov NI, Cowell SP, Brown P, Rennie PS, Guns ES, Cox ME. Lycopene differentially induces quiescence and apoptosis in androgen-responsive and -independent prostate cancer cell lines. Clin Nutr 2007; 26: 252-63.

77.   Hantz HL, Young LF, Martin KR. Physiologically attainable concentrations of lycopene induce mitochondrial apoptosis in LNCaP human prostate cancer cells. Exp Biol Med (Maywood) 2005; 230: 171-9.

78.   Liu X, Allen JD, Arnold JT, Blackman MR. Lycopene inhibits IGF-I signal transduction and growth in normal prostate epithelial cells by decreasing DHT-modulated IGF-I production in co-cultured reactive stromal cells. Carcinogenesis 2008; 29: 816-23.

79.   Mukhtar H, Ahmad N. Tea polyphenols: prevention of cancer and optimizing health.

REFERENCES

Am J Clin Nutr 2000; 71: 1698S-702S; discussion 703S-4S.

80.   Bettuzzi S, Brausi M, Rizzi F, Castagnetti G, Peracchia G, Corti A. Chemoprevention of human prostate cancer by oral administration of green tea catechins in volunteers with high-grade prostate intraepithelial neoplasia: a preliminary report from a one-year proof-of-principle study. Cancer Res 2006; 66: 1234-40.

81.   Brausi M, Rizzi F, Bettuzzi S. Chemoprevention of human prostate cancer by green tea catechins: two years later. A follow-up update. Eur Urol 2008; 54: 472-3.

82.   Choan E, Segal R, Jonker D, et al. A prospective clinical trial of green tea for hormone refractory prostate cancer: an evaluation of the complementary/alternative therapy approach. Urol Oncol 2005; 23: 108-13.

83.   Hussain T, Gupta S, Adhami VM, Mukhtar H. Green tea constituent epigallocatechin-3-gallate selectively inhibits COX-2 without affecting COX-1 expression in human prostate carcinoma cells. Int J Cancer 2005; 113: 660-9.

84.   Kang HG, Jenabi JM, Liu XF, Reynolds CP, Triche TJ, Sorensen PH. Inhibition of the insulin-like growth factor I receptor by epigallocatechin gallate blocks proliferation and induces the death of Ewing tumor cells. Mol Cancer Ther; 9: 1396-407.

85.   Siddiqui IA, Adhami VM, Afaq F, Ahmad N, Mukhtar H. Modulation of phosphatidylinositol-3-kinase/protein kinase B- and mitogen-activated protein kinase-pathways by tea polyphenols in human prostate cancer cells. J Cell Biochem 2004; 91: 232-42.

86.   Adhami VM, Siddiqui IA, Sarfaraz S, et al. Effective prostate cancer chemopreventive intervention with green tea polyphenols in the TRAMP model depends on the stage of the disease. Clin Cancer Res 2009; 15: 1947-53.

87.   Ip C, Birringer M, Block E, et al. Chemical speciation influences comparative activity of selenium-enriched garlic and yeast in mammary cancer prevention. J Agric Food Chem 2000; 48: 4452.

88.   Finley JW. Reduction of cancer risk by consumption of selenium-enriched plants: enrichment of broccoli with selenium increases the anticarcinogenic properties of broccoli. J Med Food 2003; 6: 19-26.

89.   Hell R. Molecular physiology of plant sulfur metabolism. Planta 1997; 202: 138-48.

90.   Sors TG, Ellis DR, Na GN, et al. Analysis of sulfur and selenium assimilation in Astragalus plants with varying capacities to accumulate selenium. Plant J 2005; 42: 785-97.

91.   Lyi SM, Heller LI, Rutzke M, Welch RM, Kochian LV, Li L. Molecular and

biochemical characterization of the selenocysteine Se-methyltransferase gene and Se-methylselenocysteine synthesis in broccoli. Plant Physiol 2005; 138: 409-20.

92.   Abdulah R, Faried A, Kobayashi K, et al. Selenium enrichment of broccoli sprout extract increases chemosensitivity and apoptosis of LNCaP prostate cancer cells. BMC Cancer 2009; 9: 414.

93.   Davis CD, Zeng H, Finley JW. Selenium-enriched broccoli decreases intestinal tumorigenesis in multiple intestinal neoplasia mice. J Nutr 2002; 132: 307-9.

94.   Finley JW, Ip C, Lisk DJ, Davis CD, Hintze KJ, Whanger PD. Cancer-protective properties of high-selenium broccoli. J Agric Food Chem 2001; 49: 2679-83.

95.   Gasper AV, Al-Janobi A, Smith JA, et al. Glutathione S-transferase M1 polymorphism and metabolism of sulforaphane from standard and high-glucosinolate broccoli. Am J Clin Nutr 2005; 82: 1283-91.

96.   Gasper AV, Traka M, Bacon JR, et al. Consuming broccoli does not induce genes associated with xenobiotic metabolism and cell cycle control in human gastric mucosa. J Nutr 2007; 137: 1718-24.

97.   Fahey JW, Zhang Y, Talalay P. Broccoli sprouts: an exceptionally rich source of inducers of enzymes that protect against chemical carcinogens. Proc Natl Acad Sci U S A 1997; 94: 10367-72.

98.   Kensler TW, Chen JG, Egner PA, et al. Effects of glucosinolate-rich broccoli sprouts on urinary levels of aflatoxin-DNA adducts and phenanthrene tetraols in a randomized clinical trial in He Zuo township, Qidong, People's Republic of China. Cancer Epidemiol Biomarkers Prev 2005; 14: 2605-13.

99.   Srivastava SK, Xiao D, Lew KL, et al. Allyl isothiocyanate, a constituent of cruciferous vegetables, inhibits growth of PC-3 human prostate cancer xenografts in vivo. Carcinogenesis 2003; 24: 1665-70.

100.   Thejass P, Kuttan G. Allyl isothiocyanate (AITC) and phenyl isothiocyanate (PITC) inhibit tumour-specific angiogenesis by downregulating nitric oxide (NO) and tumour necrosis factor-alpha (TNF-alpha) production. Nitric Oxide 2007; 16: 247-57.

101.   Nian H, Delage B, Ho E, Dashwood RH. Modulation of histone deacetylase activity by dietary isothiocyanates and allyl sulfides: studies with sulforaphane and garlic organosulfur compounds. Environ Mol Mutagen 2009; 50: 213-21.

102.   Chambers KF, Bacon JR, Kemsley EK, et al. Gene expression profile of primary prostate epithelial and stromal cells in response to sulforaphane or iberin exposure. Prostate

REFERENCES

2009; 69: 1411-21.

103. Wang LG, Chiao JW. Prostate cancer chemopreventive activity of phenethyl isothiocyanate through epigenetic regulation (review). Int J Oncol; 37: 533-9.

104. Xiao D, Singh SV. p66Shc is indispensable for phenethyl isothiocyanate-induced apoptosis in human prostate cancer cells. Cancer Res; 70: 3150-8.

105. Kim JH, Xu C, Keum YS, Reddy B, Conney A, Kong AN. Inhibition of EGFR signaling in human prostate cancer PC-3 cells by combination treatment with beta-phenylethyl isothiocyanate and curcumin. Carcinogenesis 2006; 27: 475-82.

106. Xiao D, Lew KL, Zeng Y, et al. Phenethyl isothiocyanate-induced apoptosis in PC-3 human prostate cancer cells is mediated by reactive oxygen species-dependent disruption of the mitochondrial membrane potential. Carcinogenesis 2006; 27: 2223-34.

107. Yao H, Wang H, Zhang Z, Jiang BH, Luo J, Shi X. Sulforaphane inhibited expression of hypoxia-inducible factor-1alpha in human tongue squamous cancer cells and prostate cancer cells. Int J Cancer 2008; 123: 1255-61.

108. Xiao D, Singh SV. Phenethyl isothiocyanate inhibits angiogenesis in vitro and ex vivo. Cancer Res 2007; 67: 2239-46.

109. Bertl E, Bartsch H, Gerhauser C. Inhibition of angiogenesis and endothelial cell functions are novel sulforaphane-mediated mechanisms in chemoprevention. Mol Cancer Ther 2006; 5: 575-85.

110. Kerbel R, Folkman J. Clinical translation of angiogenesis inhibitors. Nat Rev Cancer 2002; 2: 727-39.

111. Hanahan D, Folkman J. Patterns and emerging mechanisms of the angiogenic switch during tumorigenesis. Cell 1996; 86: 353-64.

112. Bergers G, Benjamin LE. Tumorigenesis and the angiogenic switch. Nat Rev Cancer 2003; 3: 401-10.

113. Neufeld G, Kessler O. Pro-angiogenic cytokines and their role in tumor angiogenesis. Cancer Metastasis Rev 2006; 25: 373-85.

114. Roskoski R, Jr. Vascular endothelial growth factor (VEGF) signaling in tumor progression. Crit Rev Oncol Hematol 2007; 62: 179-213.

115. Mattsson JM, Laakkonen P, Stenman UH, Koistinen H. Antiangiogenic properties of prostate-specific antigen (PSA). Scand J Clin Lab Invest 2009; 69: 447-51.

116. Kalluri R. Basement membranes: structure, assembly and role in tumour angiogenesis. Nat Rev Cancer 2003; 3: 422-33.

REFERENCES

117.   Kerbel RS, Kamen BA. The anti-angiogenic basis of metronomic chemotherapy. Nat Rev Cancer 2004; 4: 423-36.

118.   Antoniak K, Nowak JZ. [Bevacizumab: progress in the treatment of metastatic cancer and hope for patients with proliferative retinopathy]. Postepy Hig Med Dosw (Online) 2007; 61: 320-30.

119.   Traina TA, Rugo HS, Dickler M. Bevacizumab for advanced breast cancer. Hematol Oncol Clin North Am 2007; 21: 303-19.

120.   Duda DG, Batchelor TT, Willett CG, Jain RK. VEGF-targeted cancer therapy strategies: current progress, hurdles and future prospects. Trends Mol Med 2007; 13: 223-30.

121.   Goldfarb SB, Traina TA, Dickler MN. Bevacizumab for advanced breast cancer. Womens Health (Lond Engl); 6: 17-25.

122.   Abou-Alfa GK. Selection of patients with hepatocellular carcinoma for sorafenib. J Natl Compr Canc Netw 2009; 7: 397-403.

123.   Aita M, Fasola G, Defferrari C, et al. Targeting the VEGF pathway: antiangiogenic strategies in the treatment of non-small cell lung cancer. Crit Rev Oncol Hematol 2008; 68: 183-96.

124.   Jain RK. Normalization of tumor vasculature: an emerging concept in antiangiogenic therapy. Science 2005; 307: 58-62.

125.   Hellmann K. Recognition of tumor blood vessel normalization as a new antiangiogenic concept. Nat Med 2004; 10: 329; author reply -30.

126.   Hellmann K. Dynamics of tumour angiogenesis: effect of razoxane-induced growth rate slowdown. Clin Exp Metastasis 2003; 20: 95-102.

127.   Shankar S, Ganapathy S, Srivastava RK. Sulforaphane enhances the therapeutic potential of TRAIL in prostate cancer orthotopic model through regulation of apoptosis, metastasis, and angiogenesis. Clin Cancer Res 2008; 14: 6855-66.

128.   Suh SJ, Moon SK, Kim CH. Raphanus sativus and its isothiocyanates inhibit vascular smooth muscle cells proliferation and induce G(1) cell cycle arrest. Int Immunopharmacol 2006; 6: 854-61.

129.   Kumar A, D'Souza SS, Tickoo S, Salimath BP, Singh HB. Antiangiogenic and proapoptotic activities of allyl isothiocyanate inhibit ascites tumor growth in vivo. Integr Cancer Ther 2009; 8: 75-87.

130.   Marks P, Rifkind RA, Richon VM, Breslow R, Miller T, Kelly WK. Histone deacetylases and cancer: causes and therapies. Nat Rev Cancer 2001; 1: 194-202.

131.   Shahbazian MD, Grunstein M. Functions of site-specific histone acetylation and deacetylation. Annu Rev Biochem 2007; 76: 75-100.

132.   Cang S, Feng J, Konno S, et al. Deficient histone acetylation and excessive deacetylase activity as epigenomic marks of prostate cancer cells. Int J Oncol 2009; 35: 1417-22.

133.   Patra SK, Patra A, Dahiya R. Histone deacetylase and DNA methyltransferase in human prostate cancer. Biochem Biophys Res Commun 2001; 287: 705-13.

134.   Shankar S, Srivastava RK. Histone deacetylase inhibitors: mechanisms and clinical significance in cancer: HDAC inhibitor-induced apoptosis. Adv Exp Med Biol 2008; 615: 261-98.

135.   Mottet D, Castronovo V. Histone deacetylases: target enzymes for cancer therapy. Clin Exp Metastasis 2008; 25: 183-9.

136.   Bruserud O, Stapnes C, Ersvaer E, Gjertsen BT, Ryningen A. Histone deacetylase inhibitors in cancer treatment: a review of the clinical toxicity and the modulation of gene expression in cancer cell. Curr Pharm Biotechnol 2007; 8: 388-400.

137.   Lai MT, Yang CC, Lin TY, Tsai FJ, Chen WC. Depsipeptide (FK228) inhibits growth of human prostate cancer cells. Urol Oncol 2008; 26: 182-9.

138.   Venkataramani V, Rossner C, Iffland L, et al. Histone deacetylase inhibitor valproic acid inhibits cancer cell proliferation via down-regulation of the alzheimer amyloid precursor protein. J Biol Chem; 285: 10678-89.

139.   VanOosten RL, Earel JK, Jr., Griffith TS. Histone deacetylase inhibitors enhance Ad5-TRAIL killing of TRAIL-resistant prostate tumor cells through increased caspase-2 activity. Apoptosis 2007; 12: 561-71.

140.   Sonnemann J, Bumbul B, Beck JF. Synergistic activity of the histone deacetylase inhibitor suberoylanilide hydroxamic acid and the bisphosphonate zoledronic acid against prostate cancer cells in vitro. Mol Cancer Ther 2007; 6: 2976-84.

141.   Lakshmikanthan V, Kaddour-Djebbar I, Lewis RW, Kumar MV. SAHA-sensitized prostate cancer cells to TNFalpha-related apoptosis-inducing ligand (TRAIL): mechanisms leading to synergistic apoptosis. Int J Cancer 2006; 119: 221-8.

142.   Suenaga M, Soda H, Oka M, et al. Histone deacetylase inhibitors suppress telomerase reverse transcriptase mRNA expression in prostate cancer cells. Int J Cancer 2002; 97: 621-5.

143.   Abbas A, Gupta S. The role of histone deacetylases in prostate cancer. Epigenetics

2008; 3: 300-9.

144.   Mork CN, Faller DV, Spanjaard RA. A mechanistic approach to anticancer therapy: targeting the cell cycle with histone deacetylase inhibitors. Curr Pharm Des 2005; 11: 1091-104.

145.   McLaughlin F, La Thangue NB. Histone deacetylase inhibitors open new doors in cancer therapy. Biochem Pharmacol 2004; 68: 1139-44.

146.   Peck B, Chen CY, Ho KK, et al. SIRT inhibitors induce cell death and p53 acetylation through targeting both SIRT1 and SIRT2. Mol Cancer Ther; 9: 844-55.

147.   Furukawa A, Tada-Oikawa S, Kawanishi S, Oikawa S. H2O2 accelerates cellular senescence by accumulation of acetylated p53 via decrease in the function of SIRT1 by NAD+ depletion. Cell Physiol Biochem 2007; 20: 45-54.

148.   Cheng HL, Mostoslavsky R, Saito S, et al. Developmental defects and p53 hyperacetylation in Sir2 homolog (SIRT1)-deficient mice. Proc Natl Acad Sci U S A 2003; 100: 10794-9.

149.   Myzak MC, Hardin K, Wang R, Dashwood RH, Ho E. Sulforaphane inhibits histone deacetylase activity in BPH-1, LnCaP and PC-3 prostate epithelial cells. Carcinogenesis 2006; 27: 811-9.

150.   Beklemisheva AA, Fang Y, Feng J, Ma X, Dai W, Chiao JW. Epigenetic mechanism of growth inhibition induced by phenylhexyl isothiocyanate in prostate cancer cells. Anticancer Res 2006; 26: 1225-30.

151.   Ma X, Fang Y, Beklemisheva A, et al. Phenylhexyl isothiocyanate inhibits histone deacetylases and remodels chromatins to induce growth arrest in human leukemia cells. Int J Oncol 2006; 28: 1287-93.

152.   Batra S, Sahu RP, Kandala PK, Srivastava SK. Benzyl isothiocyanate-mediated inhibition of histone deacetylase leads to NF-kappaB turnoff in human pancreatic carcinoma cells. Mol Cancer Ther; 9: 1596-608.

153.   Li Y, Li X, Guo B. Chemopreventive agent 3,3'-diindolylmethane selectively induces proteasomal degradation of class I histone deacetylases. Cancer Res; 70: 646-54.

154.   Conaway CC, Yang YM, Chung FL. Isothiocyanates as cancer chemopreventive agents: their biological activities and metabolism in rodents and humans. Curr Drug Metab 2002; 3: 233-55.

155.   Pohl RJ, Fouts JR. A rapid method for assaying the metabolism of 7-ethoxyresorufin by microsomal subcellular fractions. Anal Biochem 1980; 107: 150-5.

156.   Gerhauser C, You M, Liu J, et al. Cancer chemopreventive potential of sulforamate, a novel analogue of sulforaphane that induces phase 2 drug-metabolizing enzymes. Cancer Res 1997; 57: 272-8.

157.   Keen JH, Habig WH, Jakoby WB. Mechanism for the several activities of the glutathione S-transferases. J Biol Chem 1976; 251: 6183-8.

158.   Hill KE, McCollum GW, Burk RF. Determination of thioredoxin reductase activity in rat liver supernatant. Anal Biochem 1997; 253: 123-5.

159.   Eyer P, Podhradsky D. Evaluation of the micromethod for determination of glutathione using enzymatic cycling and Ellman's reagent. Anal Biochem 1986; 153: 57-66.

160.   Trtkova K, Paskova L, Matijescukova N, Strnad M, Kolar Z. Binding of AR to SMRT/N-CoR complex and its co-operation with PSA promoter in prostate cancer cells treated with natural histone deacetylase inhibitor NaB. Neoplasma; 57: 406-14.

161.   Shechter D, Dormann HL, Allis CD, Hake SB. Extraction, purification and analysis of histones. Nat Protoc 2007; 2: 1445-57.

162.   Heltweg B, Dequiedt F, Verdin E, Jung M. Nonisotopic substrate for assaying both human zinc and NAD+-dependent histone deacetylases. Anal Biochem 2003; 319: 42-8.

163.   Sors TG, Ellis DR, Salt DE. Selenium uptake, translocation, assimilation and metabolic fate in plants. Photosynth Res 2005; 86: 373-89.

164.   Shapiro TA, Fahey JW, Wade KL, Stephenson KK, Talalay P. Chemoprotective glucosinolates and isothiocyanates of broccoli sprouts: metabolism and excretion in humans. Cancer Epidemiol Biomarkers Prev 2001; 10: 501-8.

165.   Carmeliet P. Angiogenesis in life, disease and medicine. Nature 2005; 438: 932-6.

166.   Jain RK. Molecular regulation of vessel maturation. Nat Med 2003; 9: 685-93.

167.   Nasarre P, Thomas M, Kruse K, et al. Host-derived angiopoietin-2 affects early stages of tumor development and vessel maturation but is dispensable for later stages of tumor growth. Cancer Res 2009; 69: 1324-33.

168.   Fischer C, Mazzone M, Jonckx B, Carmeliet P. FLT1 and its ligands VEGFB and PlGF: drug targets for anti-angiogenic therapy? Nat Rev Cancer 2008; 8: 942-56.

169.   Barrett JM, Rovedo MA, Tajuddin AM, et al. Prostate cancer cells regulate growth and differentiation of bone marrow endothelial cells through TGFbeta and its receptor, TGFbetaRII. Prostate 2006; 66: 632-50.

170.   Heidtmann HH, Nettelbeck DM, Mingels A, Jager R, Welker HG, Kontermann RE. Generation of angiostatin-like fragments from plasminogen by prostate-specific antigen. Br J

REFERENCES

Cancer 1999; 81: 1269-73.

171.   Lilja H, Ulmert D, Vickers AJ. Prostate-specific antigen and prostate cancer: prediction, detection and monitoring. Nat Rev Cancer 2008; 8: 268-78.

172.   Jellinck PH, Forkert PG, Riddick DS, Okey AB, Michnovicz JJ, Bradlow HL. Ah receptor binding properties of indole carbinols and induction of hepatic estradiol hydroxylation. Biochem Pharmacol 1993; 45: 1129-36.

173.   Mizokami A, Gotoh A, Yamada H, Keller ET, Matsumoto T. Tumor necrosis factor-alpha represses androgen sensitivity in the LNCaP prostate cancer cell line. J Urol 2000; 164: 800-5.

174.   Myzak MC, Tong P, Dashwood WM, Dashwood RH, Ho E. Sulforaphane retards the growth of human PC-3 xenografts and inhibits HDAC activity in human subjects. Exp Biol Med (Maywood) 2007; 232: 227-34.

175.   Kim YB, Ki SW, Yoshida M, Horinouchi S. Mechanism of cell cycle arrest caused by histone deacetylase inhibitors in human carcinoma cells. J Antibiot (Tokyo) 2000; 53: 1191-200.

176.   Desgrandchamps F, Bastien L. [Nutrition, dietary supplements and prostate cancer]. Prog Urol; 20: 560-5.

177.   Finley JW, Sigrid-Keck A, Robbins RJ, Hintze KJ. Selenium enrichment of broccoli: interactions between selenium and secondary plant compounds. J Nutr 2005; 135: 1236-8.

178.   Robbins RJ, Keck AS, Banuelos G, Finley JW. Cultivation conditions and selenium fertilization alter the phenolic profile, glucosinolate, and sulforaphane content of broccoli. J Med Food 2005; 8: 204-14.

179.   Hsu FC, Wirtz M, Heppel SC, et al. Generation of Se-fortified broccoli as functional food: Impact of Se-fertilization on S-metabolism. Plant Cell Environ.

180.   McWalter GK, Higgins LG, McLellan LI, et al. Transcription factor Nrf2 is essential for induction of NAD(P)H:quinone oxidoreductase 1, glutathione S-transferases, and glutamate cysteine ligase by broccoli seeds and isothiocyanates. J Nutr 2004; 134: 3499S-506S.

181.   Zhang Y, Talalay P. Anticarcinogenic activities of organic isothiocyanates: chemistry and mechanisms. Cancer Res 1994; 54: 1976s-81s.

182.   Zhang Y, Talalay P, Cho CG, Posner GH. A major inducer of anticarcinogenic protective enzymes from broccoli: isolation and elucidation of structure. Proc Natl Acad Sci U S A 1992; 89: 2399-403.

183. Campbell L, Howie F, Arthur JR, Nicol F, Beckett G. Selenium and sulforaphane modify the expression of selenoenzymes in the human endothelial cell line EAhy926 and protect cells from oxidative damage. Nutrition 2007; 23: 138-44.

184. Keck AS, Finley JW. Aqueous extracts of selenium-fertilized broccoli increase selenoprotein activity and inhibit DNA single-strand breaks, but decrease the activity of quinone reductase in Hepa 1c1c7 cells. Food Chem Toxicol 2006; 44: 695-703.

185. Berry MJ, Banu L, Larsen PR. Type I iodothyronine deiodinase is a selenocysteine-containing enzyme. Nature 1991; 349: 438-40.

186. Jiang ZQ, Chen C, Yang B, Hebbar V, Kong AN. Differential responses from seven mammalian cell lines to the treatments of detoxifying enzyme inducers. Life Sci 2003; 72: 2243-53.

187. Mizutani T, Fujiwara T. SBP, SECIS binding protein, binds to the RNA fragment upstream of the Sec UGA codon in glutathione peroxidase mRNA. Mol Biol Rep 2000; 27: 99-105.

188. Ip C, Lisk DJ. Characterization of tissue selenium profiles and anticarcinogenic responses in rats fed natural sources of selenium-rich products. Carcinogenesis 1994; 15: 573-6.

189. Ip C, Lisk DJ. Enrichment of selenium in allium vegetables for cancer prevention. Carcinogenesis 1994; 15: 1881-5.

190. Foster SJ, Kraus RJ, Ganther HE. The metabolism of selenomethionine, Se-methylselenocysteine, their selenonium derivatives, and trimethylselenonium in the rat. Arch Biochem Biophys 1986; 251: 77-86.

191. Gallegos A, Berggren M, Gasdaska JR, Powis G. Mechanisms of the regulation of thioredoxin reductase activity in cancer cells by the chemopreventive agent selenium. Cancer Res 1997; 57: 4965-70.

192. Fairweather-Tait S, Bao Y, Broadley M, et al. Selenium in Human Health and Disease. Antioxid Redox Signal.

193. Ishihara H, Kanda F, Matsushita T, ChiharaK, Itoh K. White muscle disease in humans: myopathy caused by selenium deficiency in anorexia nervosa under long term total parenteral nutrition. J Neurol Neurosurg Psychiatry 1999; 67: 829-30.

194. Miletic H, Niclou SP, Johansson M, Bjerkvig R. Anti-VEGF therapies for malignant glioma: treatment effects and escape mechanisms. Expert Opin Ther Targets 2009; 13: 455-68.

195. Grepin R, Pages G. [The vascular endothelial growth factor (VEGF): a model of

gene regulation and a marker of tumour aggressiveness. An obvious therapeutic target?]. J Soc Biol 2009; 203: 181-92.

196.   Hong SW, Yoo JW, Kang HS, Kim S, Lee DK. HIF-1alpha-dependent gene expression program during the nucleic acid-triggered antiviral innate immune responses. Mol Cells 2009; 27: 243-50.

197.   Fukumura D, Duda DG, Munn LL, Jain RK. Tumor microvasculature and microenvironment: novel insights through intravital imaging in pre-clinical models. Microcirculation; 17: 206-25.

198.   Moon DO, Kim MO, Kang SH, Choi YH, Kim GY. Sulforaphane suppresses TNF-alpha-mediated activation of NF-kappaB and induces apoptosis through activation of reactive oxygen species-dependent caspase-3. Cancer Lett 2009; 274: 132-42.

199.   Xu C, Shen G, Chen C, Gelinas C, Kong AN. Suppression of NF-kappaB and NF-kappaB-regulated gene expression by sulforaphane and PEITC through IkappaBalpha, IKK pathway in human prostate cancer PC-3 cells. Oncogene 2005; 24: 4486-95.

200.   Mattsson JM, Valmu L, Laakkonen P, Stenman UH, Koistinen H. Structural characterization and anti-angiogenic properties of prostate-specific antigen isoforms in seminal fluid. Prostate 2008; 68: 945-54.

201.   Fortier AH, Holaday JW, Liang H, et al. Recombinant prostate specific antigen inhibits angiogenesis in vitro and in vivo. Prostate 2003; 56: 212-9.

202.   Singh SV, Warin R, Xiao D, et al. Sulforaphane inhibits prostate carcinogenesis and pulmonary metastasis in TRAMP mice in association with increased cytotoxicity of natural killer cells. Cancer Res 2009; 69: 2117-25.

203.   Singh AV, Xiao D, Lew KL, Dhir R, Singh SV. Sulforaphane induces caspase-mediated apoptosis in cultured PC-3 human prostate cancer cells and retards growth of PC-3 xenografts in vivo. Carcinogenesis 2004; 25: 83-90.

204.   Khor TO, Keum YS, Lin W, et al. Combined inhibitory effects of curcumin and phenethyl isothiocyanate on the growth of human PC-3 prostate xenografts in immunodeficient mice. Cancer Res 2006; 66: 613-21.

205.   Patrawala L, Calhoun-Davis T, Schneider-Broussard R, Tang DG. Hierarchical organization of prostate cancer cells in xenograft tumors: the CD44+alpha2beta1+ cell population is enriched in tumor-initiating cells. Cancer Res 2007; 67: 6796-805.

206.   Saleem M, Murtaza I, Tarapore RS, et al. Lupeol inhibits proliferation of human prostate cancer cells by targeting beta-catenin signaling. Carcinogenesis 2009; 30: 808-17.

207.   Rausch V, Liu L, Kallifatidis G, et al. Synergistic activity of sorafenib and sulforaphane abolishes pancreatic cancer stem cell characteristics. Cancer Res; 70: 5004-13.

208.   Li Y, Zhang T, Korkaya H, et al. Sulforaphane, a dietary component of broccoli/broccoli sprouts, inhibits breast cancer stem cells. Clin Cancer Res; 16: 2580-90.

209.   Thapa D, Lee JS, Park MA, et al. Inhibitory effects of clotrimazole on TNF-alpha-induced adhesion molecule expression and angiogenesis. Arch Pharm Res 2009; 32: 593-603.

210.   Joseph L, Fink LM, Hauer-Jensen M. Cytokines in coagulation and thrombosis: a preclinical and clinical review. Blood Coagul Fibrinolysis 2002; 13: 105-16.

211.   Srinivasan S, Kumar R, Koduru S, Chandramouli A, Damodaran C. Inhibiting TNF-mediated signaling: a novel therapeutic paradigm for androgen independent prostate cancer. Apoptosis; 15: 153-61.

212.   Liu H, Sidiropoulos P, Song G, et al. TNF-alpha gene expression in macrophages: regulation by NF-kappa B is independent of c-Jun or C/EBP beta. J Immunol 2000; 164: 4277-85.

213.   Heiss E, Gerhauser C. Time-dependent modulation of thioredoxin reductase activity might contribute to sulforaphane-mediated inhibition of NF-kappaB binding to DNA. Antioxid Redox Signal 2005; 7: 1601-11.

214.   Myzak MC, Dashwood WM, Orner GA, Ho E, Dashwood RH. Sulforaphane inhibits histone deacetylase in vivo and suppresses tumorigenesis in Apc-minus mice. FASEB J 2006; 20: 506-8.

215.   Myzak MC, Karplus PA, Chung FL, Dashwood RH. A novel mechanism of chemoprotection by sulforaphane: inhibition of histone deacetylase. Cancer Res 2004; 64: 5767-74.

216.   Meeran SM, Patel SN, Tollefsbol TO. Sulforaphane causes epigenetic repression of hTERT expression in human breast cancer cell lines. PLoS One; 5: e11457.

217.   Visanji JM, Duthie SJ, Pirie L, Thompson DG, Padfield PJ. Dietary isothiocyanates inhibit Caco-2 cell proliferation and induce G2/M phase cell cycle arrest, DNA damage, and G2/M checkpoint activation. J Nutr 2004; 134: 3121-6.

218.   Herman-Antosiewicz A, Xiao H, Lew KL, Singh SV. Induction of p21 protein protects against sulforaphane-induced mitotic arrest in LNCaP human prostate cancer cell line. Mol Cancer Ther 2007; 6: 1673-81.

V. PUBLICATIONS

V.I   Publications

1) Kim DH*, **Kim JH*(Co-first authorship)**, Kim EH, Na HK, Cha YN, Chung JH, Surh YJ
    15-Deoxy-Delta12,14-prostaglandin J2 upregulates the expression of heme oxygenase-1 and subsequently matrix metalloproteinase-1 in human breast cancer cells: possible roles of iron and ROS.
    Carcinogenesis. 2009 Apr;4 :645-54

2) **Kim JH**, Kim EH, Na HK, Cha YN, Surh YJ
    Carbon monoxide increased HIF-1alpha protein stability by inhibition of PHD2 in human breast cancer cells.
    In preparation

3) **Kim JH**, Wieland M, Mogler C, Bub A, Bähr M, Augustin H, Gerhäuser C
    Angiostasis-induced vascular normalisation, but lack of tumor growth inhibition by kale sprout intervention in a human hormone-dependent prostate cancer xenograft model
    In preparation

4) **Kim JH**, Bähr M, Wagner J, Jung M, Gerhäuser C
    Induction of histone acetylation but no inhibition of HDAC activity by kale sprouts in LNCaP xenograft model.
    In preparation

5) **Kim JH**, Hsu FC, Hauder J, Bähr M, Bub, A, Rüfer C, De Nicola G, Iori R, Rausch T, Somoza V, Gerhäuser C
    Selenium-enriched broccoli as a functional food for prostate cancer prevention – Induction of detoxifying and antioxidant enzymes *in vitro* and in a human prostate cancer xenograft model *in vivo*
    In preparation

V.II   Poster presentations

1) **Kim JH**, Kim EH, Na HK, Surh YJ
    15-Deoxy-$\Delta^{12,14}$-prostaglandin J_2 (15d-PGJ$_2$) Upregulates MMP-1 through Activation of Heme Oxygenase-1 in Human Breast Cancer Cells
    The 10th Korea-Japan Cancer Research Workshop, Dec 2005 Tokyo, Japan

2) **Kim JH**, Kim EH, Na HK, Cha YN, Surh YJ
    15-Deoxy-$\Delta^{12,14}$-Prostaglandin J_2 Induced HO-1 Upregulates MMP-1 Expression in Human Mammary Cancer cells: The Possible Role of Iron and ROS
    Korean Society for Molecular and Cellular Biology Annual Meeting, Oct 2006 Seoul, Korea

3) **Kim JH**, Bähr M, Wagner J, Nicola GN, Rüfer C, Jung M, Iori R, Gerhäuser C

Increased histone acetylation by kale sprout intervention in a human prostate cancer xenograft model
Natural Compounds in Cancer Prevention and Treatment, Oct 2009, Smolenice, Slovakia

4) **Kim JH**, Bähr M, Wagner J, De Nicola GN, Rüfer C, Jung M, Iori R, Gerhäuser C
Increased histone acetylation, but no inhibition of HDAC activity, by kale sprout intervention in a human prostate cancer xenograft model
AACR Frontiers in Cancer Prevention Research, Dec 2009, Houston, Texas, USA

5) **Kim JH**, Bähr M, Wagner J, De Nicola GN, Bub A, Rüfer C, Jung M, Iori R, Gerhäuser C
Concomitant activation of pro- and anti-proliferative mechanisms abrogate tumor growth inhibition by kale sprout intervention in a human prostate cancer xenograft model
AACR Frontiers in Cancer Prevention Research, Dec 2009, Houston, Texas, USA

6) **Kim JH**, Wieland M, Mogler C, Bub A, Bähr M, Augustin H, Gerhäuser C
Angiostasis-induced vascular normalisation, but lack of tumor growth inhibition by kale sprout intervention in a human hormone-dependent prostate cancer xenograft model
American Institute of Cancer Research Annual Reseach Conference on Food, Nutrition, Physical Activity and Cancer, Oct. 2010, Washington DC, USA

VI. ACKNOWLEDGEMENTS

I greatly appreciate

Dr. Clarissa Gerhaeuser, who gave me the great opportunity to do my PhD at DKFZ in Germany —she gave me such an interesting project, a lot of ideas, and held long-hour discussions to teach and encourage me at the same time;

Dr. Young-Joon Surh, who supported me with the publication process and motivated me to be a better scientist—I will also never forget his mentorship;

Marion Bear, who was always with me in the lab to help my research and also in Heidelberg. It won't be possible to survive as a PhD student without her great help. I deeply appreciate her help from bottom of my heart;

Dr. Stratmann Julia, for motivating and encouraging me with great ideas and being a good friend. I will never forget her cooking! (Go ma wha!);

Dr. Antonio Rufas Garreta (Ton). He has shared many things with me, listened me, and helped me in various aspects. (I ree wha!);

Karin Klimo, Renate Steine, Dr. Carolin Konermann, Jana Faut, Marta Faryna for making my life enjoyable in the lab and giving me great support for finding old stuff and microscope fixations and maybe for the doctor hat;

Dr. Yoon-Jung Park, for greatly encouraging me and giving me challenges by holding interesting discussions and giving me suggestions. I have learned a lot about the life of post-doc from her;

Dr. Khelifa Arab, for being my science supervisor. I got a lot of motivations from him as well as real solutions for my research problems;

Anna Poetsch, for her intensive corrections;

Paster Son and his family, for praying for me and guiding me;

Jina Yoon, for being a true friend by being with me and coming to me when I am sick, encouraging me, sharing the PhD life with me;

Church members of Heidelberg;

My family,..My mom.. she always raises me up. Her prayers, phone calls, and economical support drive my life;

Parents in law, for their understanding, waiting and supporting;

My husband, Myun Hur., he was always with me even in times of both good and bad. I deeply appreciate his waiting, praying and pushing. His suggestions guide me to make right decisions;

ACKNOWLEDGEMENTS

VII. LIST OF ACADEMIC REFERENCES

Dr. Clarissa Gerhaeuser	DKFZ Heidelberg	Supervisor PhD thesis
Prof. Dr. Thomas Rausch	University Heidelberg	Supervisor PhD thesis
Prof. Dr. Bernard Watzl	Max Rubner-Institut	Supervisor PhD thesis
Prof. Dr. Young-Joon Surh	Seoul National University	Supervisor Master thesis
Prof. Dr. Hellmut Augustin	DFKZ Heidelberg	Supervisor of a project
Prof. Dr. Christoph Plass	DKFZ Heidelberg	Head of Division

VIII. CURRICULUM VITAE

Personal details

        Jung-Hyun Kim
        Div. of Epigenomics & Cancer Risk Factors (C010)
        German Cancer Research Center (DKFZ)
        Im Neuenheimer Feld 280, 69120 Heidelberg Germany
        +49 (0)6221 42 3332;   j.kim@dkfz.de

Education

Feb. 2007-present	German Cancer Research Center, University of Heidelberg, PhD Major: Biology Subject: Effects of cruciferous vegetables in prostate cancer model Name of Advisor: Dr. Clarissa Gerhaeuser
Feb. 2005-Feb.2007	Seoul National University, MS Major: Tumor Biology Subject: Breast cancer metastasis and angiogenesis Name of Advisor: Dr. Young-Joon Surh
Mar. 2001-Feb. 2005	Duksung Women's University, BS Major: Pharmacy

Award and fellowship

2006	Poster award at KSMCB Annual Meeting
2005-2006	Excellent academic records scholarship from Seoul National University
2001-2004	Un-Hyun scholarship
2001-2001	Excellent academic records scholarship from Duksung Women's University